Visual pigment evolution and the paleobiology of early mammals

Dissertation

zur Erlangung des akademischen Grades

doctor rerum naturalium

(Dr. rer. nat.)

im Fach Biologie

eingereicht an der

Mathematisch-Naturwissenschaftlichen Fakultät I

der Humboldt-Universität zu Berlin

von

Dipl.-Biol. Constanze Bickelmann

Präsident der Humboldt-Universität zu Berlin
Prof. Dr. Jan-Hendrik Olbertz

Dekan der Mathematisch-Naturwissenschaftlichen Fakultät I
Prof. Dr. Andreas Herrmann

GutachterInnen:

1. Prof. Dr. Johannes Müller
2. PD Dr. Frieder Mayer
3. Prof. Belinda S.W. Chang

Tag der mündlichen Prüfung: 30.06.2011

With love, to Leon and Gaia.

Contents

Abstract in English

The rise of mammals from premammalian cynodonts during the Late Triassic was an important transition in vertrebrate evolution. The similarities in body size, orbit size, and tooth shape of early mammalian fossils, as e.g. *Morganucodon* and *Megazostrodon*, to modern shrews, tenrecs, and hedgehogs led paleontologists to the assumption that the first mammals were nocturnal, living in the shadow of the dinosaurs. For over 30 years, this view has been generally accepted and published in textbooks. Moreover, a nocturnal lifestyle would have gone hand in hand with the evolution of fur and of endothermy, which, among other features, contributed to the origin of this highly diverse and successful animal group.

One of the limitations of paleontology is the lack of soft tissue preservation; because eye tissue is not preserved in early mammalian fossils, nocturnality as the ancestral state in these taxa will always remain an assumption. Fortunately, in recent years there have been major improvements in molecular techniques; e.g. ancestral sequence reconstructions and *in vitro* expression systems, as well as in selective constraint analyses, allowing certain types of evolutionary questions regarding the evolution of visual systems to be addressed in novel ways.

This thesis investigates whether early mammals had indeed been nocturnal by combining paleontology and molecular techniques, focusing on the only visual pigment in the vertebrate eye that is responsible for vision at night and/or dim-light; the rhodopsin.

First, for a more reliable taxon sampling, the rhodopsin gene of the echidna, one of the two living families of the most basal mammalian lineage, the monotremes, was sequenced and was successfully expressed *in vitro*, together with two self-designed mutants with unique substitutions at sites 158 and 169. Biochemical and functional analyses revealed that the echidna rhodpsin displays some cone-like characteristics, likely due to rhodopsin being expressed in cones as well. Furthermore, site 169 was found to affect the strength of photon absorption in the echidna. With the echidna being a nocturnal animal, this thesis comprises the first characterisation of a rhodopsin of a nocturnal animal.

Second, based on a comprehensive alignment of 27 tetrapod rhodopsin sequences, ancestral rhodopsin sequences for the nodes Amniota, Mammalia, and Theria (i.e. marsupials and placentals) were inferred using Maximum likelihood estimates. The most likely of these were successfully expressed *in vitro*. All expressed pigments were functional and rod-like. Most importantly, meta II half lifes, which specify the time in which rhodopsin is in its active state activating the visual transduction cascade, were found to differ; Amniota shows the same rate as bovine, whereas Mammalia and Theria display a much higher $t_{1/2}$. A high $t_{1/2}$ has been said to facilitate better vision at low-light levels. Due to inconsistency in the available data, the result also suggests that, with the visual signaling cascade being such a complex and interconnected system, erecting ecological interpretations based on single biochemical and functional reactions is problematic.

Third, selective constraint analyses that investigate positive selection were completed. Positive selection is characterised by a high number of non-synonymous substitutions that change the subsequent amino acid and, thus, lead to changes in and the adaptation of a protein. These analyses revealed that the branches leading to Theria and marsupials were the only ones that experienced positive selection acting on the rhodopsin. The positive selection found at the therian branch likely reflects the rapid diversification into modern ecological habitats during the Triassic and Jurassic, as indicated by recent additions to the fossil record. Furthermore, it has been found that the branch leading to Mammalia experienced positive selection in synonymous substitutions, which do not change the subsequent amino acid; instead, these silent sites have an effect on mRNA stability and tRNA translation efficiency, increasing the number of rhodopsin molecules. This results in a scenario where the mammalian rhodopsin might have experienced positive selection on synonymous substitutions in order to increase its molecule number as an adaptation to vision at night, followed by later adaptive changes due to ecological diversification.

Though molecular techniques permit valuble insights regarding the nocturnality of the earliest mammals, additional data as well as novel investigative approaches are needed in order to address this fascinating aspect of evolutionary history. Nonetheless, this thesis emphasises the inherent value of paleontology and molecular methods working in tandem.

Abstract in German

Die Evolution der Säugetiere in der späten Trias zählt zu den bedeutendsten Ereignissen in der Wirbeltiergeschichte.

Fossilien belegen, dass die ersten Säugetiere, z. B. *Morganucodon* oder *Megazostrodon*, klein, sehr agil und aktiv waren. Sie besaßen große Augen und hatten Zähne, die auf eine insektivore Ernährung hindeuten. Die Ähnlichkeit mit heute lebenden Igeln, Spitzmäusen und Tenreks hat Paläontologen seit über 30 Jahren zu der Annahme verleitet, diese ersten Säugetiere wären nachtaktiv gewesen. Eine nachtaktive Lebensweise hätte bei der Entstehung eines endothermen Metabolismus, einer für die Säugetierevolution entscheidenden Anpassung, unterstützend gewirkt.

Auch wenn der Fossilbericht der ersten Säugetiere in den letzten Jahren massiv an Quantität und auch Qualität zugenommen hat, kann dieser aufgrund fehlender Weichteilerhaltung keine neuen Erkenntnisse bezüglich einer nachtaktiven Lebensweise dieser Tiere liefern. Dank bedeutender Fortschritte in Wissen und Techniken der molekularen Evolutionsbiologie ist es heutzutage jedoch möglich, anzestrale Gensequenzen zu rekonstruieren und im Labor das darausfolgende Protein zu synthetisieren, sowie Selektionsdrücke, die auf Proteine gewirkt haben, genau zu analysieren.

Hier setzt die vorliegende Arbeit an. Sie untersucht das einzige Sehpigment in der Netzhaut von Wirbeltieren, welches für das Sehen bei Nacht und/oder Dämmerung verantwortlich ist: das Rhodopsin.

Zuerst wurde das Rhodopsin der nachtaktiven Echidna, die zu einer der zwei letzten lebenden Familien von Monotrematen, der basalsten lebenden Säugetiere, gehört, sequenziert. Zusammen mit zwei selbstkreierten Mutanten wurde dieses erfolgreich *in vitro* exprimiert, die biochemischen und funktionellen Eigenschaften analysiert und verglichen mit dem Rhodopsin der tagaktiven Kuh, welches bereits bestens in diversen Studien charakterisiert wurde. Die Untersuchungen ergaben, dass das Rhodopsin der Echidna auch Charakteristika von Farb-Sehpigmenten aufweist, was auf eine Expression von Rhodopsin in Zapfen hindeutet. Tests an Mutante 169 ergaben, dass diese Aminosäure an der Regulierung der Absorptionsstärke des Rhodopsins der Echidna beteiligt war.

Des Weiteren, basierend auf einem umfassenden Alignment von 27 Tetrapoden-Rhodopsinen, wurden anzestrale Proteinsequenzen für die Knotenpunkte Amniota, Mammalia und Theria (d.h. Marsupialia und Plazentalia) mithilfe der Maximum-Likelihood-Methode berechnet und wiederum erfolgreich *in vitro* synthetisiert: alle Pigmente erwiesen sich funktional und zeigten typische Rhodopsin-Charakteristika.

Ausserdem ergab die Messung der Halbwertszeit von Meta II, einem entscheidenden Aktivatorzustand des Rhodopsins in der visuellen Signalkaskade, einen im Vergleich zum Kuh-Rhodopsin erhöhten Wert, sowohl im hypothetischen Säugetier- als auch im hypothetischen Theria-Rhodopsin. Dies deutet auf eine Anpassung an besseres Sehen bei schwachen Lichtverhältnissen oder bei Dunkelheit hin. Es erwies sich aber als schwierig, aus einzelnen Funktionstests Schlussfolgerungen auf ökologisch-bedingte Anpassungen zu ziehen, da die visuelle Signalkaskade ein sehr komplexes und durch viele Proteine vernetztes System darstellt.

Zuletzt wurden mithilfe der Maximum-Likelihood-Methode Selektionsdrücke, die auf nicht-synonyme Substitutionen des Rhodopsins gewirkt haben, untersucht. Positive Selektion führt dazu, dass ein Protein sich Veränderungen in der Umwelt anpasst, wohingegen negative Selektion die ursprüngliche Funktion des Proteins manifestiert. Starke positive Selektion wurde allein entlang der Linie, die zu den Theria und auch derjenigen, die zu den Marsupialia führt, ermittelt. Entlang der Theria-Linie, im Mesozoikum, sind mehrere Einnischungsevents von Säugetiertaxa in neue Lebensräume im Fossilbericht belegt. Sehr wahrscheinlich spiegeln sich Anpassungen an neue Lebensräume in einem so adaptiven System wie dem der Sehpigmente wider. Des Weiteren wurde gezeigt, dass positive Selektion auf synonyme Substitutionen im Rhodopsin nur entlang der Mammalia-Linie gewirkt hat, was Auswirkungen auf die Stabilität der mRNA sowie die Translation der tRNA hat und weiter zu einer Zunahme der Rhodopsin-Moleküle führt. Diese Ergebnisse beschreiben ein mögliches Szenario, in dem die Säugetiere im Vergleich zu anderen Amnioten zunächst die Anzahl ihrer Rhodopsin-Moleküle gesteigert haben, möglicherweise als Anpassung an das Nachtsehen. Später erfuhr das Rhodopsin adaptive Veränderungen als Antwort auf die starke ökologische Diversifikation.

Die vorliegende Arbeit zeigt mithilfe bioinformatischer und molekularbiologischer Techniken, dass das Säugetier-Rhodopsin einige Veränderungen erfahren hat. Des Weiteren bringt sie zum Ausdruck, dass Paläontologie und Molekularbiologie sich gegenseitig unterstützen können und müssen, um interessante makroevolutionsbiologische Fragen zu lösen.

List of Figures

List of Tables

1. Introduction

1.1. The origin and evolution of mammals

1.1.1. The origin of mammals

The rise of mammals during the Mesozoic era was one of the most important events in vertebrate evolution (Kemp 2005). With over 5000 extant species and some 4000 fossil taxa, mammals are a highly diverse and successful animal group (Crompton and Sun 1985, Novacek 1992, Crompton and Luo 1993, Luo 2007). Today, mammals comprise taxa in all size ranges, from a 6 cm shrew to a 33 m blue whale (Kemp 2005, Luo 2007), and have developed an enormous number of ecological specializations such as scavenging, burrowing, gliding, arboreal, scansorial, and aquatic lifestyles (Luo and Wible 2005, Martin 2005, Ji et al. 2006, Meng et al. 2006, Luo 2007).

However, there is still a lively debate regarding the origin of this successful group. What mammalian character was the most important adaptation? So-called key innovations include lactation and preceding juvenile care, a manifold behaviour facilitated by an increase in brain size, as well as endothermy (Jerison 1971, Long 1972, Hopson 1973, Crompton et al. 1978, Koteja 2000, Kemp 2005).

An endothermic physiology, which maintains a constant body temperature, enables an animal to be active under a wider range of temperatures and allows for a more complex body plan (Kemp 2005). A high rate of sustainable aerobic activity allows for more sustained exercise and a higher maximum running speed in endotherms than in ectotherms and has advantages in e.g. predation, territory size, and predator avoidance (Koteja 2004, Kemp 2005). On the other hand, endothermy requires an immense increase in food intake (Bakker 1971, Kemp 2005, Kemp 2006).

But how did endothermy evolve? It is undoubted that such a complex character is unlikely to have evolved in a single step. Several hypotheses have been discussed, among which are the thermoregulation-first hypothesis via miniaturization, the aerobic capacity hypothesis, and the parental provision hypothesis (McNab 1978, Bennett and Ruben 1979, Ruben 1995, Farmer 2000, Koteja 2000). Also, invading a nocturnal niche is believed to be amongst the features that supported the evolution of endothermy in early mammals (Crompton et al. 1978).

1.1.2. Nocturnality – a prerequisite of endothermy

Although a nocturnal life habit in early mammals had been suggested by Jerison in 1971, Crompton et al. (1978) were the first to propose that the acquisition of homeothermy enabled early mammals to invade a nocturnal niche without having to increase their resting metabolic rate. Only in a second step, the authors proposed, did mammals become diurnal, and a higher body temperature and resting metabolic rate were only secondarily acquired (Crompton et al. 1978). This perspective has been generally accepted and published in classical textbooks. Therein, the first mammals, such as *Morganucodon* and *Megazostrodon*, are pictured to have been small, highly active, nocturnal animals, and insulated by fur, living in the shadow of the dinosaurs, with life habits similar to modern hedgehogs, tenrecs, and shrews who feed on insects (Fig. 1) (Bakker 1971, Jerison 1971, Carroll 1988, Kemp 2005).

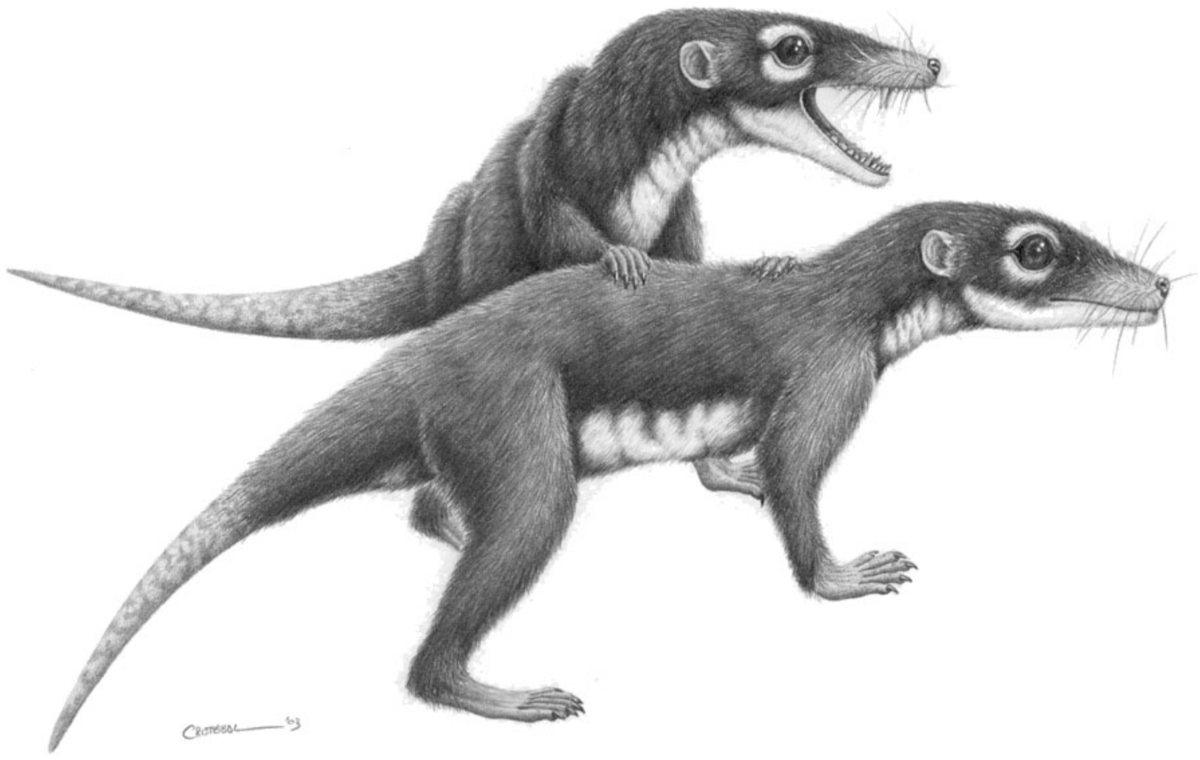

Figure 1. Reconstruction of *Morganucodon*, an early mammal from the Late Triassic of China, South Africa, India, and Europe (Kemp 2005). http://www.seirim.net/Cont/Draw/Vert/Morganucodon.jpg.

Until the mid 1970s, Mesozoic mammals were known only from teeth, but in recent years, more and more mammaliaform fossils preserving more complete skeletons have been found (Luo et al. 2001, Ji et al. 2002, Meng et al. 2006, Luo et al. 2007). Presently, the nocturnality hypothesis is supported solely by features found in the fossil record and include huge orbits, enlarged olfactory regions in the brain and improved hearing suggesting a nocturnal lifestyle, small body size, and a tooth shape similar to that of modern insectivorous animals (Carroll 1988, Kemp 2005).

In 1942, Walls described differences between the eyes of nocturnal and diurnal animals, such as eye size and shape, shape of the pupil, extent of curvature of cornea and lens, as well as visual cell shape and number, and their arrangement in the retina. Since the publication of this work, similar studies with additional information have followed (Ahnelt und Kolb 2000, Kaskan et al. 2005). However, soft-tissue morphological evidence for nocturnality as well as potential signals of endothermy in early mammals is lacking and, so far, cannot be provided by fossil findings (Ruben 1995). Ancient DNA studies have their challenges and limits, too, especially when it comes to molecules older than one million years (Hofreiter et al. 2001, Olson and Hassanin 2003, Schweitzer et al. 2009).

Hence, this thesis approaches the question of whether early mammals had indeed been nocturnal in a novel manner, i.e. by means of molecular techniques. Selection patterns acting on visual pigment genes, which support potential adaptation to changes in life habits, are investigated, and hypothetical ancestral visual pigments are inferred and resurrected, and their function is tested *in vitro*.

1.1.3. Evolution of therapsids and the acquisition of endothermy

After its erection by Linnaeus in 1758, Mammalia *sensu lato* (or Mammaliaformes according to Rowe 1988) is now recognized as a monophyletic group that includes the common ancestor of *Sinoconodon*, as well as living monotremes, and living therians (Crompton and Sun 1985, Luo et al. 2002, Kemp 2005). They form the sister group to Reptilia (Modesto and Anderson 2004) and are characterised by unique features such as insulation by fur, mammary glands, and a dentary-squamosal jaw articulation (Kemp 2005). Within synapsids, mammals belong to the clade Therapsida (Broom 1905). Therapsids originated in the Middle Permian and were one of the most successful amniote groups during the Permian, but were strongly affected by the P/T extinction event (Fig. 2) (Kemp 2005). Only anomodonts and cynodonts survived into the Triassic and the latter experienced a remarkable Middle Triassic diversification (Fig. 2) (Abdala and Ribeiro 2010). Cynodonts, more precisely Tritheledontidae and Tritylodontidae, are the closest relatives of mammals (Fig. 2) (Luo 1994). Tritylodontidae are small herbivorous forms that originated in the Early Triassic and which were abundant and remarkably diverse in the Early Jurassic (Sues 1986, Luo 1994, Abdala and Ribeiro 2010).

Tritheledontids are small insectivorous/carnivorous therapsids from the Late Triassic (Luo 1994, Kemp 2005, Abdala and Ribeiro 2010). During the Late Triassic and Early Jurassic early mammals and these cynodont tritylodontids and tritheledontids show a cosmopolitan distribution in the supercontinent Pangaea.

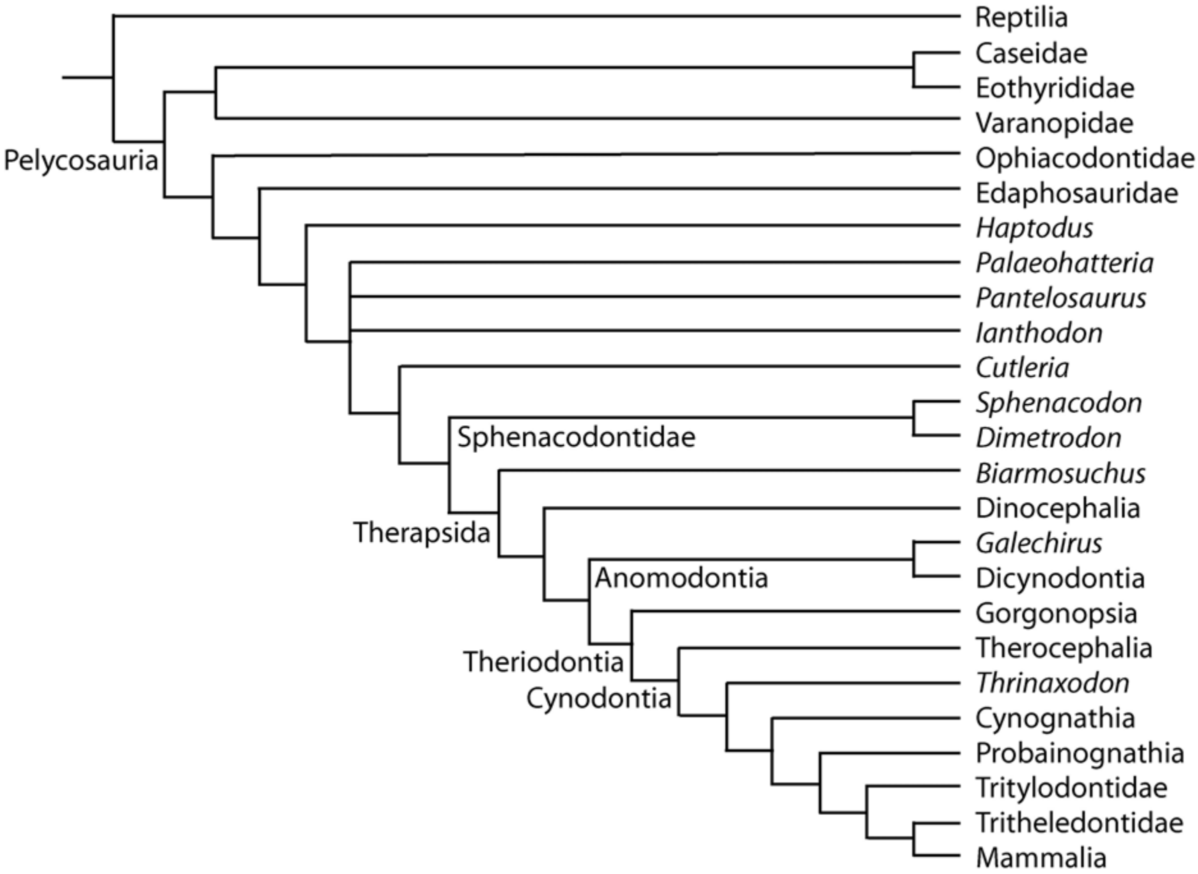

Figure 2. Simplified synapsid phylogeny based on accepted literature (Reisz 1986, Luo 1994, Abdala 2007, Abdala et al. 2008, Fröbisch et al. in press).

Gow (1985) proposed a cynodont-mammal transition characterised by sudden and profound changes, such as small body size, determinate growth, the presence of a promontorium, and diphyodonty. However, it is now widely accepted that the transition happened stepwise in transitional clades such as tritheledontids, *Sinoconodon*, and *Adelobasileus* (Brink 1956, Luo 1994, Kemp 2005, Luo 2007). For example, the stapedial process, which is part of the mammalian middle ear, is present in tritylodontids and the mammaliaform *Morganucodon*, but not found in tritheledontids and the mammaliaform *Sinoconodon* (Luo 2007). Also, the quadratojugal, which allows for more mobility in the middle ear, is already lost in *Sinoconodon* and *Morganucodon* (Luo 2007). The evolution of sensitive hearing facilitated by the middle ear in earliest mammalian forms also argues for the exploitation of nocturnal habitats (Luo 2007).

Endothermy is considered one of the major features in mammalian evolutionary history as it enables an animal to be active independent from the temperature of its surroundings and because it is thought to have been a key adaptation that gave rise to the diverse and successful mammalian group. This aspect of mammalian physiology has been the subject of various studies, in birds as well as in both living synapsids and their close extinct relatives, i.e. non-mammalian therapsids (McNab 1978, Ruben 1995, Kemp 2005, Sánchez-Villagra 2010). In contrast to pelycosaur-grade synapsids, non-mammalian therapsids have evolved many modifications in their skull and postcranium as well as presumably in their physiology towards a mammalian organisation which possibly helped to overcome temperature fluctuations of the terrestrial environment (Kemp 2005).

More precisely, in a review Sánchez-Villagra (2010) observed that fibrolamellar bone, which is an indicator of rapid osteogenesis, overall rapid growth, and endothermy, is found in some therapsids, e.g. cynodonts.

Nasal turbinal bones are found to be present in the skull of all mammals, as well as in some therapsids (Hillenius 1992, Hillenius 1994, Laaß et al. 2010). These bones are associated with reduction of respiratory water loss, but are thought to have evolved in association with elevated ventilation rates and the evolution of endothermy (Hillenius 1992).

Crompton et al. (1978) proposed that endothermy initially arose as an adaptation that permitted the exploitation of a nocturnal niche, which was facilitated by an insulating fur that reduced the rate of heat loss, while maintaining a relatively low body temperature and metabolic rate, as is also the case in living monotremes. It was only in a subsequent shift to diurnal activity that early mammals acquired a higher metabolic rate and a higher body temperature in order to withstand temperature fluctuations (Crompton et al. 1978).

1.2. Enigmatic monotremes, the most basal mammals

1.2.1. Monotremes

Monotremes are the basalmost living mammals. They form the sister group to marsupials and placentals, i.e. Theria, though, this currently widely held view is sometimes still challenged by the so-called ‘Marsupionta hypothesis’, which states that marsupials and monotremes are sister to Theria (Janke et al. 2002, Grützner and Graves 2004, Bininda-Emonds et al. 2007, Rowe et al. 2008).

The name 'Monotremata' (Bonaparte 1837) means 'single opening' and refers to the common external opening for the urinary, defecatory, and reproductive systems; the cloaca (Warren et al. 2008). Today, monotremes, also called Pro(to)theria, consist of only five species: the semi-aquatic, duck-billed platypus (*Ornithorhychus anatinus* Shaw 1799), the short-beaked echidna (*Tachyglossus aculeatus* Shaw 1792), and three species of long-beaked echidnas (*Zaglossus attenboroughi* Flannery and Groves 1998, *Zaglossus bartoni* Thomas 1907, *Zaglossus brujini* Peters and Doria 1876).

All living monotremes are nocturnal, homeothermic, endemic to the Australian continent, and show a low rate of reproduction (Dawson et al. 1979, Rissmiller 1999, Werneburg and Sánchez-Villagra 2010). They are insulated by fur, produce milk, have a single dentary and possess three middle ear bones, just like all other mammals (Campbell and Reece 2009). In sperm shape and chromosome arrangement, however, monotremes are unique among mammals (Watson et al. 1996). Unlike all other mammals, monotremes have cloacae, lay eggs, and have a reptile-like/sprawling gait (Campbell and Reece 2009). Females lack nipples, so the young suck milk directly from the abdominal skin (Warren et al. 2008, Campbell and Reece 2009). A genome analysis of the platypus revealed that the monotreme genome has many unique micro RNAs (miRNAs), but also shares some other miRNAs with either mammals or reptiles (Warren et al. 2008). Overall, monotremes exhibit an intriguing mosaic of reptilian and mammalian characters, in terms of anatomy, physiology, and reproduction (Griffiths 1989). Adult monotremes lack teeth (Warren et al. 2008), whereas fossil forms have "tribosphenic" teeth, which are one of the hallmarks of extant mammals (Li and Luo 2006, Rowe et al. 2008).

The origin of Monotremata presumably occurred sometime in the Late Triassic/Early Jurassic, a date supported by fossil as well as molecular data (Luo et al. 2002, Woodburne et al. 2003, Phillips et al. 2009). According to a recent study on *Teinolophos*, a new monotreme fossil from the Early Cretaceous of Australia, the divergence of the two residual living monotreme genera, platypus and echidna, occurred earlier than molecular estimates have suggested, i.e. in the Early Cretaceous (Rowe et al. 2008).

1.2.2. *Tachyglossus aculeatus*, the short-beaked echidna

The echidna (Tachyglossidae Gill 1872), also known as the spiny anteater, is named after the monster of Greek myth, meaning ‘she viper’. Echidnas are covered in coarse hair and spines, and have elongate and slender snouts. With their short and strong limbs and large claws, they are powerful diggers (Griffiths 1989). Echidnas have a low body temperature, which is around 7°C below the usual range of placental mammas, a low metabolic rate, and are able to reduce their energy output by torpor and hibernation (Schmidt-Nielsen et al. 1966, Nicol and Andersen 2007). During the rainy season, it is inactive and shelters under shrubs and trees (Griffiths 1989).

The short-beaked echidna is the most widely distributed extant monotreme, and can be found both in Australia and southwestern New Guinea, where it occupies a diverse range of habitats from the coast to the highlands (Griffiths 1989, Nicol and Andersen 2006, Nicol and Andersen 2007). It has an adult body mass of about 3-4 kg and with a documented lifespan of approximately 50 years, which is 3.7 times that predicted from its body mass, *Tachyglossus* is exceptionally long-living (Hulbert et al. 2008). It feeds on insects, in particular termites and ants, which it catches with its distinctive snout and specialized tongue (Griffiths and Simpson 1966, Griffiths 1989). Although not threatened by extinction, the populations of short-beaked echidnas have been reduced due to hunting, habitat destruction, and exposure to invasive predatory species and diseases.

The short-beaked echidna, *Tachyglossus aculeatus*, is nocturnal or crepuscular, depending on the temperature of its surroundings (Fig. 3) (Boisvert and Grisham 1988). The echidnan retina displays several features which are thought to result from adapting to dim-light vision, such as a circular pupil as well as the lack of oil droplets and a nictating membrane (Gresser and Noback 1935, Walls 1942, Young and Pettigrew 1991, Rowe 2000). The echidna has long been thougt to possess a pure rod retina (Bolk et al. 1934, O’Day 1952). However, Young and Pettigrew (1991) identified the presence of twin cones, which constitute 10-15% of the photoreceptors in the retina and have all the ultrastructural characteristics of the cones of placental mammals. The distribution of these cones is similar to that of cones in the retina of the nocturnal cat and their density is higher than that seen in some nocturnal primates and in the nocturnal rabbit (Young and Pettigrew 1991).

Figure 3. A short-beaked echidna, *Tachyglossus aculeatus*, in Australia (Photo: Jasmina Hugi).

1.3. Rhodopsin, a vertebrate visual pigment

1.3.1. The visual signaling cascade

Visual pigments, also called opsins, form the first crucial step in the visual transduction cascade (Yau 1994, Blumer 2004). In tetrapods, there are up to five different visual pigments, located within the rods and cones in the retina of the eye (Bowmaker and Hunt 2006). Cone opsins mediate colour (photopic) vision and include short-wavelength opsins (SWS) 1 and 2, a middle-wavelength pigment (MWS or Rh2), and a long-wavelength opsin (LWS) (Bowmaker and Hunt 2006, Yokoyama 2008, Wald 1968). Rhodopsin (Rh1) is the only visual pigment responsible for vision at night and/or dim-light (scotopic vision) (Menon et al. 2001, Yokoyama 2008). At intermediate light levels (mesopic vision), both rods and cones contribute to vision (Peichl 2005).

All opsins absorb light at different characteristic wavelengths, ranging from UV at about 350 nm to far red at about 630 nm (Fig. 4) (Yokoyama 2008). Coulour discrimination depends on

the presence of two or more types of cone photoreceptors containing opsins that show absorption maxima in different regions of the visible spectrum (Fig. 4) (Szél et al. 1996).
It has been suggested that rods have evolved from cones, with the M/LWS opsin class evolving first, followed by SWS1, SWS2, and finally the Rh class (Okano et al. 1992, Carleton et al. 2005).

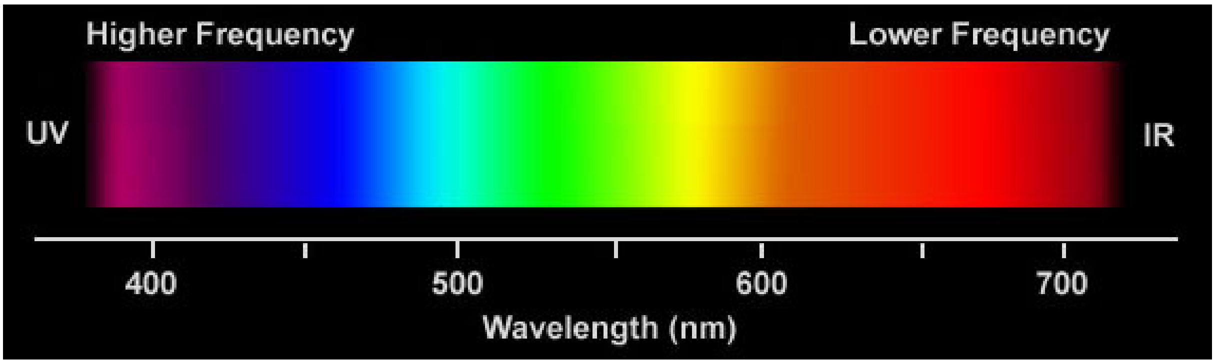

Figure 4. Wavelength diagram. SWS 1 absorbs light at 355-440 nm, SWS2 at 410-490 nm, MWS at 480-535 nm, LWS at 490-570 nm, and Rhodopsin at about 500 nm. http://www.energymedc.com/images/light spectrum.jpg.

Visual pigments are composed of a protein moiety (opsin), which is a member of the G-protein-coupled receptor family, and a light absorbing chromophore, namely 11-*cis* retinal, which is a derivative of vitamin A (Wald 1968, Sugawara et al. 2010); though some fish, reptiles, and aquatic mammals use a derivative of A_2 (Menon et al. 2001). 11-*cis* retinal, which is covalently linked to the opsin via a protonated Schiff base at a highly conserved residue Lys^{296} in transmembrane helix 7, absorbs a single photon (Fig. 5) (Baylor et al. 1979, Heck et al. 2003, Park et al. 2008).

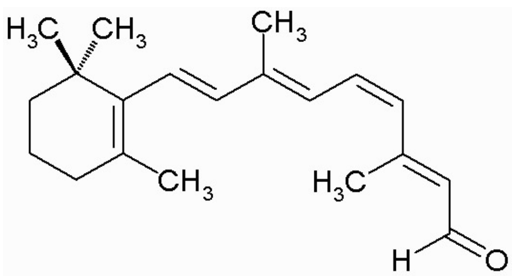

Figure 5. Structural formula of 11-*cis* retinal. http://de.academic.ru/pictures/dewiki/114/retinalcisandtrans.png.

Photon absorption causes an isomerization from 11-*cis* to all-*trans* retinal and, further, to a conformational change of the protein moiety. This results in the dissociation of all-*trans* retinal from the opsin (Palczewski et al. 2000). The active rhodopsin, also called meta II state, activates transducin, a cytoplasmic membrane G-protein, by loading it with guanosine triphosphate (GTP), which in turn causes phosphodiesterase (PDE) to increase its activity, thereby lowering the concentration of cyclic guanosine monophphate (cGMP), an intracellular second-messenger molecule (Blumer 2004, Imai et al. 2005). A decrease in cGMP concentration leads to the closure of cGMP-regulated Na^+ and Ca^{2+} ion-specific channels in the outer cell membrane and, further, to a hyperpolarized membrane potential (Blumer 2004). This light-induced hyperpolarization of the cell membrane influences second-order visual neurons by modulating the rate of neurotransmitter (glutamate) release from the synaptic terminal of the photoreceptor (Yau 1994). This chain of signaling events is also called "the vertebrate phototransduction cascade" (Fig. 6) (Blumer 2004).

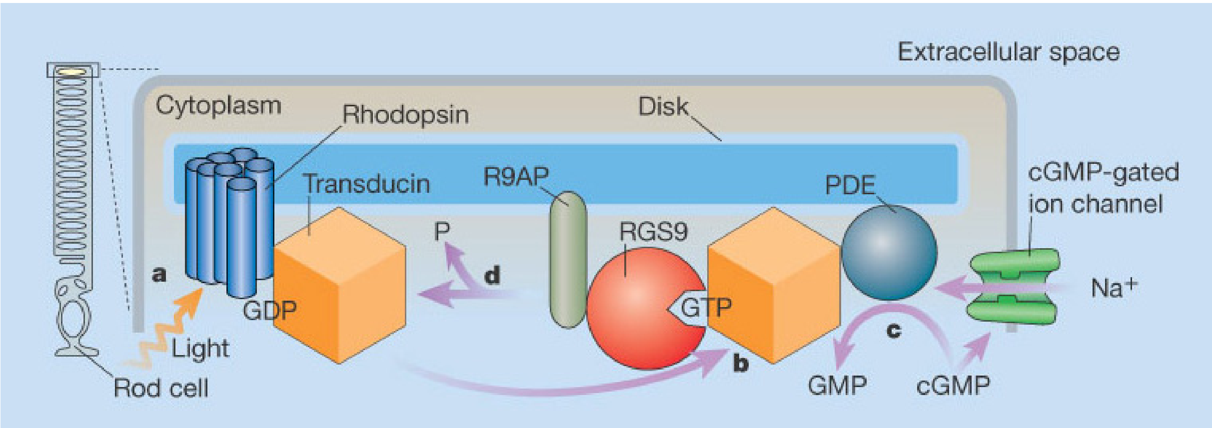

Figure 6. The phototransduction cascade in the vertebrate eye (Blumer 2004).

One photoexcited rhodopsin molecule activates hundreds of transducin copies (Sagoo and Lagnado 1997, Menon et al. 2001). Thus, the amplitude of the photoreceptor response is dependent on how efficiently the phototransduction cascade is activated by the visual pigment (Sakurai et al. 2007).

Turn-off of photoreceptor cells is accomplished by a protein called RGS9 (regulator of G-protein signaling 9), which accelerates the transducin’s ability to hydrolyse GTP, which is the rate-limiting step in the photoresponse (Sagoo and Lagnado 1997, Blumer 2004).

Eventually, rhodopsin is restored by recombining enzymatically produced 11-*cis* retinal from isomerized all-*trans* retinal in the dark, which is delivered from adjacent retinal epithelial cells (Palczewski et al. 2000, Heck et al. 2003).

1.3.2. Rhodopsin, a G protein-coupled receptor

Rhodopsin is the visual pigment mediating vision at night and/or dim-light (Menon et al. 2001, Yokoyama 2008). It consists of five exons and four introns. Its protein-coding sequence is composed of approximately 1044 nucleotides, hence, 348 amino acids (Fig. 7) (Palczewski et al. 2000). There are seven transmembrane helices (TM), which are embedded in the membrane and encompass 194 amino acids in total (Fig. 7) (Menon et al. 2001, Sakmar et al. 2002).

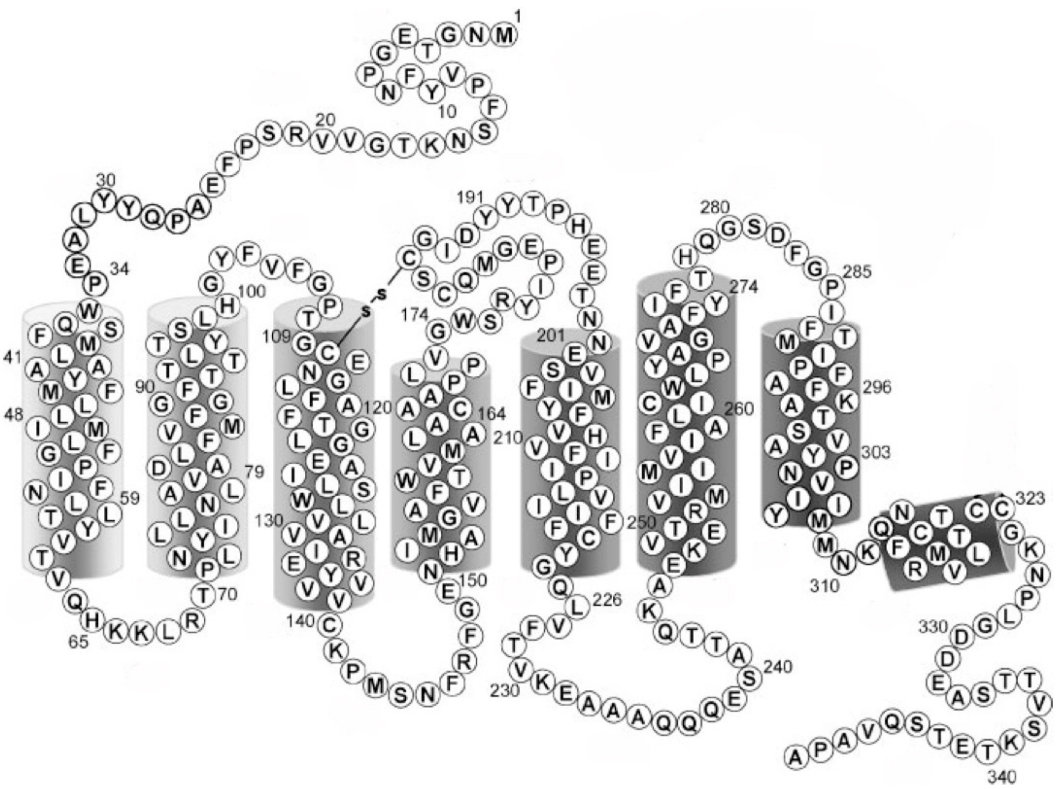

Figure 7. Secondary structure of bovine rhodopsin (Sakmar et al. 2002).

Packed in the crystal lattice to form an array of helical tubes, the extracellular surface domain comprises an amino-terminal tail and three interhelical loops; the cytoplasmic domain comprises a carboxyl-terminal tail and three cytoplasmic loops (Fig. 7) (Palczewski et al. 2000, Sakmar et al. 2002).

Rhodopsin is temperature-sensitive (McKibbin et al. 2007). With an isoelectric point at pH 5.43, rhodopsin is an acidic protein; it has more glutamic and aspartic acid than basic lysine and arginine residues (Radding and Wald 1956, Kito et al. 1968).

It is ascertained that the chromophore is covalently bound to the opsin at the highly conserved Lys^{296} (Heck et al. 2007, Park et al. 2008), but which residues participate in holding the 11-*cis* retinal inside the binding pocket before photoisomerization is still debated (Schädel et al. 2003, Park et al. 2008, Hildebrand et al. 2009).

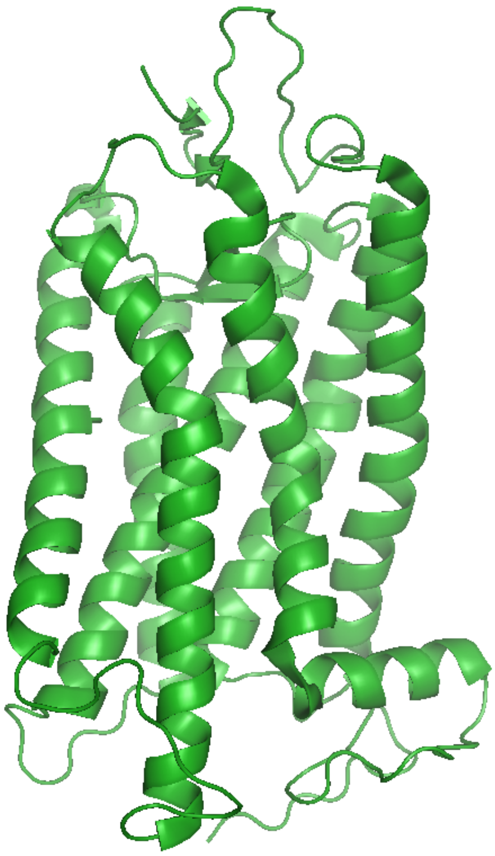

Figure 8. Three-dimensional structure of bovine rhodopsin. Downloaded from RCSB Protein Data Bank (www.pdb.org, ID: 1u19) and visualized in PyMOL (www.pymol.org - The PyMOL Molecular Graphics System, Version 1.3, Schrödinger, LLC.).

To date, the bovine rhodopsin is the best studied of all visual pigments (Fig. 8) (Menon et al. 2001, Sakmar et al. 2002, Palczewski 2006). However, not only rod opsin sequence data but also biochemical and functional properties have now been analyzed in a variety of vertebrate taxa, including fish, amphibians, reptiles, and mammals (Wald and Brown 1958, Nathans and Hogness 1983, Nathans and Hogness 1984, Kawamura and Yokoyama 1998, Sakmar et al. 2002, Imai et al. 2005, Imai et al. 2007). Surprisingly, although they are the last survivors of the most basal clade of extant mammals, not much is known about the visual capacities of monotremes. So far only the rod opsin gene sequence and absorption maximum as well as single exons of two cone opsins, i.e. SWS2 and LWS, of the platypus have been published (Davies et al. 2007). Another study on the visual pigments of both platypus and echidna only addresses cone pigments (Wakefield et al. 2008). Thus, for a more reliable taxon sampling, incorporating the echidna rod opsin in this study was elementary. Furthermore, by studying the rhodopsin of the short-beaked echidna and its biochemical and functional properties in detail, this thesis also encompasses the first characterisation of a rhodopsin from a nocturnal animal, pinpointing differences to that of a diurnal animal; in this case the bovine rhodopsin.

1.4. Ancestral sequence reconstruction and selective constraint analyses

1.4.1. Resurrecting ancient genes

Ancestral sequence reconstruction (ASR) is nowadays widely used to test hypotheses about the functional evolution of ancient genes, to provide a glimpse into their evolutionary history, and, most importantly, to get a better understanding of the paleobiology of ancient organisms that presumably possessed these genes and proteins (Chang et al. 2002a, Thornton 2004, Chang et al. 2007).

In 1963, Pauling and Zuckerkandl were the first to introduce the idea of resurrecting ancient genes, after studying amino acid sequences of vertebrate hemoglobulin chains. Then in 1971, Fitch was the first to develop an algorithm to reconstruct ancestral character states, using the parsimony principle and, thus, also taking phylogeny into account. It was not until the 1980s that this algorithm was incorporated in computer programs such as PAUP (Swofford 1985), and that the first study using this method to infer ancestral sequences was published (Baba et al. 1984). Due to concurrent improvements in DNA synthesis, in 1990, Stackhouse et al. were the first to successfully resurrect a functional ancestral gene that had been inferred by parsimony. Since parsimony has some intrinsic limitations (Thornton 2004), it was a significant step in ancestral sequence reconstruction methods when Yang et al. developed PAML in 1995, a program which uses a maximum likelihood algorithm to infer ancestral sequences (Koshi and Goldstein 1996), thus allowing further knowledge about the process of molecular evolution to be included (Thornton 2004). Since then, resurrecting ancient proteins has become an increasingly popular tool for addressing evolutionary questions as it provides a great opportunity to study the mechanisms of functional change during evolution at a molecular level (Fig. 9) (Chang and Donoghue 2000, Chang et al. 2002a, Gaucher et al. 2003, Shi and Yokoyama 2003). Though it has its limitations, e.g. its hypothetical nature, the dubious accuracy of selecting the right algorithm to fit the data, as well as the limited interpretations based on recreating single molecules, ASR can provide data where paleontologists and the fossil record reach their limits (Chang et al. 2002a, Chang et al. 2007).

Ancestral sequences are usually inferred using a maximum likelihood phylogenetic algorithm, an alignment of extant sequences, a specific phylogeny, and a probabilistic model of sequence evolution. For each internal node in the phylogeny as well as each site in the sequence, an ancestral state with the highest likelihood is calculated. The confidence in any inferred ancestral state is described as its posterior probability, which is defined as the likelihood of the state divided by the sum of the prior-weighted likelihoods for all states. One uncertainty in the maximum likelihood approach is the assumption that the alignment, tree, model, and model parameters are a priori known to be correct. Another method, the Bayesian approaches addresses these sources of uncertainty by estimating likelihoods over several possible trees or parameter values, each weighted by its posterior probability (Smith et al. 2010). However, it has recently been suggested that maximum likelihood estimates are as reliable as Bayesian methods (Smith et al. 2010).

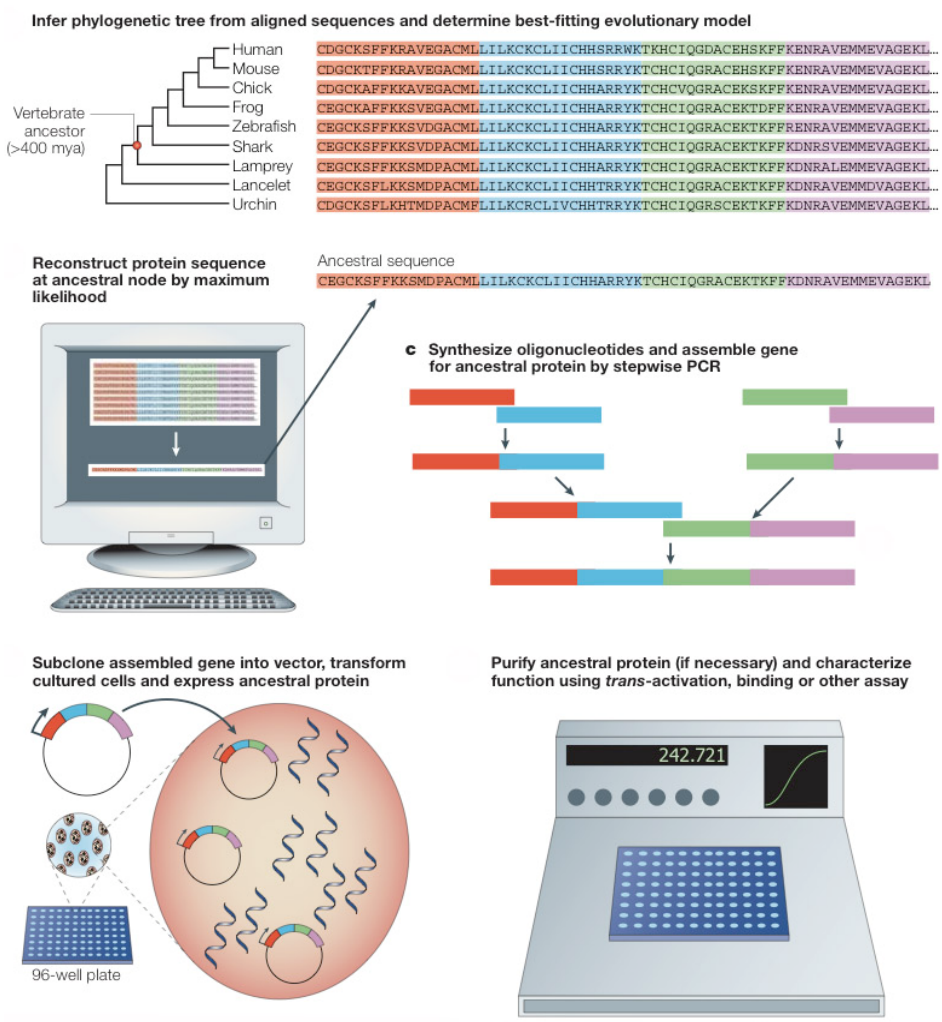

Figure 9. The ancestral gene resurrection strategy (Thornton 2004).

Ancestral sequence reconstruction methods allow researchers to address fascinating evolutionary questions and peer deep into the past. For example, Gaucher et al. (2003) were able to infer information about the lifestyle of Precambrian organisms. In order to understand in what environment the earliest life forms evolved, they investigated EF-Tu, a GDP-binding elongation factor which regulates the rate of protein synthesis and which is highly temperature-sensitive, in the common ancestor of all bacteria (Gaucher et al. 2003). Measuring the thermostability and GDP-binding affinity of *E.coli* bacteria containing resurrected EF-Tu genes indicate that bacterial ancestors had EF-Tus with an optimal GDP-binding temperature of 65°C, suggesting that bacteria originated in a thermophilic environment (Gaucher et al. 2003). Chang et al. (2002a) investigated the visual capacities of ancestral archosaurs living in the early Triassic, approximately 240 million years ago. Their data suggests that inferred ancestral archosaur rod opsins had been functional for vision at night and/or in dim-light (Chang et al. 2002a). Another study focused on steroid hormone receptors that evolved before the origin of Bilateria (Thornton et al. 2003). They found that these receptors were lost in invertebrates (Thornton et al. 2003). In chordates, they had experienced an increase in affinity for steroids after having first evolved oestrogen receptor-like functions (Thornton et al. 2003).

Since the vertebrate visual system is so adaptive, ancestral sequence reconstruction is a great tool for investigating rhodopsin, the visual pigment mediating scotopic vision, which then allows for fathoming visual capacities and life habits of early mammals. Hence, this approach was used to infer hypothetical ancestral mammalian rhodopsins, among others.

1.4.2. *In vitro* expression systems in vision research

The visual system is one of the five senses that provide input for perception. This highly specialized and adaptive system is triggered by a large range of different light levels. It is instrumental in the survival of an animal, and changes can have profound consequences for the organism it inhabits.

In order to understand this crucial system and the proteins involved better, the evolutionary history of the different opsins involved in the visual signaling cascade and the differences they exhibit have been subject to various studies (Okano et al. 1992, Bowmaker and Hunt 2006); permitted by major improvements in *in vitro* expression systems in recent years. *In vitro* expression systems allow not only for studying molecular properties of visual pigments but also for synthesising hypothetical ancestral opsins (Oprian et al. 1987, Chang et al. 2002a, Sakmar et al. 2002, Chang 2003, Parry et al. 2005).

Furthermore, various biochemical assays have now been developed in order to characterise visual pigments and to identify differences between rod and cone opsins, including hydroxylamine stability, meta II decay and retinal regeneration, transducin activation, as well as acid bleaching (Kito et al. 1968, Shichida et al. 1994, Starace and Knox 1998, Imai et al. 2005, Imai et al. 2007, Sakurai et al. 2007).

Simultaneously, site-directed mutagenesis experiments have become a popular approach in vision research as they allow for the identification of key sites that are potentially responsible for changes in the different types of visual pigments (Sakmar et al.1989, Imai et al. 1997, Carvalho et al. 2006). Altering a specific amino acid can test if this exact amino acid has a significant impact on a protein's function, eventually leading to a far-reaching adaptation and possibly to the origination of a newly adapted protein (Chang et al. 2007).

Thus, to date, much is known about biochemical and functional differences between cone and rod pigments, but detailed studies characterising and comparing differences in the rhodopsin of a nocturnal animal to that of a diurnal one are lacking. This thesis in part comprises the in vitro expression and the first detailed characterisation of a rod opsin from a nocturnal animal, the short-beaked echidna, potentially allowing the biochemical and functional properties of inferred and synthesised ancestral pigments to a nocturnal or a diurnal lifestyle to be determined.

1.4.3. Selective constraint analyses

In addition to ancestral gene reconstruction, the identification of selective constraint acting on genes of interest, has become a more popular approach in molecular evolutionary research in recent years (Yang and Bielawski 2000, Tan et al. 2005, Zhao et al. 2009a).

If mutations do not code for another amino acid, as is often the case if they occur in the third codon position, they are called synonymous (silent) substitutions (Page and Holmes 2006). Whereas those that lead to the translation of a different amino acid are referred to as non-synonymous (replacement) substitutions (Page and Holmes 2006).

In a highly adaptive system, adaptive changes, which can be a result of an accelerated rate of non-sysnonymous substitutions (d_N) over synonymous substitutions (d_S), can be traced using selective constraint analysis. The strength of selection acting on protein-coding genes is assessed by estimating ω, which is the ratio of non-synonymous (d_N) to synonymous (d_S)

substitutions (Yang 2002). Positive selection is identified whenever $\omega = d_N/d_S > 1$ (Yang 2002, Pie 2006). For if $\omega = 1$ and $\omega < 1$ this would indicate neutral and purifying selection, respectively (Yang 2002, Pie 2006). Detected positive selection is a clear signal of adaptive evolution driven by selection (Yang 2002).

Selective constraint methods are now widely used. For example, Bakewell et al. (2007) investigated the degree of positive selection in human and chimpanzee genes and found more genes undergoing positive selection in chimp than in humans since their split; a finding which is in sharp contrast to the common belief that humans experienced more phenotypic adaptations than chimpanzees. Metzger and Thomas (2010) studied other G-protein coupled receptors, the CC chemokine receptor proteins, and found evidence for positive selection acting on residues in extracellular domains rather than in intracellular domains, which might be due to ligand-binding and pathogen interactions in the extracellular domains. Although selective constraint analyses provide a glimpse into the evolution of protein-coding genes, one must be aware that these analyses need to be carried out with care. For example, Tan et al. (2005) investigated the selective constraint acting on several opsins in primates and concluded that nocturnality could not have been the ancestral state. However, they did not take all exons of the short-, middle-, and long-wavelength opsins into account, and thus, disregarded important information (Tan et al. 2005).

With the visual system being a highly adaptive system, this method is nowadays often used in vision research, addressing not only paleobiological questions concerning e.g. vision capacities in ancestral primates and bats, but also ecological diversification in fish due to adaptations in their visual pigments (Sugawara et al. 2002, Spady et al. 2005, Tan et al. 2005, Zhao et al. 2009a, Shen et al. 2010).

Thus, this approach was used in this thesis to investigate the vertebrate rhodopsin and its single amino acids were inferred for mammalian and other branches, in order to make inferences of if and how the visual pigment responsible for dark and dim-light had experienced significant modifications in early mammals presumably due to changes in life habits.

1.5. Objectives of this thesis

This thesis represents the first study that investigates whether the first mammals had indeed been nocturnal, as indicated by the fossil record, by means of molecular evolution. Its focus lies on rhodopsin, the one visual pigment which is responsible for vision at night and/or dim-light.

1) The rhodopsin of the short-beaked echidna was expressed *in vitro* and investigated in detail. The echidna was interesting because, on the one hand, it represents one of the two last survivors of monotremes, the most basal mammals. On the other hand, it is a nocturnal animal and, so far, a detailed characterisation of a rhodopsin of a nocturnal animal is lacking.

2) Hypothetical ancestral rhodopsin amino acid sequences for the nodes Amniota, Mammalia, and Theria were inferred by maximum likelihood estimates and the proteins were expressed *in vitro*. Their biochemical and functional properties were examined and compared to rhodopsins of a nocturnal and a diurnal animal, i.e. echinda and bovine, respectively.

3) Selective constraint analyses were carried out in order to evaluate if the rhodopsin had experienced any dramatic changes in its function in tetrapods and along the branch leading to Mammalia in particular.

2. Material and methods

2.1. In the molecular lab

2.1.1. Genomic DNA isolation

Blood samples of a female short-beaked echidna ("Annie"), *Tachyglossus aculeatus*, were obtained from the Toronto Zoo, and stored 1:2 in Lysis buffer (Shaw et al. 2003). Genomic DNA was extracted using a DNeasy Blood and Tissue Kit (Quiagen, Cat No.69504). Because the blood sample was very viscous, it was further diluted 1:4 in AL buffer, which comes with the kit. Contrary to the instructions in the manual, 200 µl blood was adjusted with 80 µl PBS and 120 µl AL buffer. The rest of the procedure was carried out according to the manual instructions. All three elutions were visualized on a 1% agarose gel and elution 1, which showed the clearest band, was used for further procedures (Fig. 10).

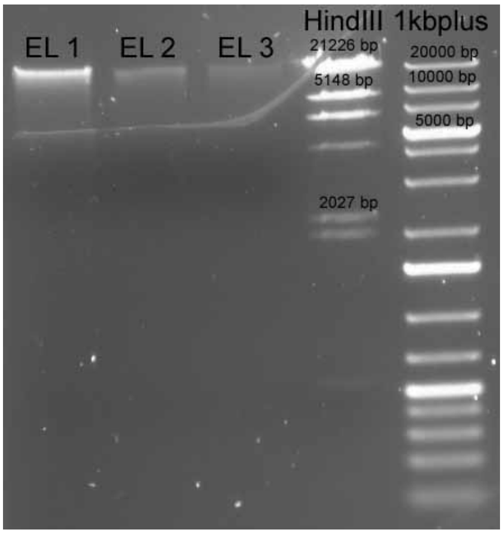

Figure 10. 1% agarose gel showing all three elutions and two DNA ladders.

2.1.2. Genome-walking PCR

Elution 1 was used to establish a genome walker library using a Universal GenomeWalker™ Kit (Clontech, Cat. No.K1807-1) (Fig. 11). In short, four genomic libraries with a size of around 4000 base pairs were created by blunt-end digestion with the four restriction enzymes *Eco* R, *Dra* I, *Pvu* II, and *Ssp* I (Fig. 11). Restriction digests were phenol-chloroform purified and ligated to GenomeWalker Adaptors using T4 DNA Ligase (Fermentas, Cat. No.EL0011) (Fig. 11).

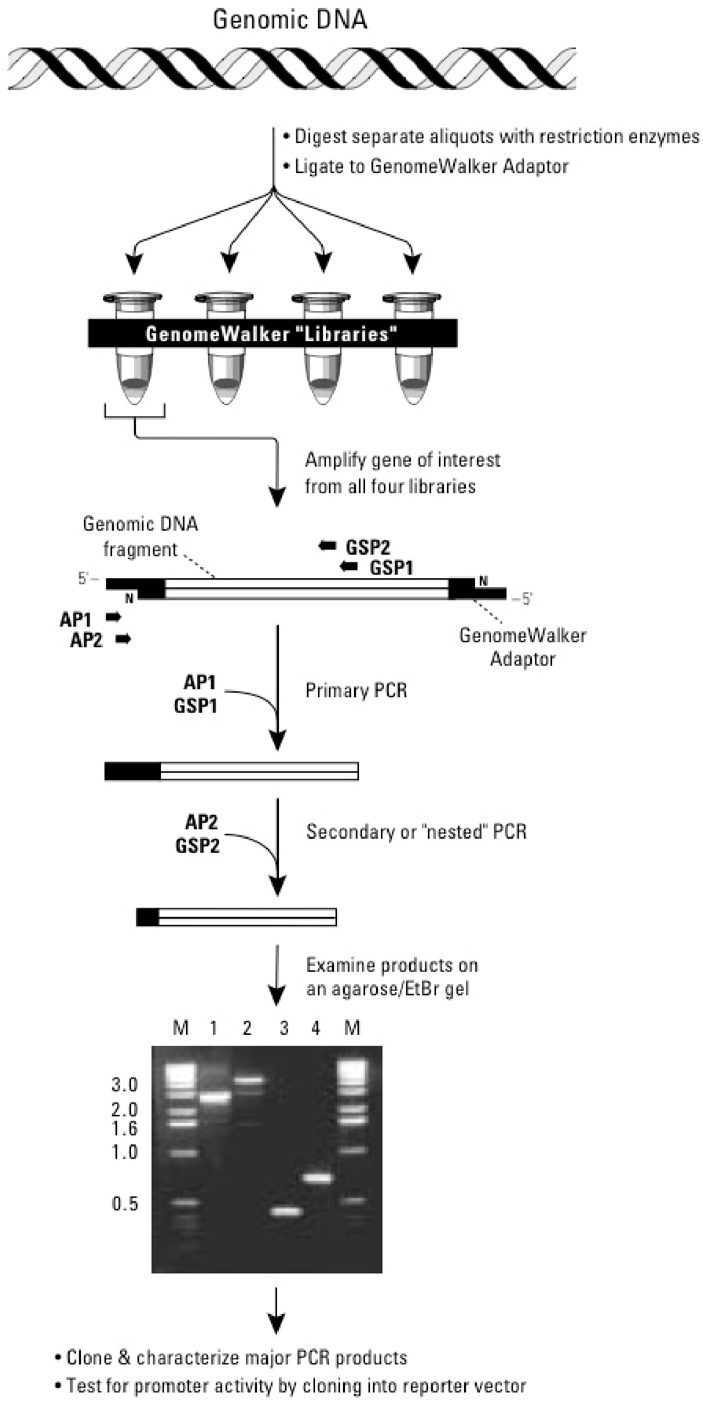

Figure 11. Establishing a genome walker library (Universal GenomeWalker™ Kit User Manual, 2000).

First round hot-start PCR was carried out using 1 µl of each genomic library as follows: an initial 1 min denaturation at 95°C followed by 7 cycles of denaturation at 94°C for 25 sec and primer annealing at 72°C for 3 min; another 32 cycles of denaturation at 94°C for 25 sec and primer annealing at 67°C for 3 min; product extension was at 67°C for 7 min. PCR products were generated using the adaptor primers (AP1 and AP2) from the GenomeWalker kit, as well as degenerate PCR primers 1, 2, and 3 obtained from Davies et al. (2007) and self-designed degenerate primers (Tab. 1).

Table 1. Self-designed degenerate primers used in first round hot-start PCR.

Sequence name	Sequence 5' to 3'
gw_91F	TAC CTG GCA GAG CCA TGG CAG TAC TCG GTC
gw_182F	ACG TCA CCA TCC AGC ACA AGA AMINO ACIDC TCC GCA
gw_121R	GAC CGA GTA CTG CCA TGG CTC TGC CAG GTA
gw_212R	TGC GGA GTT TCT TGT GCT GGA TGG TGA CGT

PCR products were visualized on a 1% agarose gel, fragments of interest were cut out and ligated into the pJet1.2 vector following the "sticky-end ligation" protocol from the CloneJet PCR Cloning Kit (Fermentas, Cat. No.1231). Each construct was then transformed into α-Select Silver Competent Cells (Bioline, Cat. No.85025). Cell transformation mixture was spread onto LB agar plates containing ampicillin. Three clones each were screened with a screening PCR using EconoTaq DNA Polymerase (Lucigen, Cat. No.30031-1) under following conditions: an initial denaturation of 95°C for 3 min, 30 cycles of 94°C for 1 min, 54°C for 1 min, 72°C for 1 min, and 72°C for 7 min. PCR products were visualized on a 1% agarose gel, and PCR products that had the correct band size were sequenced on a 3130XL Genetic Analyzer (Applied Biosystems) using standard T7 and pIRES primers.

2.1.3. Gene synthesis and site-directed mutagenesis

Gene synthesis can be assessed via PCR of several fragments (Chang et al. 2007). In this study, rhodopsin protein-coding sequences of the echidna and three inferred ancestral pigments were synthesised by Geneart AG, Regensburg, Germany (www.geneart.com). In order to account for different codon usage biases (i.e. preferential use of certain DNA codons over others that code for the same amino acid) in different monophyletic groups (Sharp et al. 1988), the three hypothetical gene sequences were optimized for expression in mammalian cells. Since the echidna rhodopsin gene came from a living animal, it was not modified.

Using the echidna construct as template, coding sequences of echidna mutants at sites 158 and 169 were generated by site-directed mutagenesis according to the Quick-change method (www.stratagene.com). Sites 158 and 169 were chosen to be mutated because they are both unique to the echidna (Tab. 4) and located at interesting sites within the 3D structure of rhodopsin (Borhan et al. 2000) (Fig. 8). These sites were mutated to the condition in bovine, i.e. T158A and F169A.

For creating these mutants, a PCR was performed using a Pfu Polymerase (Fermentas, Cat. No.EP0501) and specific primers (Tab. 2) under following conditions: an initial denaturation of 95°C for 1 min; 13 cycles of 95°C for 30 s, 55°C for 1 min, 68°C for 4 min; before a final extension of 37°C for 60 min, 1 µl of DpnI was added to each reaction in order to destroy methylated, nascent DNA derived from *E.coli*.

Table 2. Primers used in site-directed mutagenesis PCR in order to create echidna mutants T158A and F169A.

Sequence name	Sequence 5' to 3'
EcRho_T158A_s	CAT GCC ATC ATG GGT GTG GCC TTC ACT TGG ATC ATG GCC
EcRho_T158A_as	GGC CAT GAT CCA AGT GAA GGC CAC ACC CAT GAT GGC ATG
EcRho_F169A_s	CCC TGG CCT GTG CCG CGC CCC CAC TCG TTG G
EcRho_F169A_as	CCA ACG AGT GGG GGC GCG GCA CAG GCC AGG G

2.1.4. An adequate expression vector

All constructs were delivered by Geneart AG in a custom pMA vector. After transformation into α-Select Silver Competent Cells, purifications of all four plasmid DNAs were prepared with a Plasmid Maxi Kit (Quiagen, Cat. No. 12169), according to the instructions. First, the pMA vector was digested with EcoRI and BamHI restriction enzymes and 10x buffer (Fermentas), each construct was then glycogen precipitated, and ligated into the p1D4 expression vector (Morrow and Chang 2010), thereby tagged with eight amino acids (ETSQVAPA) at the carboxy terminus to allow for later purification of expressed proteins from HEK293 cells (Oprian et al. 1991). These amino acids correspond exactly to the carboxy terminus of bovine rhodopsin and are known to be the epitope for the monoclonal antibody rho 1D4 (Molday and MacKenzie 1983, MacKenzie et al. 1984). These constructs were again transformed, screened, sequenced, stored in 30% glycerol at -80°C, and finally purified according to the Plasmid Maxi kit instructions.

2.1.5. Protein expression

In order to express the various rod visual pigments, HEK293 cells were transfected with 8 µg/plate Lipofectamine 2000 (Invitrogen, Cat No.11668-019) and 24.8 µg/plate DNA. After 48 hours, cells were harvested according to a modified protocol from Starace and Knox (1998) with 1x PBS (Sigma-Aldrich) and 10 µg/ml aprotinin and leupeptin, incubated with 4 µM 11-*cis* retinal (R.K. Crouch, Medical University of South Carolina and the National Eye Institute, National Institutes of Health, USA) in the dark for 2-3 hrs at 4°C, and solubilized for 3-4 hours at 4°C in 50 mM Tris (pH 6.8), 100mM MaCl, 1mM $CaCl_2$, 0.1 mM PMSF (all

Sigma-Aldrich), and 1% DM (Anatrace). After immunoaffinity purification following a modified protocol from Chang et al. (2002a) using the 1D4 monoclonal antibody, the extracted pigments were washed several times with 50 mM Tris (pH 6.8), 0.1% DM, 100mM NaCl, and 50 mM NaPhos (pH 6.5), finally eluted by elution buffer (0.1% DM, 50 mM NaPhos (pH 6.5), and 0.18 mg/ml 1D4 peptide (University of British Columbia, Canada)) for 2-3 hours, and subjected to spectrophotometry.

2.1.6. Western blot

In order to confirm that the correct protein had indeed been expressed, the first step was to separate the protein in the extract of the host cell tissue by PAGE (Wong 2006). The resolved protein bands in the gel were then transferred to a membrane by a technique called western blot, and subjected to immunological detection (Wong 2006).

Harvested protein lysates were resolved on a SDS-polyacrylamide gel (BioRad, Cat. No.161-1100EDU) at 20 mA for around 1 hr. Proteins were electroblotted onto a polyvinylidene fluoride (PVDF) membrane (Pal Corporation) at 50 V for 1 hr. Membranes were blocked in 1% TBS, 0.05% Tween, and 3% dry milk (all Sigma-Aldrich), and were washed in 1% TBS and 0.05% Tween. Afterwards, they were incubated with 0.2 μg/ml mouse 1D4 monoclonal antibody (GE Healthcare, Cat No.NA931) in 1% TBS, 0.05% Tween, and 3% dry milk for 2 hrs. After washing, they were incubated with 0.2 μg/ml sheep anti-mouse antibody linked to horseradish peroxidase (GE Healthcare, Cat No.NA931) for 1 hr. After final washes, membranes were developed using an ECL Plus Western Blotting Detection System (GE Healthcare, Cat No.RPN2132).

2.1.7. Spectrophotometry

The characteristic wavelength at which a visual pigment absorbs light (λ_{max}) is regulated by opsin-chromophore interactions (Sakmar et al. 1989).

A spectrophotometer is used to measure not only the amount of light that a sample absorbs but also at what characteristic wavelength. The instrument operates by passing a beam of light through a sample and measuring the intensity of light reaching a detector.

Here, all absorption spectra, including the ones during hydroxylamine and acid assays, were taken with a Cary4000 Spectrophotometer (Varian Inc.) at 25°C, using a temperature control. Spectra were recorded continuously between 560 nm-250 nm, with a scan rate of 400 nm/min, average time 0.1 sec, data interval of 0.667 nm, integration time 0.12 sec, and slit width 2 nm. Pigments were photoexcited with light from a fiber optic lamp for 60 sec. Dark spectra were curve fitted following Govardovskii's method (Govardovskii et al. 2000).

Meta II decay assays were carried out on a CaryEclipse Fluorescence Spectrophotometer (Varian Inc.), with excitation at 295 nm and emission at 330 nm. Excitation slit width was 1.5 nm and emission slit width 10 nm. Data was collected every 30 sec, with an average time of 2 sec.

2.1.8. Functional assays: acid bleach, hydroxylamine sensitivity, and meta II decay rate

Nowadays, various functional and biochemical assays have been developed in order to characterise the different types of visual pigments and to elucidate differences between rod and cone opsins (Kito et al. 1968, Shichida et al. 1994, Starace and Knox 1998, Imai et al. 2005, Imai et al. 2007, Sakurai et al. 2007).

In this study, three assays characterising each expressed rhodopsin were performed.

For the first functional assay, the acid bleach, successfully expressed pigments were treated with freshly prepared hydrochloric acid (HCl) such that they were at a final concentration of 2 M in 130 µl sample. Samples were kept in the dark, and the temperature was maintained at 25ºC. After the addition of HCl, absorption spectra were taken every 2-5 minutes.

If pigments react to hydrochloric acid, the Schiff base linkage between opsin and 11-*cis* retinal will break off and the absorption peak will shift to reach a plateau at 440 nm, which is the characteristic λ_{max} of a protonated Schiff base 11-*cis* retinal free in solution (Kito et al. 1968).

In addition, the molar extinction coefficient of a visual pigment can be estimated using this method. The molar extinction coefficient is a measurement of how strongly a substance absorbs light at a given wavelength. It can be determined by the Lambert-Beer law

$$A = \varepsilon * c * l \text{ (in } M^{-1} cm^{-1}\text{)}$$

with A being the actual absorbance, ε the extinction coefficient, c the concentration, and l the path length. Based on the molar extinction coefficient, the concentration of a protein in solution can also be estimated.

The molar extinction coefficient of 11-cis retinal bound to a denatured opsin is known to be 30 800 M^{-1} cm^{-1} (Starace and Knox 1998). Following the formula

$$\varepsilon = \varepsilon_{ret} * (\text{Abs } \lambda_{max} / \text{Abs } \lambda_{440\text{ nm}})$$

extinction coefficients for all expressed rhodopsins were determined.

Second, hydroxylamine assays were performed. Hydroxylamine (NH_2OH) is a chemical compound that is remarkably close in structure to ammonia and differs only by an additional hydroxyl, which gives it basic properties (Fig. 12). It competes with the 11-*cis* retinal for rhodopsin at the Schiff base linkage at Lys^{296} (Kawamura and Yokoyama 1998). If it enters the chromophore binding pocket, it forms a retinal oxime with 11-*cis* retinal, thereby relinquishing the rhodopsin, i.e. the apoprotein (Kawamura and Yokoyama 1998). This oxime absorbs light at 363 nm (Kawamura and Yokoyama 1998).
Testing the sensitivity to hydroxylamine has been used in previous studies to distinguish rod opsins from cone opsins, since this reaction is substantially faster in cone opsins (Wald et al. 1955, Fager and Fager 1981, Okano et al. 1989, Wang et al. 1992, Starace and Knox 1998).

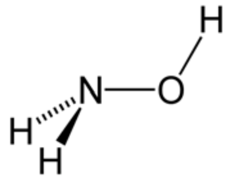

Figure 12. Structural formula of hydroxylamine. http://de.academic.ru/pictures/dewiki/72/Hydroxylamine-2D.png.

Freshly prepared hydroxylamine in PBS was added to samples with a concentration around 0.007-0.01 µM such that the final concentration of hydroxylamine was 1 M in 130 µl sample. Samples were kept in the dark, and the temperature was maintained at 25ºC. After the addition of hydroxylamine, absorption spectra were recorded every 2-3 minutes for the first 30 min and then every 30 min for another 90 min. At the end of the experiment, the rhodopsin was exposed to light.
Curves were fitted in SigmaPlot 11 using the nonlinear regression

$$f = y_0 + a\,(1 - e^{-bx})$$

which is a first order 'Exponential Rise to Maximum' equation with 3 parameters.

Third, meta II decay rate analyses were carried out. After photoisomerization of 11-*cis* retinal, rhodopsin passes through a series of photoproducts, which show different characteristic absorption maxima (Fig. 13) (Weitz and Nathans 1993, Imai et al. 2005, Kuwayama et al. 2005, Palczewski 2006, Sugawara et al. 2010).

Meta II is the key state for catalyzing the transducin GDP-GTP exchange (Fig. 13) (Weitz and Nathans 1993, Imai et al. 2005), and one of the fastest photochemical reactions known in biology (Palczewski 2006). One single molecule of photoexcited rhodopsin activates hundreds copies of transducin (Sagoo and Lagnado 1997, Menon et al. 2001).

Meta II is the active state of rhodopsin, in which the original Schiff base is intact but deprotonated, and has its absorption peak at 380 nm (Sakmar et al. 2002, Heck et al. 2003). In its ground state of rhodopsin, there is a quenching of an intrinsic Tryptophan fluorescence in the ground state of rhodopsin (Farrens and Khorana 1995). After photoexcitation and after the chromophore leaves the binding pocket, this intrinsic Tryptophan fluorescence is not quenched anymore and a rise in absorbance at 380 nm can be detected (Fig. 13) (Farrens and Khorana 1995, Schädel et al. 2003).

Upon decay, meta II converts via meta III to opsin in the correctly folded form without all-*trans* retinal and, subsequently, binds fresh 11-*cis* retinal (Fig. 13) (Sakamoto and Khorana 1995, Heck et al. 2003, Palczewski 2006). Its decay rate is much faster in cones than in rods (Shichida et al. 1994, Sakurai et al. 2007).

Samples, which were at a concentration of around 0.007-0.01 µM, were kept in the dark, and the temperature was maintained at 25ºC. After 5 minutes, samples were bleached with a fiber optic lamp for 60 sec, and recordings were taken every 30 sec for 30-40 min. Curves were fitted in SigmaPlot 11 using the nonlinear regression

$$f = y_0 + a\,(1 - e^{-bx})$$

which is a first order 'Exponential Rise To Maximum' equation with 3 parameters.

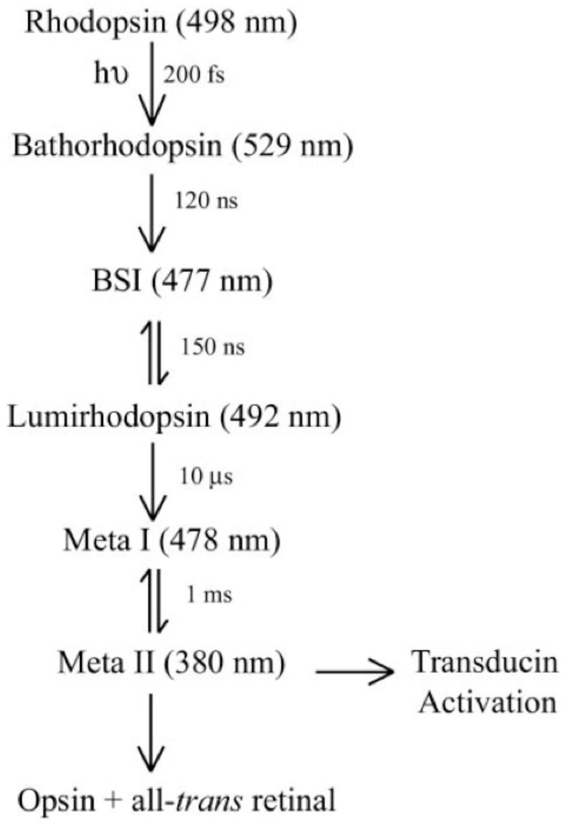

Figure 13. Reaction scheme of rhodopsin photoproducts (Yan et al. 2003).

2.2. Maximum likelihood analyses

2.2.1. PAML

Ancestral sequence reconstructions and selective constraint analyses were carried out with the program PAML 4 (Yang 2007). PAML is a package of programs that phylogenetically analyses DNA and protein sequences using maximum likelihood (Yang 2007). Its strength lies in the many sophisticated substitution models that help to understand the process of sequence evolution (Yang 2007). Maximum likelihood analyses in PAML start with an alignment of extant gene sequences, a tree describing their phylogenetic relationships, and a specified statistical model of evolution (Yang 2007, Hanson-Smith et al. 2010).

2.2.2. The dataset

The protein-coding rhodopsin sequence of the short-beaked echidna was included in an alignment together with 25 other tetrapod rhodopsin sequences downloaded from the GenBank database at NCBI (Tab. 3). The protein-coding sequence of the snake rhodopsin was kindly provided by the Chang Lab (Toronto). Sequences were aligned using MEGA 4 (Tamura et al. 2007) and checked by eye. Premature stop codons were removed from all

sequences prior to the analysis. For genomic DNA, intron-exon boundaries were identified by comparison with published cDNA sequences. All sequences show intact ORFs, suggesting the genes are functional (Table 4). Amino acid positions mentioned throughout the text are numbered according to bovine rhodopsin (Palczewski et al. 2000). A tetrapod phylogeny was established manually, based on accepted literature (Fig. 14) (Bininda-Emonds et al. 2007, Meredith et al. Murphy et al. 2007, Wible et al. 2007, Asher and Helgen 2010). Taxa were sampled from a broad range of tetrapods, with only one or two representatives from closely related species being chosen in order to maximize the divergence. The amount of 27 sequences was considered reasonable, since it has been suggested that more taxa are not necessarily better for reconstructing ancestral states (Li et al. 2008). As required by PAML 4, the tree is unrooted with coelacanth and lungfish considered as outgroups.
The data acquisition was carried out in close collaboration with Jingjing Du (Toronto).

Table 3. Accession numbers of all sequences which were downloaded from NCBI and used in this study.

Species name	Common name	NCBI accession numbers
Alligator mississippiensis	American alligator	U23802.1
Ambystoma tigrinum	Tiger salamander	U36574.1
Anolis carolinensis	Green anole	L31503.1
Bos taurus	Cattle	NM_001014890.1
Bufo bufo	European toad	U59921.1
Caluromys philander	Fat-tailed dunnart	AY159786.2
Canis lupus familiaris	Dog	NM_001008276.1
Cavia porcellus	Guinea pig	EF457995
Cricetulus griseus	Chinese hamster	X61084.1
Felis catus	Domestic cat	NM_001009242.1
Gallus gallus domesticus	Chicken	NM_001030606.1
Homo sapiens	Human	NM_000539.2
Latimeria chalumnae	Coelacanth	AF131256.1
Loxodonta africana	African elephant	AY686752.1
Macaca fascicularis	Rhesus macaque	XM_001094250.1
Neoceratodus forsteri	Australian lungfish	EF526295
Ornithorhynchus anatinus	Platypus	EF050076.1
Oryctolagus cuniculus	European rabbit	NM_001082349.1
Otolemur crassicaudata	Galago	AB112594.2
Rana temporaria	European common frog	U59920.1
Sminthopsis crassicaudata	Bare-tailed woolly opossum	AY313946.1
Sus scrofa	Wild boar	NM_214221.1
Trichechus manatus	West-Indian manatee	AF055319.1
Ursus maritimus	Polar bear	AY883926.1
Uta stansburiana	Common side-blotched lizard	DQ100323.1

Table 4. Alignment of rhodopsin amino acid sequences used in this study.

	0	1	2	3	4	5
Coelacanth	MNGTEGPNFY	VPMSNKTGVV	RNPFEYPQYY	LADPWKYSAL	AAYMFFLILV	GFPINFLTLF
Lungfish	MNGTEGPNFY	VPMTNKTGVV	RSPFEYPQYY	LADPWKYSAL	AAYMFFLILT	GFPINFLTLY
Frog	MNGTEGPNFY	IPMSNKTGVV	RSPFEYPQYY	LAEPWKYSIL	AAYMFLLILL	GFPINFMTLY
Toad	MNGTEGPNFY	IPMSNKTGVV	RSPFEYPQYY	LAEPWQYSIL	CAYMFLLILL	GFPINFMTLY
Salamander	MNGTEGPNFY	VPFSNKSGVV	RSPFEYPQYY	LAEPWQYSVL	AAYMFLLILL	GFPVNFLTLY
Snake	MNGTEGLNFY	IPMSNKTGIV	RSPFEYPQYY	LADPWQYSAL	AAYMFLLILL	GFPINFLTLY
Anole	MNGTEGQNFY	VPMSNKTGVV	RNPFEYPQYY	LADPWQFSAL	AAYMFLLILL	GFPINFLTLF
Lizard	MNGTEGQNFY	IPMSNKTGVV	RSPFEYPQYY	LADPWQFSAL	AAYMFLLILL	GFPINFLTLF
Alligator	MNGTEGPDFY	IPFSNKTGVV	RSPFEYPQYY	LAEPWKYSAL	AAYMFMLIIL	GFPINFLTLY
Chicken	MNGTEGQDFY	VPMSNKTGVV	RSPFEYPQYY	LAEPWKFSAL	AAYMFMLILL	GFPVNFLTLY
Platypus	MNGTEGQDFY	IPMSNKTGVV	RSPFEYPQYY	LAEPWQYSVL	AAYMFMLIML	GFPINFLTLY
Echidna	MNGTEGQDFY	IPMSNKTGIV	RSPFEYPQYY	LAEPWQYSVL	AAYMFMLIML	GFPINFLTLY
Opossum	MNGTEGPNFY	VPFSNKTGVV	RSPFEEPQYY	LAEPWQFSCL	AAYMFMLIVL	GFPINFLTLY
Dunnart	MNGTEGPNFY	VPYSNKSGVV	RSPYEEPQYY	LAEPWMFSCL	AAYMFMLIVL	GFPINFLTLY
Elephant	MNGTEGPNFY	VPFSNKTGVV	RSPFEYPQYY	LAEPWQFSML	AAYMFLLIVL	GFPINFLTLY
Manatee	MNGTEGPNFY	VPFSNKTGVV	RSPFEYPQYY	LAEPWQFSML	AAYMFLLIVL	GFPINFLTLY
Pig	MNGTEGPNFY	VPFSNKTGVV	RSPFEYPQYY	LAEPWQFSML	AAYMFMLIVL	GFPINFLTLY
Cattle	MNGTEGPNFY	VPFSNKTGVV	RSPFEAPQYY	LAEPWQFSML	AAYMFLLIML	GFPINFLTLY
Cat	MNGTEGPNFY	VPFSNKTGVV	RSPFEYPQYY	LAEPWQFSML	AAYMFLLIVL	GFPINFLTLY
Bear	----------	-----?TGVV	RSPFESPQYY	LAEPWQFSML	AAYMFLLIVL	GFPINFLTLY
Dog	MNGTEGPNFY	VPFSNKTGVV	RSPFEYPQYY	LAEPWQFSML	AAYMFLLIVL	GFPINFLTLY
Hamster	MNGTEGPNFY	VPFSNATGVV	RSPFEYPQYY	LAEPWQFSML	AAYMFLLIVL	GFPINFLTLY
Guinea pig	MNGTEGENFY	IPFSNATGVV	RSPFEYPQYY	LAEPWQFSIL	AAYMFMLIVL	GFPINFLTLY
Rabbit	MNGTEGPDFY	IPMSNQTGVV	RSPFEYPQYY	LAEPWQFSML	AAYMFLLIVL	GFPINFLTLY
Galago	MNGTEGPNFY	VPFSNATGVV	RSPFEYPQYY	LAEPWQFSML	AAYMFMLIVL	GFPINFLTLY
Macaque	MNGTEGPNFY	VPFSNATGVV	RSPFEYPQYY	LAEPWQFSML	AAYMFLLIVL	GFPINFLTLY
Human	MNGTEGPNFY	VPFSNATGVV	RSPFEYPQYY	LAEPWQFSML	AAYMFLLIVL	GFPINFLTLY

	6	7	8	9	10	11
Coelacanth	VTIQHKKLRT	PLNYILLDLA	VADLCMVFGG	FFVTMYSSMN	GYFVLGPTGC	NIEGFFATLG
Lungfish	VTVQHKKLRT	PLNYILLNLA	VADLFMVFGG	FTTTMYTAMN	GYFVFGVVGC	NLEGFFATFG
Frog	VTIQHKKLRT	PLNYILLNLA	FANHFMVLCG	FTITLYTSLH	GYFVFGQSGC	YFEGFFATLG
Toad	VTIQHKKLRT	PLNYILLNLA	FANHFMVLCG	FTVTMYSSMN	GYFILGATGC	YVEGFFATLG
Salamander	VTIQHKKLRT	PLNYILLNLA	FANHFMVFGG	FPVTMYSSMH	GYFVFGQTGC	YIEGFFATMG
Snake	VTIQHKKLRT	PLNYILLNLA	VANLFMVLVG	FTTTMYTSMN	GYFIFGTVGC	NVEGFFATLG
Anole	VTIQHKKLRT	PLNYILLNLA	VANLFMVLMG	FTTTMYTSMN	GYFIFGTVGC	NIEGFFATLG
Lizard	VTIQHKKLRT	PLNYILLNLA	IANLFMVLIG	FTTTMYTSMN	GYFIFGTIGC	SIEGFFATLG
Alligator	VTVQHKKLRS	PLNYILLNLA	VADLFMVLGG	FTTTLYTSMN	GYFVFGVTGC	YFEGFFATLG
Chicken	VTIQHKKLRT	PLNYILLNLV	VADLFMVFGG	FTTTMYTSMN	GYFVFGVTGC	YIEGFFATLG
Platypus	VTIQHKKLRT	PLNYILLNLA	FANHFMVLGG	FTTTLYTSLH	GYFVFGPTGC	NIEGFFATLG
Echidna	VTIQHKKLRT	PLNYILLNLA	FANHFMVLGG	FTTTLYTSLH	GYFVFGPTGC	NIEGFFATLG
Opossum	VTIQHK???T	PLNYILLNLA	IADLFMVFGG	FTTTLYTSLH	GYFVFGPTGC	DLEGFFATLG
Dunnart	VTIQHKKLRT	PLNYILLNLA	VADLFMVICG	FTTTLVTSLN	GYFVFGTTGC	LVEGFFATTG
Elephant	VTVQHKNVRT	PLNYILLNLA	VANHFMVFGG	FTTTLYTSLH	GYFVFGSTGC	NLEGFFATLG
Manatee	VTVQHKKLRT	PLNYILLNLA	VADLFMVFGG	FTTTLYTSLH	GYFVFGPTGC	NVEGFFATLG
Pig	VTVQHKKLRT	PLNYILLNLA	VADLFMVFGG	FTTTLYTSLH	GYFVFGPTGC	NLEGFFATLG
Cattle	VTVQHKKLRT	PLNYILLNLA	VADLFMVFGG	FTTTLYTSLH	GYFVFGPTGC	NLEGFFATLG
Cat	VTVQHKKLRT	PLNYILLNLA	VADLFMVFGG	FTTTLYTSLH	GYFVFGPTGC	NLEGFFATLG
Bear	VTVQHKKLRT	PLNYILLNLA	VADLFMVFGG	FTTTLYTSLH	GYFVFGPTGC	NLEGFFATLG
Hamster	VTVQHKKLRT	PLNYILLNLA	VADLFMVFGG	FTTTLYTSLH	GYFVFGPTGC	NLEGFFATLG
Dog	VTVQHKKLRT	PLNYILLNLA	VADLFMVFGG	FTTTLYTSLH	GYFVFGPTGC	NVEGFFATLG
Guinea pig	VTVQHKKLRT	PLNYILLNLA	VANLFMVLGG	FTTTLYTSMN	GYFVFGPTGC	NLEGFFATLG
Rabbit	VTVQHKKLRT	PLNYILLNLA	VADLFMVLGG	FTTTLYTSLH	GYFVFGPTGC	NVEGFFATLG
Galago	VTVQHKKLRT	PLNYILLNLA	VADLFMVFGG	FTTTLYTSLH	GYFVFGPTGC	NLEGFFATLG
Macaque	VTVQHKKLRT	PLNYILLNLA	VADLFMVFGG	FTTTLYTSLH	GYFVFGPTGC	NAEGFFATLG
Human	VTVQHKKLRT	PLNYILLNLA	VADLFMVLGG	FTSTLYTSLH	GYFVFGPTGC	NLEGFFATLG

	1	1	1	1	1	1
	2	3	4	5	6	7
Coelacanth	GQVALWALVV	LAIERYVVVC	KPMSNFRFGE	NHAIMGVIFT	WIMALSCAVP	PLFGWSRYIP
Lungfish	GIIALWCLVV	LAIERYIVVC	KPISNFRFGE	NHAIMGVVFT	WIMALACAGP	PLFGWSRYIP
Frog	GEIALWSLVA	LAIERYIVVC	KPMSNFRFGE	NHAMMGVAFT	WIMALACAVP	PLFGWSRYIP
Toad	GEIALWSLVV	LAIERYVVVC	KPMSNFRFSE	NHAVMGVAFT	WIMALSCAVP	PLLGWSRYIP
Salamander	GEIALWSLVV	LAIERYVVVC	KPMSNFRFGE	NHAIMGVMMT	WIMALACAAP	PLFGWSRYIP
Snake	GEIALWSLVI	LAVERYVVVC	KPMSNFRFTQ	THAIIGVSLT	WIMALACAVP	PLIGWSRYIP
Anole	GEMGLWSLVV	LAVERYVVIC	KPMSNFRFGE	THALIGVSCT	WIMALACAGP	PLLGWSRYIP
Lizard	GEIALWSLVV	LAVERYVVVC	KPMSNFRFSE	THAIIGVGFT	WIMALACAGP	PLLGWSRYIP
Alligator	GEVALWCLVV	LAIERYIVVC	KPMSNFRFGE	NHAIMGVVFT	WIMALTCAAP	PLVGWSRYIP
Chicken	GEIALWSLVV	LAVERYVVVC	KPMSNFRFGE	NHAIMGVAFS	WIMAMACAAP	PLFGWSRYIP
Platypus	GEIALWSLVV	LAIERYIVVC	KPMSNFRFGE	NHAIMGVAFT	WIMALACALP	PLVGWSRYIP
Echidna	GEIALWSLVV	LAIERYIVVC	KPMSNFRFGE	NHAIMGVTFT	WIMALACAFP	PLVGWSRYIP
Opossum	GEIALWSLVV	LAIERYIVXC	KXMSNFRFGE	NHAIMGVAFT	WVMALACAAP	PLVGWSRYIP
Dunnart	GEVALWALVV	LAIERYIVVC	KPMSNFRFGE	NHAIMGVAFT	WIMALACSVP	PIFGWSRYIP
Elephant	GEIALWSLVV	LAIERYVVVC	KPMSNFRFGE	NHAIMGVAFT	WVMALACAAP	PLVGWSRYIP
Manatee	GEIALWSLVV	LAIERYVVVC	KPMSNFRFGE	NHAIMGVAFT	WVMALACAAP	PLAGWSRYIP
Pig	GEIALWSLVV	LAIERYVVVC	KPMSNFRFGE	NHAIMGLALT	WVMALACAAP	PLVGWSRYIP
Cattle	GEIALWSLVV	LAIERYVVVC	KPMSNFRFGE	NHAIMGVAFT	WVMALACAAP	PLVGWSRYIP
Cat	GEIALWSLVV	LAIERYVVVC	KPMSNFRFGE	NHAIMGVAFT	WVMALACAAP	PLVGWSRYIP
Bear	GEIALWSLVV	LAIERYVVVC	KPMSNFRFGE	NHAIMGVAFT	WVMALACAAP	PLVGWSRYIP
Dog	GEIALWSLVV	LAIERYVVVC	KPMSNFRFGE	NHAIMGVAFT	WVMALACAAP	PLAGWSRYIP
Hamster	GEIALWSLVV	LAIERYVVIC	KPMSNFRFGE	NHAIMGVVFT	WIMALACAAP	PLVGWSRYIP
Guinea pig	GEIALWSLVV	LAIERYVVVC	KPMSNFRFGE	NHAIMGVVFT	WIMALACAAP	PLVGWSRYIP
Rabbit	GEIALWSLVV	LAIERYVVVC	KPMSNFRFGE	NHAIMGVAFT	WIMALACAAP	PLVGWSRYIP
Galago	GEIALWSLVV	LAIERYVVVC	KPMSNFRFGE	NHAIMGLVFT	WIMALACAAP	PLVGWSRYIP
Macaque	GEIALWSLVV	LAIERYVVVC	KPMSNFRFGE	NHAIMGVAFT	WVMALACAAP	PLFGWSRYIP
Human	GEIALWSLVV	LAIERYVVVC	KPMSNFRFGE	NHAIMGVAFT	WVMALACAAP	PLAGWSRYIP

	1	1	2	2	2	2
	8	9	0	1	2	3
Coelacanth	EGMQSSCGVD	YYTLKPEVNN	ESFVIYMFVV	HFTIPLIVIF	FCYGRLVCTV	KDAAAQQQES
Lungfish	EGMQCSCGID	YYTLKPEVNN	ESFVIYMFIV	HFTIPLIIIF	FCYGRLMCTV	KEAAAQQQES
Frog	EGMQCSCGVD	YYTLKPEINN	ESFVIYMFVV	HFLIPLIIIT	FCYGRLVCTV	KEAAAQQQES
Toad	EGMQCSCGVD	YYTLKPEVNN	ESFVIYMFVV	HFTIPLIIIF	FCYGRLVCTV	KEAAAQQQES
Salamander	EGMQCSCGVD	YYTLKPEVNN	ESFVIYMFLV	HFTIPLMIIF	FCYGRLVCTV	KEAAAQQQES
Snake	EGMQSSCGVD	YYTPTPEVHN	ESFVIYMFLV	HFVIPLTVIF	FCYGRLICTV	KEAAAQQQES
Anole	EGMQCSCGVD	YYTPTPEVHN	ESFVIYMFLV	HFVTPLTIIF	FCYGRLVCTV	KAAAAQQQES
Lizard	EGMQCSCGVD	YYTPNPEVHN	ESFVIYMFLV	HFVTPLTIIF	FCYGRLLCTV	KAAAAQQQES
Alligator	EGMQCSCGVD	YYTLKPEVNN	ESFVIYMFVV	HFAIPLAVIF	FCYGRLVCTV	KEAAAQQQES
Chicken	EGMQCSCGID	YYTLKPEINN	ESFVIYMFVV	HFMIPLAVIF	FCYGNLVCTV	KEAAAQQQES
Platypus	EGMQCSCGID	YYTLRPEVNN	ESFVIYMFVV	HFTIPMTIIF	FCYGRLVFTV	KEAAAQQQES
Echidna	EGMQCSCGID	YYTLKPEVNN	ESFVIYMFVV	HFTIPMTIIF	FCYGRLVFTV	KEAAAQQQES
Opossum	EGMQCSCGID	YYTLKPEVNN	ESFVIYMFVV	HFTIPMVVIF	FCYGQLVFTV	KEAAAQQQES
Dunnart	EGMQCSCGID	YYTLNPEFNN	ESFVIYMFVV	HFIIPLTVIF	FCYGQLVFTV	KEAAAQQQES
Elephant	EGMQCSCGID	YYTLKPEVNN	ESFVIYMFVV	HFTIPMTIIF	FCYGQLVFTV	KEAAAQQQES
Manatee	EGMQCSCGID	YYTLKPEVNN	ESFVIYMFVV	HFTIPMIVIF	FCYGQLVFTV	KEAAAQQQES
Pig	EGLQCSCGID	YYTLKPEVNN	ESFVIYMFVV	HFSIPLVIIF	FCYGQLVFTV	KEAAAQQQES
Cattle	EGMQCSCGID	YYTPHEETNN	ESFVIYMFVV	HFIIPLIVIF	FCYGQLVFTV	KEAAAQQQES
Cat	EGMQCSCGID	YYTLKPEVNN	ESFVIYMFVV	HFTIPMIVIF	FCYGQLVFTV	KEAAAQQQES
Bear	EGMQCSCGID	YYTLKPEVNN	ESFVIYMFVV	HFTIPMIVIF	FCYGQLVFTV	KEAAAQQQES
Dog	EGMQCSCGID	YYTLKPEINN	ESFVIYMFVV	HFAIPMIVIF	FCYGQLVFTV	KEAAAQQQES
Hamster	EGMQCSCGVD	YYTLKPEVNN	ESFVIYMFVV	HFTIPLIVIF	FCYGQLVFTV	KEAAAQQQES
Guinea pig	EGMQCSCGID	YYTLKPEVNN	ESFVIYMFVV	HFTIPMIIIF	FCYGQLVFTV	KEAAAQQQES
Rabbit	EGMQCSCGID	YYTLKPEVNN	ESFVIYMFVV	HFTIPLIIIF	FCYGQLVFTV	KEAAAQQQES
Galago	EGMQCSCGID	YYTLKPEVNN	ESFVIYMFVV	HFFIPLFVIF	FCYGQLVFTV	KEAAAQQQES
Macaque	EGLQCSCGID	YYTLKPEVNN	ESFVIYMFVV	HFTIPMIVIF	FCYGQLVFTV	KEARAQQQES
Human	EGLQCSCGID	YYTLKPEVNN	ESFVIYMFVV	HFTIPMIIIF	FCYGQLVFTV	KEAAAQQQES

	2	2	2	2	2	2
	4	5	6	7	8	9
Coelacanth	ATTQKAEKEV	TRMVIVMVIS	FLVCWVPYAS	VAAYIFFNQG	SEFGPVFMTA	PSFFAKSASF
Lungfish	ATTQKAEKEV	TRMVYIMVIS	YLVCWLPYAS	VSFYIFTHQG	SDFGPVFMTV	PAFFAKTASV
Frog	ATTQKAEKEV	TRMVIIMVIF	FLICWVPYAY	VAFYIFCNQG	SEFGPIFMTV	PAFFAKSSAI
Toad	ATTQKAEKEV	TRMVIIMVVF	FLICWVPYAS	VAFFIFSNQG	SEFGPIFMTV	PAFFAKSSSI
Salamander	ATTQKAEKEV	TRMVIIMVVA	FLICWVPYAS	VAFYIFSNQG	TDFGPIFMTV	PAFFAKSSAI
Snake	ATTQKAEKEV	TRMVILMVIA	FLICWVPYAS	VAFYIFTHQG	SDFGPVFMTI	PSFFAKSSAI
Anole	ATTQKAEREV	TRMVVIMVIS	FLVCWVPYAS	VAFYIFTHQG	SDFGPVFMTI	PAFFAKSSAI
Lizard	ATTQKAEREV	TRMVILMVIS	FLICWVPYAS	VAFYIFTHQG	SDFGPVFMTI	PAFFAKSSAI
Alligator	ATTQKAEKEV	TRMVIIMVVS	FLICWVPYAS	VAFYIFSNQG	SDFGPVFMTI	PAFFAKSSAI
Chicken	ATTQKAEKEV	TRMVIIMVIA	FLICWVPYAS	VAFYIFTNQG	SDFGPIFMTI	PAFFAKSSAI
Platypus	ATTQKAEKEV	TRMVIIMVIA	FLICWVPYAS	VAFYIFTHQG	SNFGPIFMTV	PAFFAKSSAI
Echidna	ATTQKAEKEV	TRMVIIMVIA	FLICWVPYAS	VAFYIFTHQG	SNFGPIFMTA	PAFFAKSSAI
Opossum	ATTQKAEKEV	TRMVIIMVIA	FLICWLPYAG	VAFYIFTHQG	SNFGPILMTL	PAFFAKTSAV
Dunnart	ATTQKAEKEV	TRMVIIMVIA	FLICWVPYAS	VAFYIFTHQG	SDFGPIFMTL	PAFFAKSSSI
Elephant	ATTQKAEKEV	TRMVIIMVIA	FLICWVPYAS	VAFYIFTHQG	SDFGPILMTL	PAFFAKSSAI
Manatee	ATTQKAEKEV	TRMVIIMVIA	FLICWVPYAS	VAFYIFTHQG	SNFGPIFMTL	PAFFAKSASI
Pig	ATTQKAEKEV	TRMVIIMVVA	FLICWLPYAS	VAFYIFTHQG	SDFGPIFMTI	PAFFAKSASI
Cattle	ATTQKAEKEV	TRMVIIMVIA	FLICWLPYAG	VAFYIFTHQG	SDFGPIFMTI	PAFFAKTSAV
Cat	ATTQKAEKEV	TRMVIIMVIA	FLICWVPYAS	VAFYIFTHQG	SNFGPIFMTL	PAFFAKSSSI
Bear	ATTQKAEKEV	TRMVIIMVIA	FLICWLPYAG	VAFYIFTHQG	SNFGPIFMTL	PAFFAKSSSI
Dog	ATTQKAEKEV	TRMVIIMVIA	FLICWVPYAS	VAFYIFTHQG	SDFGPIFMTL	PAFFAKSSSI
Hamster	ATTQKAEKEV	TRMVILMVVF	FLICWFPYAG	VAFYIFTHQG	SNFGPIFMTL	PAFFAKSSSI
Guinea pig	ATTQKAEKEV	TRMVIIMVIA	FLICWVPYAS	VAAYIFTHQG	SNFGPIFMTV	PAFFAKSSSI
Rabbit	ATTQKAEKEV	TRMVIIMVIA	FLICWVPYAS	VAFYIFTHQG	SNFGPIFMTI	PAFFAKSSSI
Galago	ATTQKAEKEV	TRMVIIMVIA	FLICWLPYAG	VAFYIFTHQG	SNFGPIFMTL	PAFFAKTASI
Macaque	ATTQKAEKEV	TRMVIIMVIA	FLICWVPYAS	VAFYIFTHQG	SNFGPIFMTI	PAFFAKSASI
Human	ATTQKAEKEV	TRMVIIMVIA	FLICWVPYAS	VAFYIFTHQG	SNFGPIFMTI	PAFFAKSAAI

	3	3	3	3	3	3
	0	1	2	3	4	5
Coelacanth	YNPVIYILLN	KQFRNCMITT	LCCGKNPFGD	EDATSAAGSS	KTEASSVSSS	SVSPA
Lungfish	YNPVIYILMN	KQFRNCMITT	LCCGKNPFGD	EETTSA-GTS	KTEASSVSSS	QVSPA
Frog	YNPVIYIMLN	KQFRNCMITT	LCCGKNPFGD	DDASSAA-TS	KTEATSVSTS	QVSPA
Toad	YNPVIYIMLN	KQFRNCMITT	LCCGKNPFGE	DDASSAA-TS	KTEASSVSSS	QVSPA
Salamander	YNPVIYIVLN	KQFRNCMITT	ICCGKNPFGD	DETTSAA-TS	KTEASSVSSS	QVSPA
Snake	YNPVIYIVMN	KQFRNCMLTT	LCCGKNPLAE	DDTSAG---T	KTETSTVSTS	QVSPA
Anole	YNPVIYILMN	KQFRNCMIMT	LCCGKNPLGD	EETSAG---T	KTETSTVSTS	QVSPA
Lizard	YNPVIYILMN	KQFRNCMIMT	LCCGKNPLAE	EDTSAG---T	KTETSTVSTS	QVSPA
Alligator	YNPVIYIVMN	KQFRNCMITT	LCCGKNPLGD	DETATG---S	KTETSSVSTS	QVSPA
Chicken	YNPVIYIVMN	KQFRNCMITT	LCCGKNPLGD	EDTSAG----	KTETSSVSTS	QVSPA
Platypus	YNPVIYIMMN	KQFRNCMLTT	ICCGKNPLGD	DEASATA--S	KTEQSSVSTS	QVSPA
Echidna	YNPVIYIMMN	KQFRNCMLTT	ICCGKNPLGD	DEASATA--S	KTEQSSVSTS	QVSPA
Opossum	YNPVIYIMLN	KQFRTCMLTT	LCCGKIPLGD	DEASATA--S	KTETSQVA--	---PA
Dunnart	YNPVIYIMMN	KQFRNCMITT	LCCGKNPLGD	DEASTTA--S	KTETSQVA--	---PA
Elephant	YNPVIYIMMN	KQFRNCMLTT	ICCGKNPFGE	EEGSTTA--S	KTETSQVA--	---PA
Manatee	YNPVIYIMMN	KQFRNCMLTT	ICCGKNPFAE	EEGATTV--S	KTETSQVA--	---PA
Pig	YNPVIYIMMN	KQFRNCMLTT	LCCGKNPLGD	DEASTTT--S	KTETSQVA--	---PA
Cattle	YNPVIYIMMN	KQFRNCMVTT	LCCGKNPLGD	DEASTTV--S	KTETSQVA--	---PA
Cat	YNPVIYIMMN	KQFRNCMLTT	LCCGKNPLGD	DEASTTG--S	KTETSQVA--	---PA
Bear	YNPVIYIMMN	KQFRNCMITT	LCCGKNPLGD	DEASASA--?	----------	-----
Dog	YNPVIYIMMN	KQFRNCMITT	LCCGKNPLGD	DEASASA--S	KTETSQVA--	---PA
Hamster	YNPVIYIMMN	KQFRNCMLTT	LCCGKNILGD	DEASATA--S	KTETSQVA--	---PA
Guinea pig	YNPVIYIMMN	KQFRNCMLTT	ICCGKNPLGD	DEASTTV--S	KTETSQVA--	---PA
Rabbit	YNPVIYIMMN	KQFRNCMLTT	ICCGKNPLGD	DEASATA--S	KTETSQVA--	---PA
Galago	YNPVIYIMMN	KQFRTCMITT	LCCGKNPLGD	DEASTTA--S	KTETSQVA--	---PA
Macaque	YNPVIYIMMN	KQFRNCMLTT	ICCGKNPLGD	DEASATV--S	KTETSQVA--	---PA
Human	YNPVIYIMMN	KQFRNCMLTT	ICCGKNPLGD	DEASATV--S	KTETSQVA--	---PA

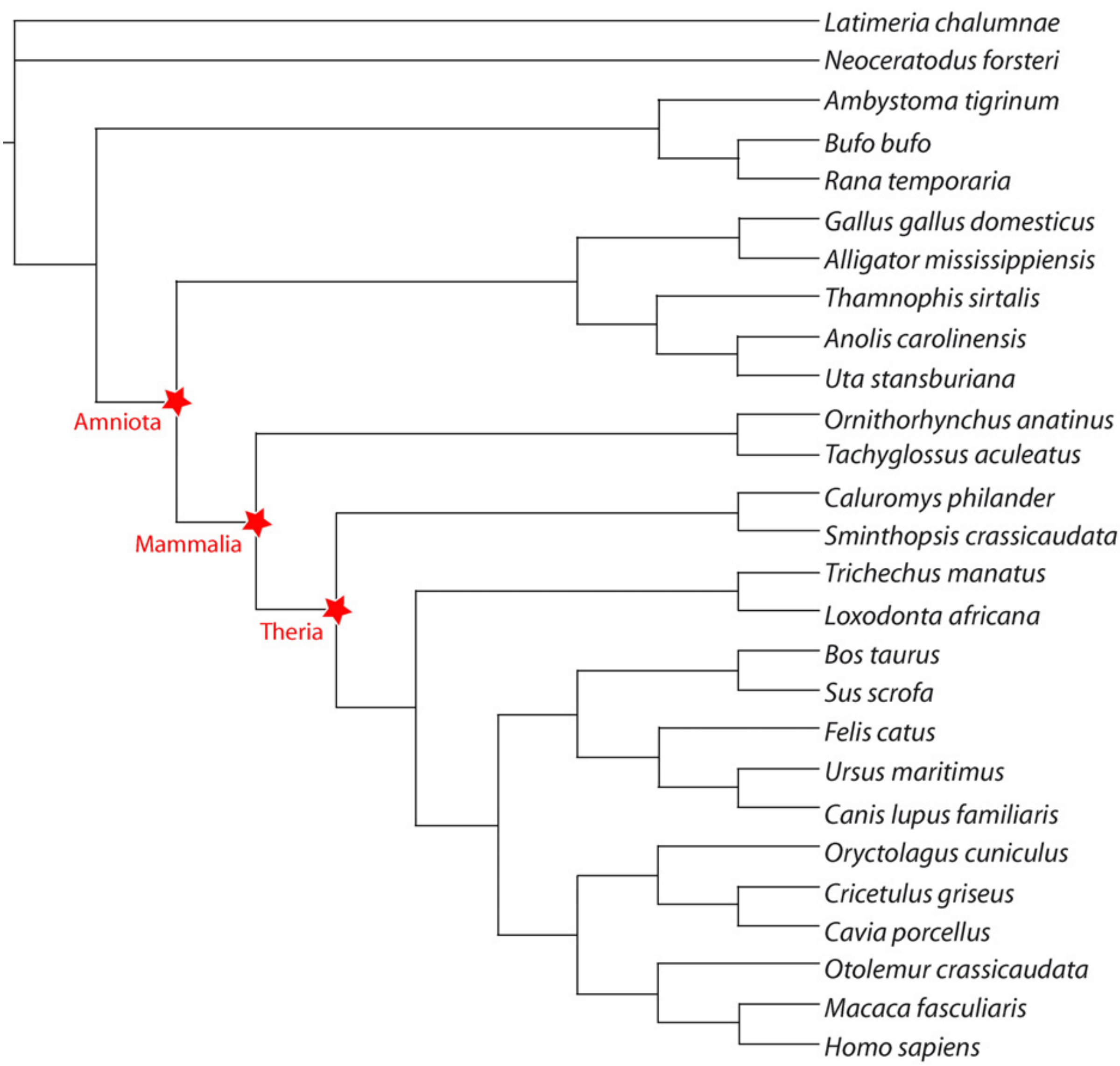

Figure 14. Tetrapod phylogeny used in this study, with coelacanth and lungfish as outgroups. Nodes for which ancestral rhodopsin sequences were reconstructed are indicated by a red star.

2.2.3. Selective constraint analyses

2.2.3.1. Introduction

$\omega = d_N/d_S$ is the measure of natural selection acting at protein level, with values of $\omega < 1$, $= 1$, > 1 indicating purifying selection, neutral evolution (i.e. no selection), and positive selection, respectively (Kimura 1983). In order to investigate the d_N/d_S ratio in different amniote branches, the CODEML program in PAML 4 was used (Yang 2007).

In order to detect positive selection, two different codon models were used: branch models and branch-site models. Codon substitution models, compared to nucleotide or amino acid substitution models, consider the codon triplet as unit of evolution (Goldman and Yang 1994).

They account for transition/transversion rate bias, ω ratio, and equilibrium frequency of codons (Goldman and Yang 1994).

Branch models allow some branches in a given phylogeny to have d_N/d_S values estimated seperately from the rest of the tree and are useful for detecting positive selection acting on particular lineages (Yang 1998, Yang and Nielsen 1998). However, positive selection acts on sites rather than branches. If there are a lot of sites changing along a branch, their signals together would be very strong and positive selection is more likely to be detected along that branch using branch models. However, if only a few sites experience selection, their signal might be overruled along that branch. Thus, branch-site models that allow the d_N/d_S ratio to vary among both branches and sites are also implemented to account for the positive selection at only a few sites (Yang and Nielsen 2002, Yang et al. 2005, Zhang et al. 2005).

Branch and branch-site models require an a priori specification of the foreground branches, i.e. the branches of interest, and which have their own ω estimated (Yang 1998, Yang and Nielsen 1998). Background branches comprise all other branches in the phylogeny and have only one ω ratio estimated.

Statistical significance is assessed by using likelihood ratio tests (LRTs) comparing nested statistical models (Yang 2007).

2.2.3.2. Likelihood ratio test

A likelihood ratio test determines the feasibility of any tree for which the maximum likelihood can be computed (Navidi et al. 1991). For nested models, the alternative model with additional parameters (p_1) should fit the data better than the null model (p_0), as judged by the likelihood score of each model (l_0 and l_1) (Chang et al. 2002b, Yang 2007). If the null model is true, the difference in fit to data can be approximated by a χ^2 distribution, with degrees of freedom (d.f.) being equal to the number of parameters ($p_1 - p_0$) between the two models (Chang et al. 2002b, Yang 2007). So, the test statistic $2\Delta l$ can be compared with that χ^2 distribution to test whether the null model is rejected against the alternative model (Chang et al. 2002, Yang 2007).

$$2 * \Delta * l = \chi^2$$

In general, positive selection is detected if, both, ω is bigger than 1 in the alternative model and if the LRTs show significance.

2.2.3.3. Branch models

For assessing selective constraint acting on branches of interest, two-ratio models were used in this study (Yang 1998). For these models, there are no standard names. Names here were conceived.

One alternative model (MB2a) was compared to two null models (MB1n, also known as M0, and MB2n) (Tab. 5). The alternative model MB2a estimates separate background (ω_0) and foreground (ω_1) ratios. In the first null model MB1n, the foreground branch was set to have the same d_N/d_S ratio estimated as the background branches ($\omega_0 = \omega_1$). By comparison with the alternative model, together with significant LRTs, it is estimated if the foreground ω of a pre-specified branch is significantly different from the background ω. If ω_1 were estimated to be greater than 1 while ω_0 is smaller than 1, this would indicate either relaxed purifying or positive selection acting on the foreground branch (Yang 1998).

The second null model MB2n estimates a background ratio and the foreground ratio is constrained to 1. The comparison of this model with the alternative model, accompanied by significant LRTs, indicates if ω_1 is significantly different from 1, i.e. either bigger or smaller than 1. Further, only if ω_1 was estimated to be bigger 1, this would indicate positive selection (Yang 1998).

Table 5. Parameters of branch models used in this study.

Model	Background ω_0	Foreground ω_1
Alternative model MB2a	ω_0	ω_1
First null model MB1n	ω_0	$\omega_1 = \omega_0$
Second null model MB2n	ω_0	$\omega_1 = 1$

2.2.3.4. Branch-site models

Branch-site models assume that the ω ratio varies among codon sites, and that there are four site classes in the sequence, each having their own estimated ω (Yang and Nielsen 2002, Zhang et al. 2005). Here, branch-site model A was used (Zhang et al. 2005). The names are standard.

Again, we have one alternative model (MA) and two null models (M1a and MA1) (Tab. 6). In the alternative model MA, site class ω_0 is free to vary, but restricted to be smaller than 1, which represents purifying selection. In site lass ω_1, sites are fixed to 1, representing neutral selection. ω_{2a} and ω_{2b} are set to be bigger than or equal to 1.

In the first null model M1a, there are only two site classes. ω_0 is free to vary, but restricted to be smaller than 1. ω_1 is fixed to 1. Site classes ω_{2a} and ω_{2b} are not considered. By comparison with the alternative model, one identifies sites which have elevated ω ratios and whether these sites experienced relaxed purifying or positive selection.

The second null model MA1 has four site classes. ω_0 is free to vary, as long as it is bigger than 1, which represents purifying selection. ω_1 is fixed to 1 and represents neutral evolution. ω_{2a} and ω_{2b} are fixed to 1. Thus, comparing MA1 and MA identifies whether the sites in ω_{2a} and ω_{2b} classes of the MA model have ω ratios significantly bigger than 1 and if positive selection is acting.

If the likelihood ratio test suggests that some sites, i.e. codons, estimated by the branch-site model, are under positive selection, the Bayes Empirical Bayes (BEB) method is used to calculate the posterior probability that each site is from a particular site class (Yang et al. 2005, Yang 2007). Sites with high posterior probabilities that come from the class where $\omega > 1$ are likely to be under positive selection (Yang et al. 2005). Here, posterior probabilities with a p-value greater than 0.95 were considered reliable.

Table 6. Parameters of branch-site models used in this study.

Model	Site class	ω
Alternative model MA	0	$0 < \omega_0 < 1$
	1	$\omega_1 = 1$
	2a	$\omega_{2a} >= 1$
	2b	$\omega_{2b} >= 1$
First null model M1a	0	$0 < \omega_0 < 1$
	1	$\omega_1 = 1$
Second null model MA1	0	$0 < \omega_0 < 1$
	1	$\omega_1 = 1$
	2a	$\omega_{2a} = 1$
	2b	$\omega_{2b} = 1$

2.2.4. Ancestral sequence reconstruction

Using information of present-day sequences, nucleotide and amino acid sequences of extinct ancestors can be reconstructed in PAML 4 (Yang 2007). The likelihood approach uses branch lengths and the substitution pattern for ancestral reconstruction (Yang et al. 1995). It starts with an alignment of extant sequences, a phylogeny relating those sequences, and a statistical model of evolution, and calculates the likelihood of each possible ancestral state given that sequence, tree, and model (Smith et al. 2010). The maximum likelihood ancestral state is the state with the highest likelihood (Smith et al. 2010).

There are two, fairly similar approaches, i.e. marginal and joint reconstruction (Yang 2007). The marginal approach assigns a single character state to a single node in the tree (Koshi and Goldstein 1996, Yang et al. 2005), whereas the joint reconstruction assigns a set of character states to all ancestral nodes in the tree (Pupko et al. 2000). The marginal approach is more suitable and often used when a gene or protein sequence in an extinct ancestor is sought after (Chang et al. 2002a, Thornton 2004). It is also the default setting in PAML 4. Hence, it was also used in this study.

Ancestral reconstruction can be conducted under nucleotide, amino acid, and codon-based models (Yang 2007). Here, different (codon and amino acid) models were first compared with each other to ascertain their consistency. For codon models, branch-site model MA, with Theria marked as foreground, and site model M3 were found to be most consistent; in amino acid models it was JTT+gamma distribution. Generally, site model M3 fits most data better than branch and branch-site models (Yang 2007). First, MA and M3 models were compared with each other. Whenever amino acids differed, model JTT+gamma distribution was always consistent with model M3. Also, sites that differ were never BEB sites, except for site 218, which has a low posterior probability anyways. Also, model M3 has a much higher likelihood and less parameters than model MA.

3. Results

3.1. In the molecular lab

3.1.1. The echidna rhodopsin sequence

The sequencing of the echidna rhodopsin gene sequence was successful. Table 7 shows the genomic DNA (gDNA) and complementary (cDNA) sequence, and Figure 15 shows the protein-coding amino acid sequence with amino acids differing from bovine rhodopsin highlighted in green.

Table 7. Genomic DNA (gDNA) sequence, and complementary DNA (cDNA) sequence of the rhodopsin of the short-beaked echidna, *Tachyglossus aculeatus*. Exons are highlighted in red.

	1					
gDNA	ATGAATGGGA	CGGAGGGCCA	GGACTTTTAC	ATCCCCATGT	CCAATAAGAC	GGGGATTGTC
cDNA	ATGAATGGGA	CGGAGGGCCA	GGACTTTTAC	ATCCCCATGT	CCAATAAGAC	GGGGATTGTC
gDNA	AGGAGTCCCT	TTGAGTATCC	CCAGTATTAC	CTGGCAGAGC	CATGGCAGTA	CTCGGTCCTC
cDNA	AGGAGTCCCT	TTGAGTATCC	CCAGTATTAC	CTGGCAGAGC	CATGGCAGTA	CTCGGTCCTC
gDNA	GCTGCGTATA	TGTTCATGCT	CATCATGCTG	GGGTTCCCCA	TCAACTTCCT	CACGCTGTAC
cDNA	GCTGCGTATA	TGTTCATGCT	CATCATGCTG	GGGTTCCCCA	TCAACTTCCT	CACGCTGTAC
gDNA	GTCACCATCC	AGCACAAGAA	ACTCCGCACC	CCTCTCAACT	ACATCCTCCT	GAACCTGGCA
cDNA	GTCACCATCC	AGCACAAGAA	ACTCCGCACC	CCTCTCAACT	ACATCCTCCT	GAACCTGGCA
gDNA	TTTGCCAACC	ACTTCATGGT	GTTGGGTGGT	TTCACCACAA	CCCTGTATAC	TTCCCTGCAT
cDNA	TTTGCCAACC	ACTTCATGGT	GTTGGGTGGT	TTCACCACAA	CCCTGTATAC	TTCCCTGCAT
						360
gDNA	GGCTACTTTG	TTTTTGGACC	TACGGGCTGC	AACATCGAAG	GCTTCTTTGC	CACACTGGGA
cDNA	GGCTACTTTG	TTTTTGGACC	TACGGGCTGC	AACATCGAAG	GCTTCTTTGC	CACACTGGGA
gDNA	GGTAAGTTTC	CTCCAGGAGT	CCCCCTAGGA	GACGCTCTCC	TGGGCTATGA	CTTTTTTCCT
cDNA	----------	----------	----------	----------	----------	----------
gDNA	CCTGAAGGGA	GAGGAAAGAT	GTCAGCACCT	CCTCCCCACC	TGGGTAGGCC	GCCTTGCCGG
cDNA	----------	----------	----------	----------	----------	----------
gDNA	CGGAAGTCAT	TTTCGAGCTA	ATACCGAGAA	GAGGCTGCTT	TGGCTAATAC	TGGGGACCGA
cDNA	---------	---------	---------	---------	---------	---------
gDNA	GGTCACAGCA	GATCGGGTCA	GTCACTCCAG	AGTCTCTGTC	CCACTCAGCC	CTGGCCCTTT
cDNA	----------	----------	----------	----------	----------	----------
gDNA	CTCTTGGAAT	TCTGAGTCTT	TTGGAAGGAG	AGTGCGGGCC	CCGAGATGAG	GACTGTTAAT
cDNA	----------	----------	----------	----------	----------	----------
gDNA	CGTTAACAGA	GAATGGCAGA	GACCAGCCTG	AGGCCTCCGA	GCAGGAGGTC	TTGTGGGATC
cDNA	----------	----------	----------	----------	----------	----------
gDNA	TGAGGGCAGG	GAGGACAGAA	ATATGGCACT	GGGGCGGAGA	GGGAGGCAGG	TCACCTTCTG
cDNA	----------	----------	----------	----------	----------	----------
gDNA	TTTGGCACCC	AAGTCTCTGG	TAAGGAGTAT	GGGGTTCAGG	GAAGCCATCA	GGGAGCACAC
cDNA	----------	----------	----------	----------	----------	----------

```
gDNA    AGAGGCTTGG  AGTCTGACCC  CATTCTGCCA  CAAGCTTCCC  TTAAATGAGT  TCCTCGACCT
cDNA    ----------  ----------  ----------  ----------  ----------  ----------

gDNA    CTCTGCCCTT  CAGTTTGTCC  ACTGAGACTG  GGGTGGGGAG  AGAGACCCAG  GGGAGCAGAC
cDNA    ----------  ----------  ----------  ----------  ----------  ----------

gDNA    ACCTCAAAAC  ATGAAGTTCC  ATTATCAATC  CTAAAACCGC  CCTGAGAGTC  TAAATCAGGG
cDNA    ----------  ----------  ----------  ----------  ----------  ----------

gDNA    GAGATTGGGA  GAGGTTGCCC  TTTTGTTCTG  GACCTGTAGC  TTCCCCAAGG  ATATCGCTAT
cDNA    ----------  ----------  ----------  ----------  ----------  ----------

gDNA    CTGGGGCAGG  AACCTATGGC  TCTTGCCTCA  GCTCAACCTC  CTGCTCCTGC  AGCCAGAGTG
cDNA    ----------  ----------  ----------  ----------  ----------  ----------

gDNA    GGAGCCTGGC  ATGGGACAGG  GACGGTGTCT  GATCTGATGA  GCTGGTATCT  ACCCCCGCAC
cDNA    ----------  ----------  ----------  ----------  ----------  ----------

gDNA    CTTAGCCCAG  TGCTTTGGCA  CACATGAGCA  CTAAATAGAT  ACCCTAACTA  GCTTTGTGTC
cDNA    ----------  ----------  ----------  ----------  ----------  ----------
             1266
gDNA    TTGCAGGTGA  GATTGCGCTC  TGGTCTCTGG  TGGTGTTGGC  TATCGAGCGG  TATATCGTGG
cDNA    -----GGTGA  GATTGCGCTC  TGGTCTCTGG  TGGTGTTGGC  TATCGAGCGG  TATATCGTGG

gDNA    TCTGCAAGCC  TATGAGCAAC  TTCCGGTTTG  GGGAGAACCA  TGCCATCATG  GGTGTGACTT
cDNA    TCTGCAAGCC  TATGAGCAAC  TTCCGGTTTG  GGGAGAACCA  TGCCATCATG  GGTGTGACTT
                                                                  1434
gDNA    TCACTTGGAT  CATGGCCCTG  GCCTGTGCCT  TCCCCCCACT  CGTTGGCTGG  TCCAGGTACA
cDNA    TCACTTGGAT  CATGGCCCTG  GCCTGTGCCT  TCCCCCCACT  CGTTGGCTGG  TCCA------

gDNA    GGAGCTGCCT  GAAACCTGCT  CAGTAGCCCA  AGGGAAAGCC  CTGAAATGCC  AGGAGGAGGA
cDNA    ----------  ----------  ----------  ----------  ----------  ----------

gDNA    ACTCAGAGGG  GTTGGGATGG  GAGGGCATCC  TCAACTGTGC  CAGTGACGAA  GCTAGGTCTG
cDNA    ----------  ----------  ----------  ----------  ----------  ----------

gDNA    CCAGGGTACC  TGCTCCCCTT  CTTCAACTTG  GCTTTTCCCT  AATCCTTAGC  TAACCTGGGG
cDNA    ----------  ----------  ----------  ----------  ----------  ----------

gDNA    TTTCAAGTCA  AGCATCTTGA  ACAGAGCTAC  CCAAATCCTC  TGATGCAGCG  CTCCCATTGA
cDNA    ----------  ----------  ----------  ----------  ----------  ----------

gDNA    TATTGACCAT  GAGTTCTCCG  AGCCCATGGA  GATGGGGAGA  GATCACGTCT  CTGGAATTGG
cDNA    ----------  ----------  ----------  ----------  ----------  ----------

gDNA    TGTTTGACAG  TGGGGAAATG  GCAGCTGTGG  AGGTGGTGTG  AGTTGGGAGT  GTCATTTGTT
cDNA    ----------  ----------  ----------  ----------  ----------  ----------

gDNA    TTAAAGAGAA  CAACCATAAT  AAAAATGACA  TTTGTTAAGC  GCTCTTTCTG  TGCCAAGCAC
cDNA    ----------  ----------  ----------  ----------  ----------  ----------

gDNA    TGTACTAAGC  GCTGGGGTAG  GTACAGGATA  ATCAGGTTAG  GCACAGTCCC  TGTCCCACCT
cDNA    ----------  ----------  ----------  ----------  ----------  ----------

gDNA    GGGATGAAGA  GTCTAAGTGG  AGGGGACTAT  TCATCCATAA  AGGTGTTTAG  TCCTGCTGAG
cDNA    ----------  ----------  ----------  ----------  ----------  ----------

gDNA    GTGCAAAGAA  GTTCAGTGAC  TTGCTTAAAG  TCACACAGCA  GGCAGGTGGC  AGCTCTGGGA
cDNA    ----------  ----------  ----------  ----------  ----------  ----------

gDNA    TTAGAACCCA  GGTCCTCTGA  CTTCTAGTCT  GGTGCTCTCT  CCACTAAGCC  ACACTGCTTC
cDNA    ----------  ----------  ----------  ----------  ----------  ----------

gDNA    TCCCAGCTCT  AAAGGGTGAT  TAGAGAATCC  TTGGGCCAGA  GGAATCTCCC  TCAGCAGATT
cDNA    ----------  ----------  ----------  ----------  ----------  ----------

gDNA    GTCTCCACTT  CAGCCTCCAG  CAAAGCTATC  CCAGCCTCAG  CAGGCACCAA  CATGCCTGAC
cDNA    ----------  ----------  ----------  ----------  ----------  ----------
```

```
gDNA     CAACTGTCAA  GAAGATTCTA  CACCCTCTCC  CGGGGATCTG  TCATAGCTAA  GGAATACCAG
cDNA     ----------  ----------  ----------  ----------  ----------  ----------

gDNA     ATCTCTTCTG  CAGTCGAAGC  CCATGCCTTG  ATCAAAAGCT  GTTCCCCTTC  CTCCTTACAG
cDNA     ----------  ----------  ----------  ----------  ----------  ----------

gDNA     AAAGTCTAAA  CCCATCATAT  AATCTTTAGG  TTGAATGCCT  CCAATATGCC  CTCTTTGCCA
cDNA     ----------  ----------  ----------  ----------  ----------  ----------

gDNA     ATCTCCTCAC  ACATCTACCT  AGGGGGGCTG  CTAAATGGTA  ATGCGGTCAA  TCTGTCTGCA
cDNA     ----------  ----------  ----------  ----------  ----------  ----------
         2461
gDNA     GATATATCCC  CGAGGGTATG  CAGTGTTCGT  GTGGGATTGA  CTACTACACT  CTCAAACCTG
cDNA     GATATATCCC  CGAGGGTATG  CAGTGTTCGT  GTGGGATTGA  CTACTACACT  CTCAAACCTG

gDNA     AGGTCAACAA  TGAGTCCTTT  GTCATCTACA  TGTTTGTGGT  TCACTTCACC  ATCCCAATGA
cDNA     AGGTCAACAA  TGAGTCCTTT  GTCATCTACA  TGTTTGTGGT  TCACTTCACC  ATCCCAATGA
                                                            2628
gDNA     CAATCATTTT  CTTCTGCTAC  GGCCGCCTGG  TCTTCACTGT  CAAAGAGGTG  AGCAAACCGT
cDNA     CAATCATTTT  CTTCTGCTAC  GGCCGCCTGG  TCTTCACTGT  CAAAGAGG--  ----------

gDNA     CTCACGTGCA  TCTACCTGGG  GAGATTGGTT  CTGGTGTTCT  CTGCTGGCCT  AGCCCCTTTC
cDNA     ----------  ----------  ----------  ----------  ----------  ----------
                                                                           2760
gDNA     CTCAACTGCT  CCCCTCACGA  TTTCCTGCCT  GACCATCCCT  CTCTGCCCCC  CATTTTAGGC
cDNA     ----------  ----------  ----------  ----------  ----------  ---------C

gDNA     TGCAGCCCAG  CAGCAGGAGT  CCGCCACCAC  GCAGAAAGCT  GAGAAGGAAG  TCACCCGCAT
cDNA     TGCAGCCCAG  CAGCAGGAGT  CCGCCACCAC  GCAGAAAGCT  GAGAAGGAAG  TCACCCGCAT

gDNA     GGTGATCATC  ATGGTCATTG  CTTTCCTGAT  CTGCTGGGTG  CCCTACGCCA  GTGTGGCATT
cDNA     GGTGATCATC  ATGGTCATTG  CTTTCCTGAT  CTGCTGGGTG  CCCTACGCCA  GTGTGGCATT

gDNA     CTACATCTTC  ACACACCAGG  GATCAAACTT  CGGCCCCATC  TTCATGACTG  CCCCGGCTTT
cDNA     CTACATCTTC  ACACACCAGG  GATCAAACTT  CGGCCCCATC  TTCATGACTG  CCCCGGCTTT
                                                                       2998
gDNA     CTTTGCCAAG  AGTTCTGCGA  TCTACAACCC  AGTCATCTAC  ATTATGATGA  ACAAGCAGGT
cDNA     CTTTGCCAAG  AGTTCTGCGA  TCTACAACCC  AGTCATCTAC  ATTATGATGA  ACAAGCAG--

gDNA     AACCGAGAGC  GTGTCTGGTT  TGTCCTTACA  TATAAGTTAA  GGTGCGGCAA  GAGCCCCCAG
cDNA     ----------  ----------  ----------  ----------  ----------  ----------

gDNA     CAGGCCGGGG  GGCGGGGGGG  AGGCAGGCAG  ATTCAATCAG  TCAATGGCAT  TTATCTAGTT
cDNA     ----------  ----------  ----------  ----------  ----------  ----------

gDNA     CTTGCTTATG  GTGGGCAGAG  TACTGGCCTG  AGCGTGTGGG  AAAATCCAAT  ACAATGGGGC
cDNA     ----------  ----------  ----------  ----------  ----------  ----------

gDNA     AGGTAGATGT  GATCCCTGCC  CCCAAGGAGC  TTACAGTCTA  GAGGGTCTAA  GTGGGTAGGG
cDNA     ----------  ----------  ----------  ----------  ----------  ----------

gDNA     CAGGACAAGA  GTCTCGGAAG  GGCCCAGCCA  ATCGGCATGA  GGTAACAGGG  CCCCAAAAGT
cDNA     ----------  ----------  ----------  ----------  ----------  ----------

gDNA     TGGGAGACAG  GGGTTCTGGT  CTCCGTCCCT  CTTCCAGCTT  TGGTCCCCTC  TGACCTCCGG
cDNA     ----------  ----------  ----------  ----------  ----------  ----------

gDNA     TAAACTTCTC  TATCCATACC  TCAGGGTGAC  AGTACTTGCC  TTCTCCCTTC  ACCTCTCAAG
cDNA     ----------  ----------  ----------  ----------  ----------  ----------

gDNA     GATGAAGTAG  GGCAGAGTGA  AAGGGAACCC  AGATGAAGCC  AAATTCTCCG  GAGGGAGGTG
cDNA     ----------  ----------  ----------  ----------  ----------  ----------

gDNA     CTCGCTCTGC  CAAGGTTGAA  GTCTGTTCCG  TTGACATCCT  CATGGGCTTC  TGTGGGCCTG
cDNA     ----------  ----------  ----------  ----------  ----------  ----------

gDNA     CAAAAATTGG  GTGGAAGACC  CCCCAAGTAC  CCTGCTGCAC  TGGTGCCAGA  ACTCAAGCTG
cDNA     ----------  ----------  ----------  ----------  ----------  ----------
```

```
gDNA       TCTGCTACCT  CCCCCTCCTC  ATTGTGCCAT  TGTTAGCATC  CTGCTGGGGA  TGGGGTGGGC
cDNA       ----------  ----------  ----------  ----------  ----------  ----------

gDNA       CTGGCGTGCC  TGAGCTTGGC  TATCAGCCTG  ATCTAGAAAG  GGGCTGACTG  TTGATTGTGG
cDNA       ----------  ----------  ----------  ----------  ----------  ----------

                                                             3762
gDNA       TCTCCTTGTC  CTGGTTTCCA  ACCTAATGCT  TCCTCCCCCA  GTTCCGGAAC  TGCATGCTCA
cDNA       ----------  ----------  ----------  ----------  -TTCCGGAAC  TGCATGCTCA

gDNA       CCACCATCTG  CTGCGGCAAG  AACCCGCTGG  GCGATGATGA  GGCTTCGGCC  ACAGCTTCCA
cDNA       CCACCATCTG  CTGCGGCAAG  AACCCGCTGG  GCGATGATGA  GGCTTCGGCC  ACAGCTTCCA

                                                               3887
gDNA       AGACCGAGCA  GTCTTCCGTG  TCCACCAGCC  AGGTTTCTCC  AGCATAG
cDNA       AGACCGAGCA  GTCTTCCGTG  TCCACCAGCC  AGGTTTCTCC  AGCATAG
```

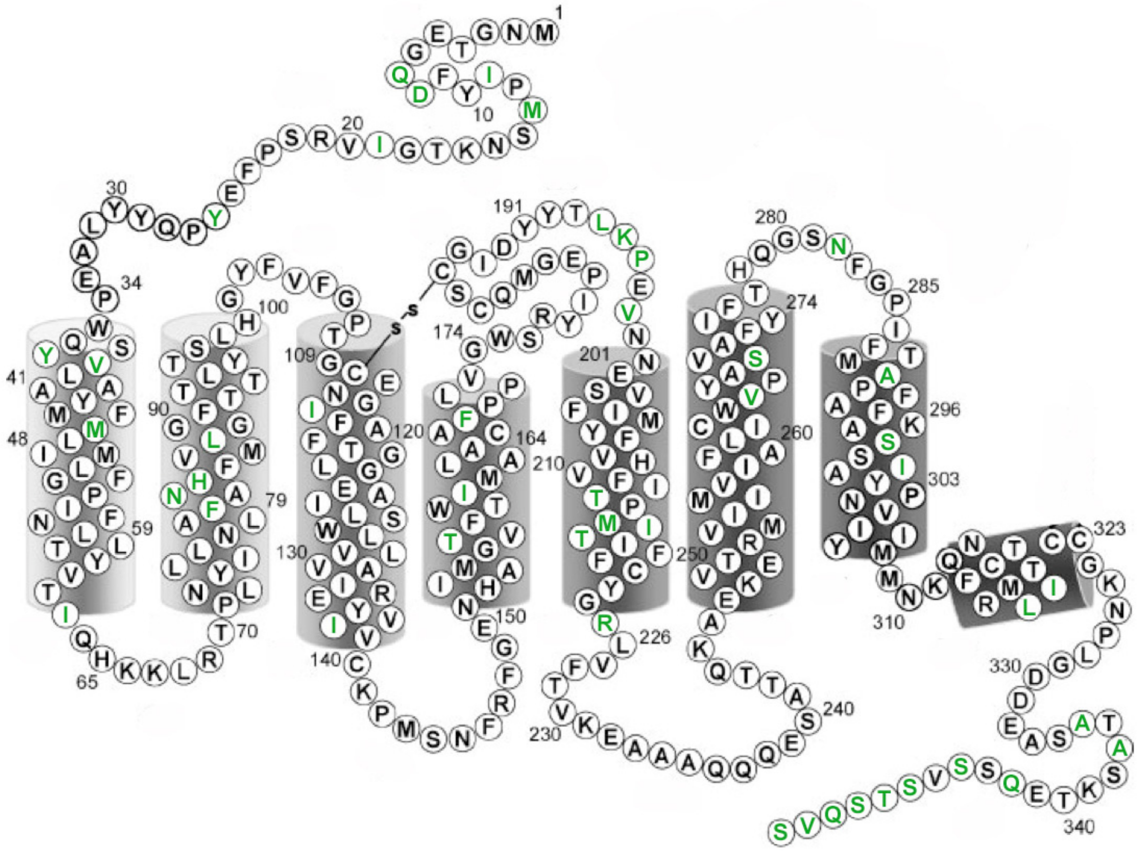

Figure 15. Secondary structure of the echidna rhodopsin (modified after Sakmar et al. 2002). Amino acids differing from bovine rhodopsin are highlighted in green.

3.1.2. Three ancestral sequences

Three inferred ancestral sequence for the nodes Amniota, Mammalia, and Theria were inferred by the M3 model in PAML (Tab. 8).

Table 8. Most likely hypothetical ancestral nucleotide sequences for the nodes Amniota, Mammalia, and Theria, inferred by maximum likelihood estimates.

	0	1	2	3	4	5
Amniota	MNGTEGPNFY	VPMSNKTGVV	RSPFEYPQYY	LAEPWQYSAL	AAYMFMLILL	GFPINFLTLY
Mammalia	MNGTEGPNFY	VPMSNKTGVV	RSPFEYPQYY	LAEPWQYSVL	AAYMFMLIVL	GFPINFLTLY
Theria	MNGTEGPNFY	VPFSNKTGVV	RSPFEYPQYY	LAEPWQFSVL	AAYMFMLIVL	GFPINFLTLY
	6	7	8	9	1 0	1 1
Amniota	VTIQHKKLRT	PLNYILLNLA	VADLFMVLGG	FTTTMYTSMN	GYFVFGPTGC	NIEGFFATLG
Mammalia	VTIQHKKLRT	PLNYILLNLA	VADLFMVFGG	FTTTLYTSLH	GYFVFGPTGC	NIEGFFATLG
Theria	VTIQHKKLRT	PLNYILLNLA	VADLFMVFGG	FTTTLYTSLH	GYFVFGPTGC	NLEGFFATLG
	1 2	1 3	1 4	1 5	1 6	1 7
Amniota	GEIALWSLVV	LAIERYVVVC	KPMSNFRFGE	NHAIMGVAFT	WIMALACAAP	PLFGWSRYIP
Mammalia	GEIALWSLVV	LAIERYVVVC	KPMSNFRFGE	NHAIMGVAFT	WIMALACAAP	PLVGWSRYIP
Theria	GEIALWSLVV	LAIERYIVVC	KPMSNFRFGE	NHAIMGVAFT	WIMALACAAP	PLVGWSRYIP
	1 8	1 9	2 0	2 1	2 2	2 3
Amniota	EGMQCSCGVD	YYTLKPEVNN	ESFVIYMFVV	HFTIPLTIIF	FCYGRLVCTV	KEAAAQQQES
Mammalia	EGMQCSCGID	YYTLKPEVNN	ESFVIYMFVV	HFTIPMTIIF	FCYGRLVFTV	KEAAAQQQES
Theria	EGMQCSCGID	YYTLKPEVNN	ESFVIYMFVV	HFTIPMIVIF	FCYGQLVFTV	KEAAAQQQES
	2 4	2 5	2 6	2 7	2 8	2 9
Amniota	ATTQKAEKEV	TRMVIIMVIS	FLICWVPYAS	VAFYIFTNQG	SDFGPIFMTV	PAFFAKSSAI
Mammalia	ATTQKAEKEV	TRMVIIMVIA	FLICWVPYAS	VAFYIFTHQG	SNFGPIFMTV	PAFFAKSSAI
Theria	ATTQKAEKEV	TRMVIIMVIA	FLICWVPYAS	VAFYIFTHQG	SNFGPIFMTL	PAFFAKSSAI
	3 0	3 1	3 2	3 3	3 4	3 5
Amniota	YNPVIYIVMN	KQFRNCMITT	LCCGKNPLGD	DETSAAAGTT	KTETSSVSTS	QVSPA
Mammali a	YNPVIYIMMN	KQFRNCMLTT	LCCGKNPLGD	DEASATAGTS	KTETSSVSTS	QVSPA
Theria	YNPVIYIMMN	KQFRNCMLTT	LCCGKNPLGD	DEASATAGTS	KTETSQVATS	QVSPA

3.1.3. Western blot

In order to confirm that the correct proteins had been expressed in HEK293 cells, a SDS-PAGE analysis transferred onto a nitrocellulose membran was performed on harvested samples (Fig. 16).

Fig. 16A shows the bovine rhodopsin used as control, as well as the echidna protein and the two mutants. Fig. 16B shows the bovine control and the three ancestral pigments. The bovine sample was diluted 1:2 due to its high expression yield.

Bovine rhodopsin has a molecular weight of around 30 kDa (Frank and Rodbard 1975, Reeves et al. 1996); the corresponding band is seen in Fig. 16. All other samples display two distinct bands at around 36 and 40 kDa (Fig. 16). The echidna rhodopsin and the two mutants are 363 amino acids long, which is 5 amino acids longer than bovine rhodopsin, due to a non-therian insertion from AA 358 to 363 in the former (Tab. 4, chapter 2.2.2.). The ancestral pigments also carry this insertion and are 367 amino acids long (Tab. 8, chapter 3.1.2.). This is responsible for the greater size of expressed visual pigments other than bovine. Bovine rhodopsin monomers are seen in an additional band at around 32 kDa (Fig. 16). In addition, echidna rhodopsin and the two mutants show two additional faint bands at around 50 kDa (Fig. 16A). However, the presence of multiple bands is most likely due to proteins undergoing different post-translational modifications, which can differ in different cell types (Reeves et al. 1996, Wong 2006). Proteins are often synthesized with an extra short peptide in the N-terminal end in order to keep the protein in a nonfunctional form until it is activated into the more mature form, or to guide the protein through various compartments in the cell (Wong 2006). Thus, a subsequent treatment with N-glycosidase F would help to remove all N-linked glycosidation, but unfortunately this was not possible due to technical reasons.

The molecular weight (MW) of each expressed protein was determined with an online tool for calculating the MW based on an input protein sequence (Tab. 9). The results indicate that the upper band in each lane in the western blot, which is at around 40 kDa, is the correct one.

Table 9. Molecular weight estimates based on protein sequences (http://www.expasy.ch/tools/pi_tool.html).

Rhodopsin	MW
Bovine	38.54
Echidna	39.96
Mutant T158A	39.93
Mutant F169A	39.88
Amniota	39.60
Mammalia	39.67
Theria	39.69

Interestingly, the echidna rhodopsins and the two mutants show only faint bands after being exposed for 3 minutes, whereas bovine and the ancestral pigments show a very strong band, after being exposed for only 1 second. This indicates that the ancestral pigments were expressed much better, which could be due to the fact that their gene sequences had been optimized for expression in mammalian cells.

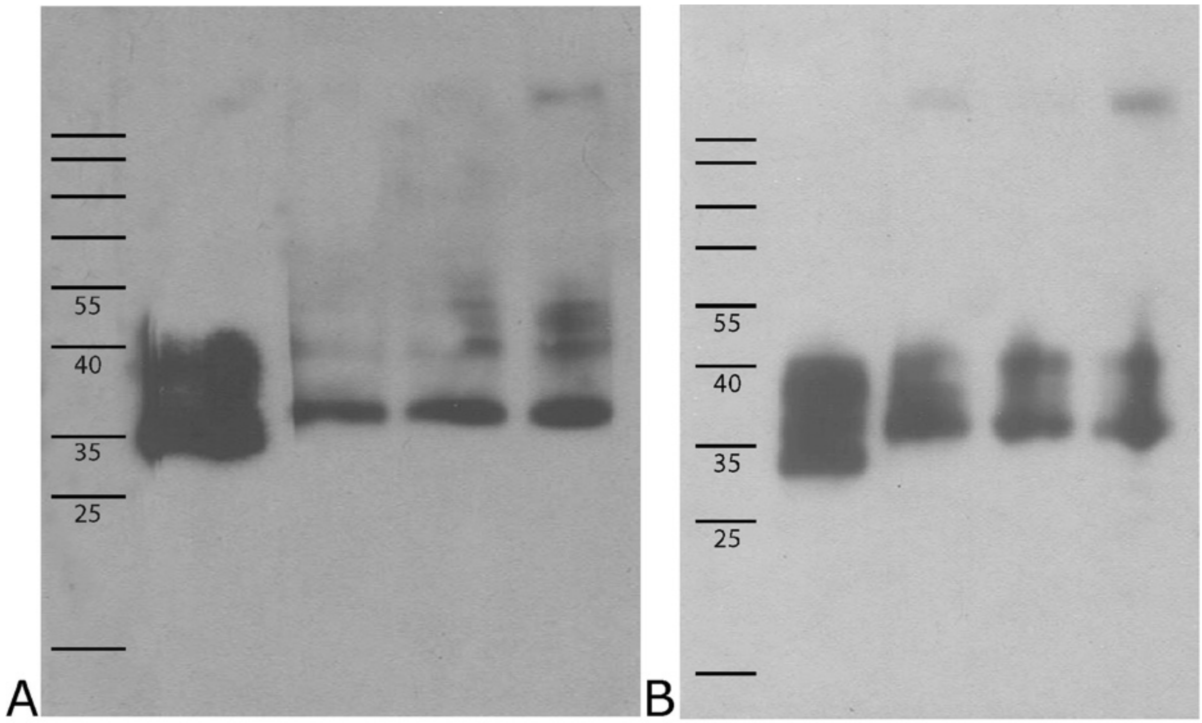

Figure 16. Western blot analysis of expressed rhodopsin pigments. (A) From left to right: Bovine, Echidna, mutant T158A, and mutant F169A rhodopsin. (B) From left to right: Bovine, Amniota, Mammalia, and Theria rhodopsin.

3.1.4. Dark and light spectra

Figure 17 shows dark aborption spectra of all visual pigments expressed in this study. For an accurate determination of λ_{max}, absorption spectra were curve fitted following Govardovskii's method (Govardovskii et al. 2000). Ideally, for a reliable determination of λ_{max}, the curve fitting should be performed at least three times on rhodopsin data from different expressions. However, this was not possible due to technical reasons.

Nonetheless, the following absorption peaks were determined and are shown in Table 10. With a determined λ_{max} at 500 nm, the bovine rhodopsin expressed in this study shows an absorption peak that falls within the published range (Oprian et al. 1987, Stavenga et al. 1993).

Table 10. Absorption peaks of all rhodopsins expressed in this study. Absorption spectra were curve fitted following Govardovskii's method (Govardoskii et al. 2000).

Rhodopsin	λ_{max} in nm
Bovine	500
Echidna	496.5
Mutant T158A	494.5

Rhodopsin	λ_{max} in nm
Mutant F169A	495.5
Amniota	500
Mammalia	501
Theria	500.5

After the dark absorption spectra were taken, pigments were bleached with light for 60s (Fig. 17). A light-bleached opsin shows a characteristic absorption curve with a peak at 380 nm, due to the unquenching of tryptophan after irradiation and subsequent deprotonation of the Schiff base (Farrens and Khorana 1995, Schädel et al. 2003, Salom et al. 2006). This shift in λ_{max} indicates that each expressed pigment is indeed functional (Fig. 17).

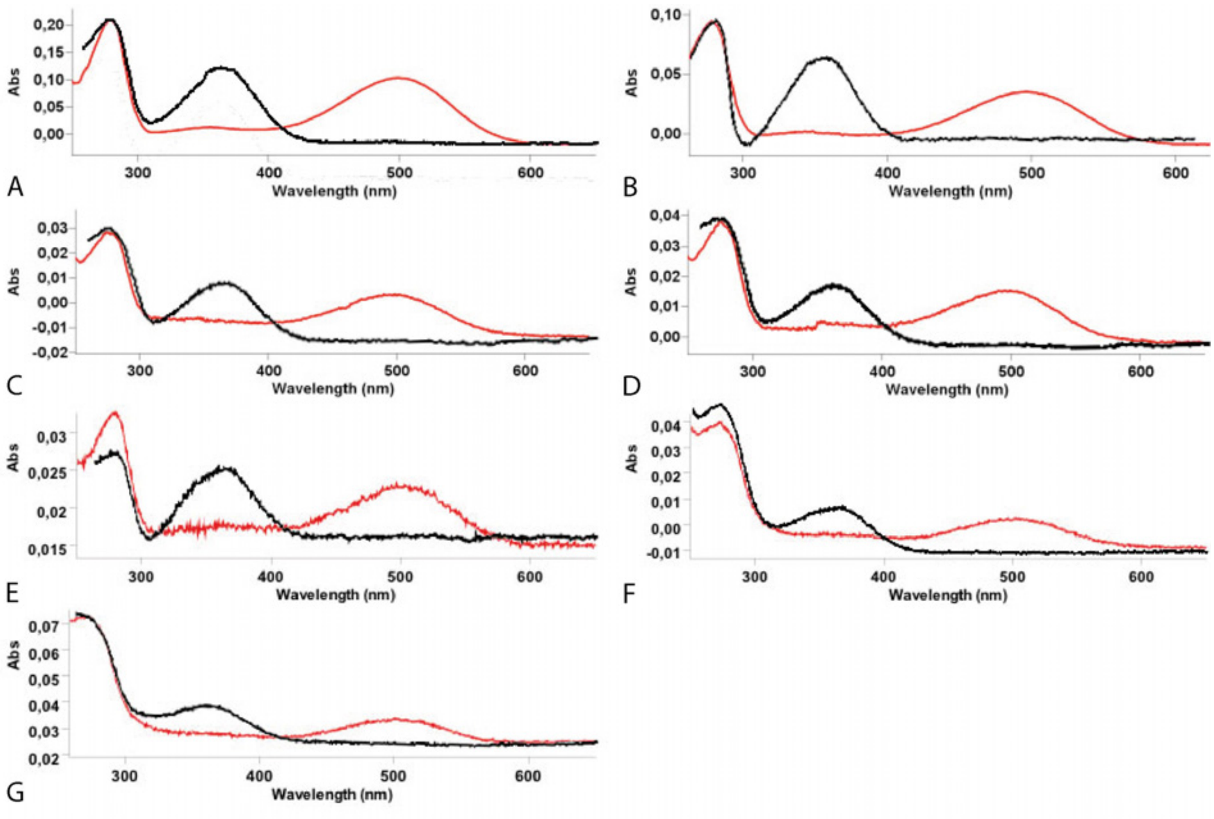

Figure 17. Dark (in red) and light (in black) absorption spectra of expressed and purified rhodopsins, i.e. (A) bovine, (B) echidna, (C) mutant T158A, (D) mutant F169A, (E) Amniota, (F) Mammalia, and (G) Theria rhodopsin. λ_{max} of expressed rhodopsins: Bovine: 500 nm, Echidna: 496.5 nm, mutant T158A: 494.5 nm, mutant F169A: 495.5 nm, Amniota: 500 nm, Mammalia: 501 nm, and Theria: 500.5 nm.

The ratio of UV to visible absorbance (A_{280}/A_{max}) was also determined using the dark absorption spectra data. It is the amount of protein in a sample over the amount of absorbing protein in the sample, i.e. the expression yield. For expression in COS-1 cells, a ratio of around 3 was observed (Oprian et al. 1987), as opposed to a ratio of 1.6-1.7 when prepared from rod outer segments (ROS) (Hong et al. 1982). Sakamoto and Khorana (1995) prepared bovine rhodopsin from ROS and reported a ratio of 1.7-1.8. ROS prepared bovine rhodopsin displayed a ratio of around 2 (Radding and Wald 1956). A ratio below 1.6 is considered to indicate a purity close to 100% (Ernst et al. 2007).

All rhodopsins expressed in this study, including bovine, showed a A_{280}/A_{max} ratio in the same range per expression. Ratios between 2.3 to 3.7 were observed.

3.1.5. Acid bleach

Acid bleaches were performed on echidna and its mutants as well as on the three ancestral rhodopsin pigments, including bovine as positive control (Fig. 18). A shift from λ_{max} to 440 nm at 20°C indicates the break-off of the chromophore from the opsin, relinquishing a protonated Schiff base 11-*cis* retinal free in solution (Kito et al. 1968); hence, a functional rod pigment.

Figure 18 shows the difference absorbance over time of all acid treated pigments. The white circles indicate difference absorbance at 440 nm and are expected to increase and then stabilize once the chromophore and the opsin are indeed detached. The black circles indicate difference absorbance at λ_{max} of each rhodopsin and are expected to decline.

In Figures 18B-D there is an initial drop in difference absorbance at 440 nm, which can be explained by bubbles that formed when adding the HCl and which disturbed the reading of the spectrophotometer.

However, the echidna rhodopsin and the two mutants did not react to the acid as quickly as bovine, which occured immediately right after the addition (Figs. 18A, B). Still, within 10 minutes the protonated Schiff base (PSB) had formed. The two mutants reacted to HCl similar to echidna (Figs. 18C, D). For all ancestral rhodopsins, the acidification was complete within 5 minutes; the therian rhodopsin reacted as quickly as the bovine one (Figs. 18E-G).

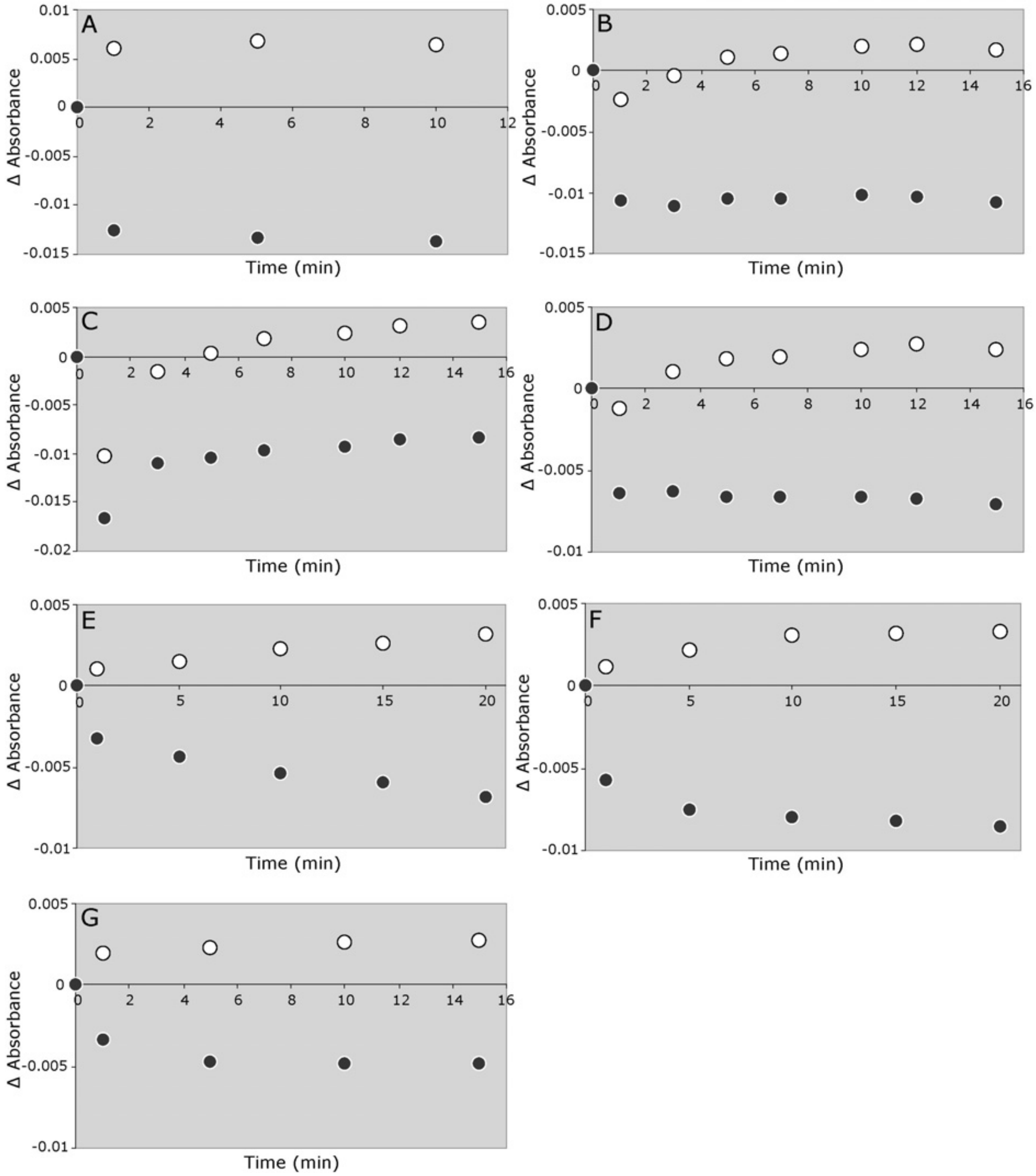

Figure 18. Acid bleaches of (A) bovine, (B) echidna, (C) mutant T158A, (D) mutant F169A, (E) Amniota, (F) Mammalia, and (G) Theria rhodopsin. White circles indicate absorption at 440 nm; black ones indicate absorption at λ_{max}.

In addition, the molar extinction coefficient of a visual pigment can be estimated based on acid treatment data (Radding and Wald 1956, Starace and Knox 1998). It is a measure of how strongly a chemical absorbs light at a given wavelength.

There are various extinction coefficients published for bovine rhodopsin (estimated λ_{max} = 498 - 500 nm), ranging from 40 600 to 43 000 M^{-1} cm^{-1} (Wald and Brown 1953, Shichi et al.

1969, Daemen et al. 1970, Hong and Hubbell 1972, Oprian et al. 1987). All estimated extinction coefficients are shown in Table 11.

Table 11. Molar extinction coefficients determined for all proteins expressed in this study.

Rhodopsin	ε in M^{-1} cm^{-1}
Bovine	40 622
Echidna	34 921
Mutant T158A	31 411
Mutant F169A	40 254
Amniota	49 169
Mammalia	46 961
Theria	45 460

3.1.6. Hydroxylamine sensitivity

All pigments, including bovine rhodopsin as positive control, were treated with 1 M hydroxylamine (NH_2OH) for 2 hrs (Fig. 19). Hydroxylamine assays are used to distinguish between rod and cone opsins, with cone opsins reacting quickly to the compound and forming a retinal oxime, which absorbs light at around 363 nm, and rod opsins not shifting their absorption peak for an extended period of time (Wald et al. 1955, Fager and Fager 1981, Okano et al. 1989, Wang et al. 1992, Starace and Knox 1998). Bovine rhodopsin is known to stay stable in the presence of hydroxylamine for at least 12 hrs (Kawamura and Yokoyama 1998).

In this study, the bovine rhodopsin positive control reacted little to hydroxylamine for the 2 hours during which the measurements were taken, though the dots are very scattered, which is due to the spectrophotometer (Fig. 19A). Also, the degree of increase in difference absorbance at $\lambda_{363\ nm}$ is not very high. An incipient rise is normal, as long as the curve evens out after several minutes. The observed drop in difference absorbance is due to the presence of bubbles or a change in properties of the solution, as was also the case in the acid bleach (Fig. 19A).

Interestingly, the echidna rhodopsin and the two mutants reacted to hydroxylamine more than bovine, as indicated by an increase in difference absorbance of more than 0.005 (Figs. 19B-D). However, cone opsins react to hydroxylamine much stronger (Kawamura and Yokoyama 1998, Starace and Knox 1998). Also, since there were only two runs performed for each mutant, a third run should be performed for a more reliable result.

Figures 19E-F show, though the data points are also somewhat scattered, that the amniote and mammalian rhodopsins react to hydroxylamine just as little as the bovine one. For the Theria rhodopsin, one of the three curves rises slightly, but the other two do not show a strong increase in absorption (Fig. 19G).

The determination of $t_{1/2}$ of hydroxylamine treated pigmnents was not possible, because the data points are too scatterered and R^2 values are not reliable.

In conclusion, there is some indication that echidna and the two mutants are not as stable in the presence of hydroxylamine as bovine rhodopsin, which indicates cone-like characteristics. All ancestral pigments, however, are as insensitive to hydroxylamine as bovine rhodopsin.

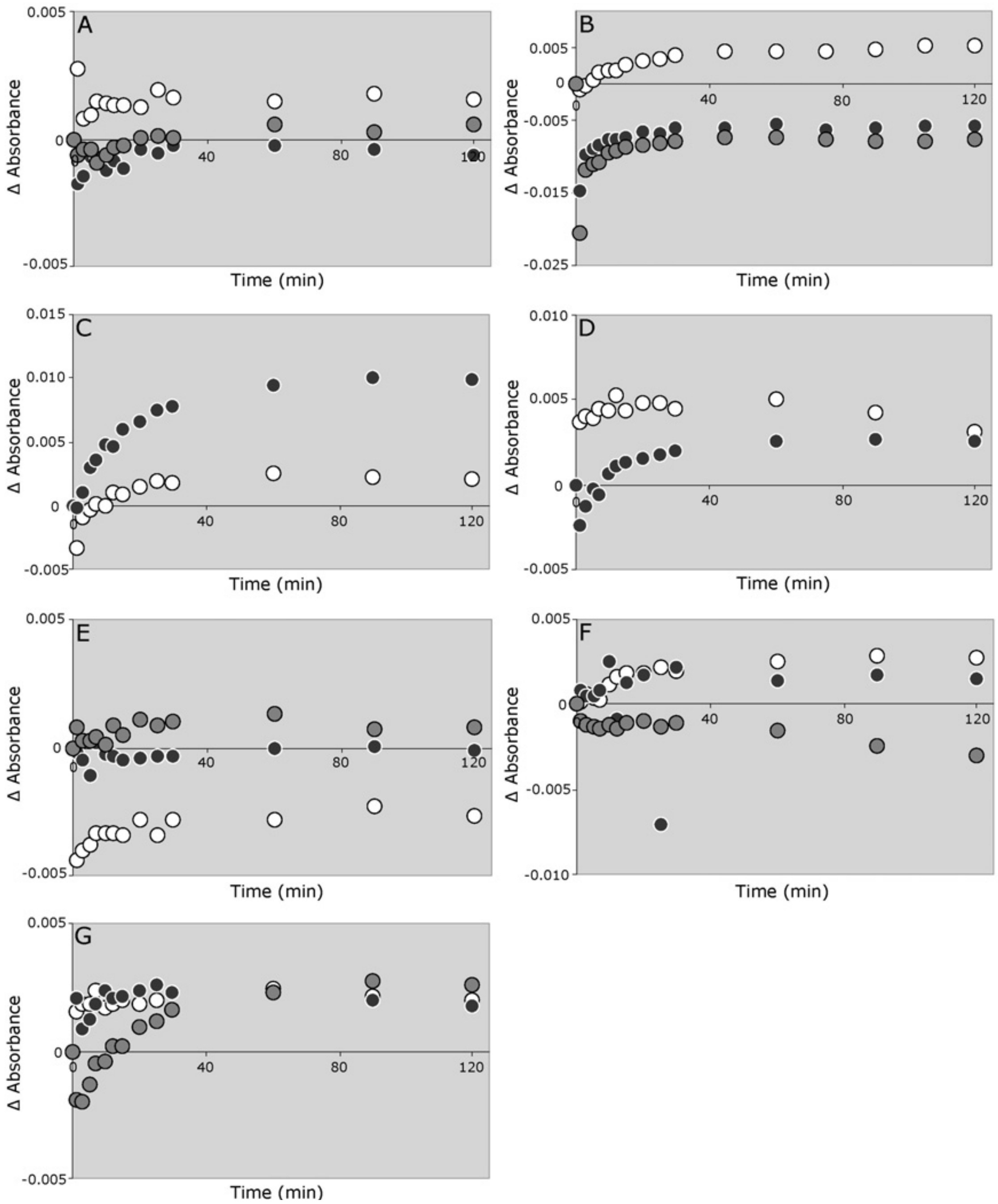

Figure 19. Hydroxylamine assays performed on (A) bovine, (B) echidna, (C) mutant T158A, (D) mutant F169A, (E) Amniota, (F) Mammalia, and (G) Theria rhodopsins. Circles indicate different runs.

3.1.7. Meta II decay by fluorescence spectroscopy

Meta II is the active state of rhodopsin and a key intermediate in the visual signaling cascade where the crucial transducin activation takes place (Fig. 13, chapter 2.1.8.) (Weitz and Nathans 1993, Imai et al. 2005, Sugawara et al. 2010). Here, the opsin and the chromophore are still bound but the Schiff base is deprotonated, unquenching tryptophan, and has its λ_{max} at 380 nm (Farrens and Khorana 1995, Sakmar et al. 2002, Heck et al. 2003, Salom et al. 2006). The rhodopsin meta II state is induced by light bleach and finished with the addition of fresh 11-*cis* retinal, which binds to rhodopsin molecules.

The results of the meta II decay rate assays performed in this study are given in tables 12 and 13. Bovine meta II decay rates are more or less within the expected range of 15 min^{-1} (Tab. 12, 13) (Janz and Farrens 2001, Reeves et al. 1996). The amniote rhodopsin displays a $t_{1/2}$ similar to bovine (Tab. 12). Most striking are the results for the mammalian ancestor, where $t_{1/2}$ is much higher than those of bovine and amniote (Tab. 12). Also, the therian rhodopsin displays a high $t_{1/2}$, similar to the mammalian one (Tab. 12). On the other hand, the echidna displays a much lower $t_{1/2}$ than bovine (Tab. 13). Due to technical reasons, meta II decay rates were not determined for the two mutants.

Table 12. Meta II decay results and their coefficient of determination (R^2) of ancestral pigments and bovine rhodopsin as positive control. Hyphenated numbers in brackets indicate number of expression and assay run.

Expressed rod pigment	$t_{1/2}$ in min^{-1}	R^2
Bovine	16.46 (1)	0.9985
	17.24 (2)	0.9990
	21.39 (3)	0.9932
	12.95 (4)	0.9921
Amniota	16.74 (1)	0.9989
	16.54 (2)	0.9992
	17.07 (3)	0.9976
	13.85 (4)	0.9924
Mammalia	21.33 (1)	0.9986
	22.36 (2)	0.9994
	22.43 (3)	0.9938
	30.54 (4)	0.9989
Theria	33.98 (1)	0.9988
	25.30 (2)	0.9987
	38.72 (3)	0.9977
	14.69 (4)	0.9120

Table 13. Meta II decay results and coefficients of determination (R^2) of echidna rhodopsin and bovine as positive control. Hyphenated numbers in brackets indicate number of expression and assay run.

Expressed rod pigment	$t_{1/2}$ in min^{-1}	R^2
Bovine	12.2 (5)	0.9979
	13.8 (6)	0.9979
	13.0 (7)	0.9977
	14.1 (8)	0.999
	13.8 (9)	0.9987
Echidna	10.3 (5)	0.9957
	9.9 (6)	0.9968
	6.6 (7)	0.9943
	6.1 (8)	0.9974
	6.7 (9)	0.9972

3.2. The ancestral sequences and their structure

3.2.1. Interesting sites

Site-directed mutagenesis is often used in vision research in order to identify key sites being responsible for causing dramatic changes within the visual pigment (Imai et al. 1997, Carvalho et al. 2006).

For the three inferred ancestral proteins, there are 10 residues at which Amniota and Mammalia differ from the Therian sequence (Fig. 20). Amniota differs from Mammalia and Theria at 28 sites (Fig. 20).

According to Hildebrand et al. (2009), residues 37, 39, and 290 are located within the hole where the chromophore enters the binding pocket and might be involved in holding it. Site 95 is not believed to be involved in shifting λ_{max} (Yokoyama et al. 2008). Residue 112 may be of interest as it is next to 113, which was found to be a negatively charged counterion that stabilizes the positively charged PBS (Hildebrand et al. 2009, Shichida and Matsuyama 2009). Substitutions at site 189 cause differences in the molecular properties of rods and cones (Imai et al. 2007, Lamb et al. 2007). Mutants with substitutions at this site were found to fold incorrectly (Doi et al. 1990). A site-directed mutagenesis study by Chang et al. (2002a) showed that site 218 does not have any effect on spectral tuning or transducin activation. According to Wakefield et al. (2008), site 308 causes spectral tuning in human and platypus.

Interestingly, all three ancestral sequences have the insertion of five amino acids between position 349 and 353, which is lost in all living Theria, but retained in living monotremes and living non-mammalian tetrapods (Tab. 4, chapter 2.2.2.). Its presence in the hypothetical

Theria sequence reflects the arithmetic of the Maximum Likelihood approach and indicates that it became lost independently in marsupials and placentals.

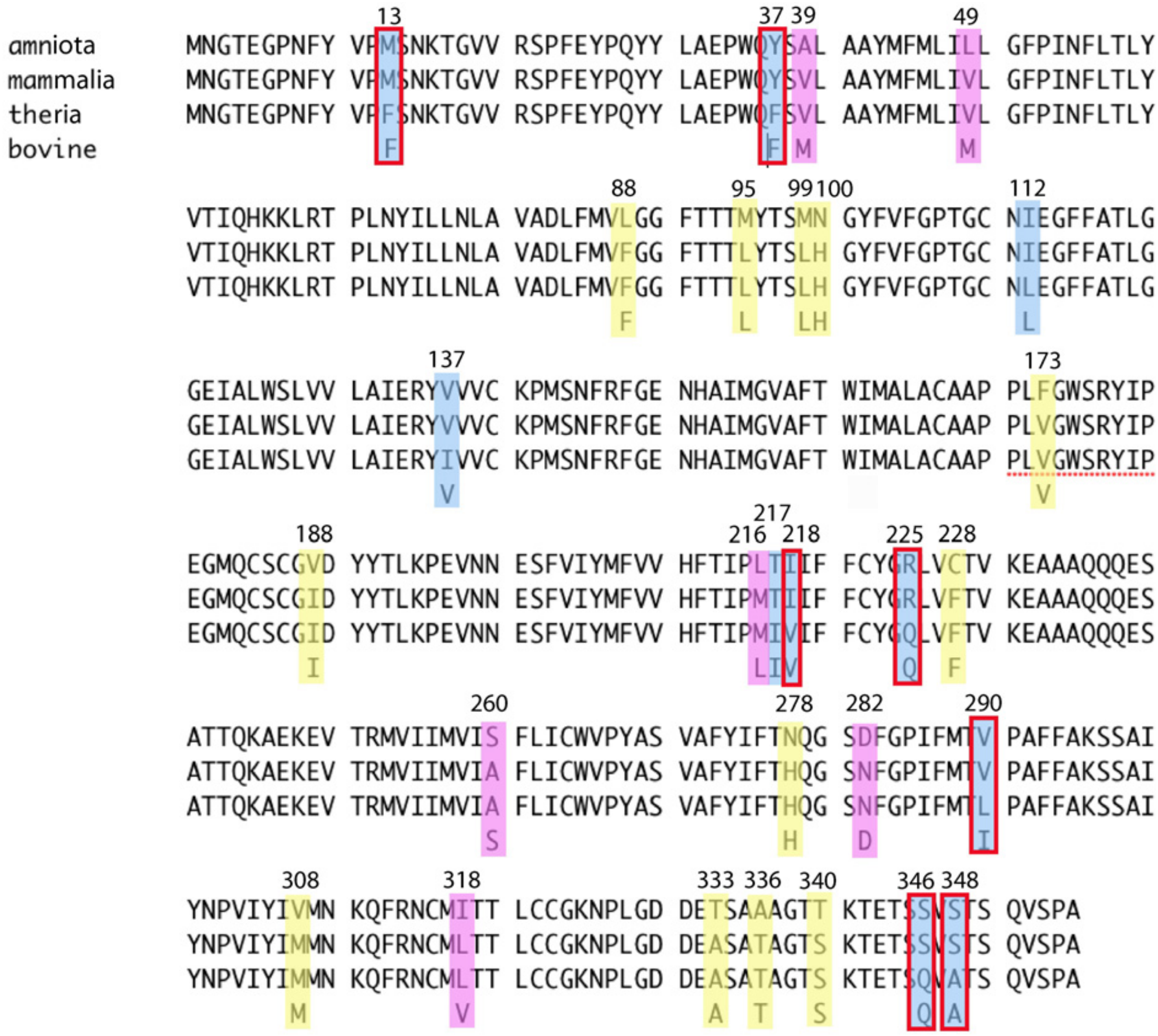

Figure 20. Amino acid alignment of the three inferred ancestral rhodopsins. Blue bars indicate residues where Amniota and Mammalia differ from Theria. Pink bars indicate residues where Amniota differs from Mammalia and Theria, and where Bovine is different from Mammalia and Theria. Yellow bars indicate residues where Amniota differs from Mammalia and Theria, and where Bovine shares the same residue with Mammalia and Theria. The red boxes indictate BEB sites inferred by PAML (Tab. 22, chapter 3.4.3.).

Future directions for research already involve creating and expressing mutants at some of these interesting sites, allowing the determination of if and which ones are responsible for differences in the biochemistry and functionality of the ancestral pigments. Such a study could potentially elucidate which changes these sites experienced while the organism was adapting to a new environment.

3.2.2. Rhodopsin 3D structure

Rhodopsin is a well studied G protein-coupled receptor. It is now possible to examine its 3D structure with the help of molecular visualization programs, such as PyMOL (www.pymol.org). This method helps to locate sites that might influence the biochemical and functional properties of the rhodopsin of various taxa. In addition, it is possible to infer the 3D structure of hypothetical rhodopsins based on their protein-coding sequence, in order to see if differing amino acids have any effect on the 3D structure of the protein.

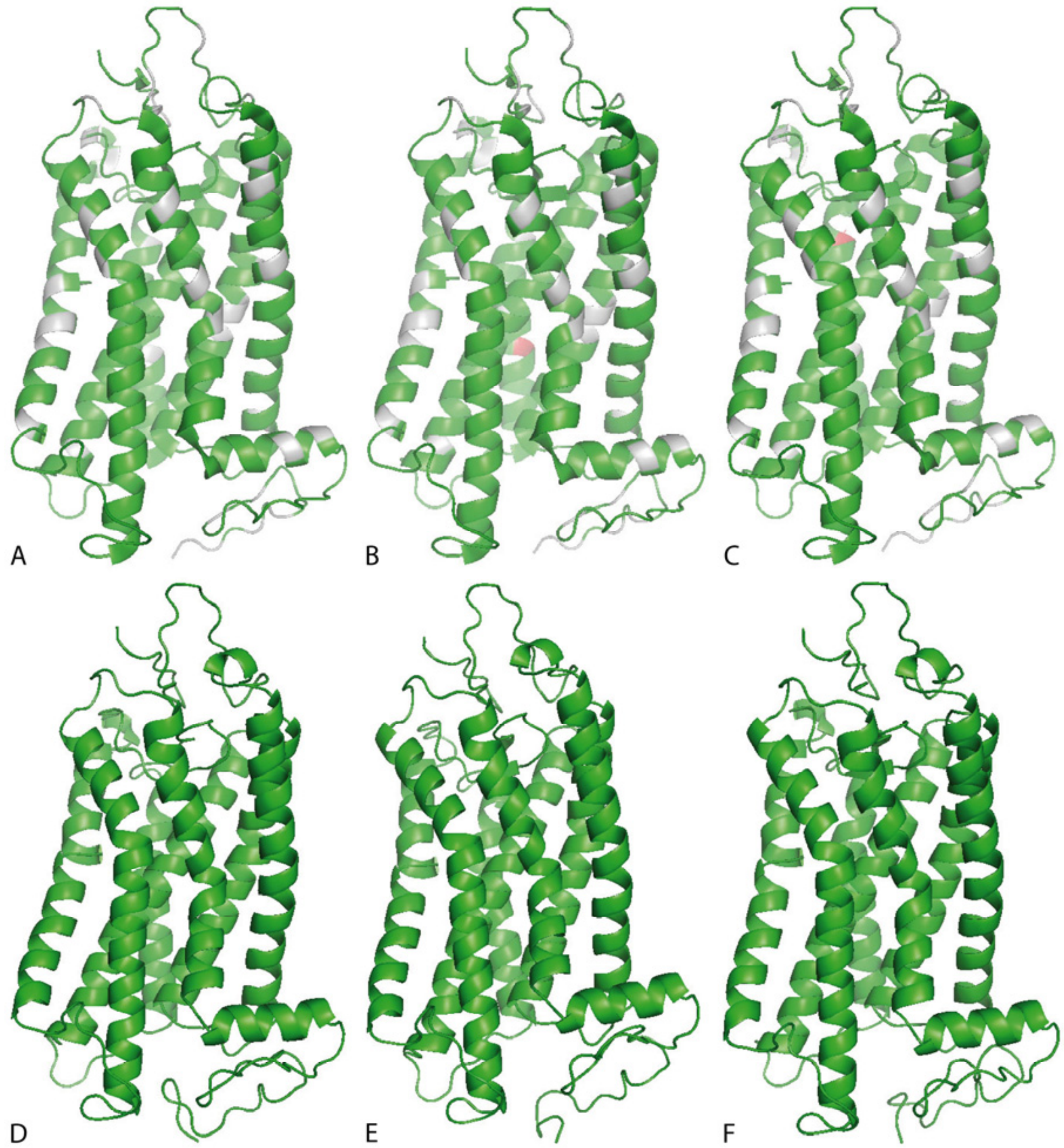

Figure 21. Rhodopsin 3D structure of all pigments from this study. (A) shows the echidna rhodopsin with amino acids differing from bovine rhodopsin highlighted in gray. Red marks indicate the substitutions of mutants (B) T158A and (C) F169A. (D-F) Ancestral pigments, i.e. (D) Amniota, (E) Mammalia, and (F) Theria.

3.3. Comparing protein-coding rhodopsin sequences from living taxa

Taking a closer look at the 27 tetrapod rhodopsin amino acid sequences, several interesting substitutions were identified, i.e. substitutions unique to a taxon, a monophyletic group, or individual clades (Tab. 4, chapter 2.2.2.).

3.3.1. Substitutions unique to a taxon

The lungfish bears the highest number of unique substitutions of all taxa studied, which is nine in total. This is followed by dunnart (seven substitutions), and toad, snake, anole, and bovine (five substitutions each).

The echidna has two unique substitutions at site 158 and 169, which were also chosen for site-directed mutagenesis (see chapter 2.1.3).

Interestingly, rhodopsin sequences from eutherian (placental) taxa, especially Euarchontoglires (i.e. Glires and Primates), do not exhibit that many unique substitutions compared to the rest of tetrapods. Furthermore, sequences of the manatee, dog, guinea pig, and human do not display a single unique substitution.

3.3.2. Substitutions unique to monophyletic groups

Reptiles, including birds, have a couple of very interesting unique features in their rhodopsin sequences: together with the lungfish, they have lost a residue at site 337; and at site 133, except for the alligator, they share a Valine instead of the Isoleucine present in all other taxa.

Amino acids shared by most mammalian sequences are at residues 95, 99, 100, 107, 216, 228, 308, 318, and 333.

Monotremes carry two unique substitutions, i.e. at residues 39 and 344. In general, they share more amino acids with reptilian and other non-mammalian vertebrates than with Theria, such as at residues 13, 83, 88, 112, 225, 346, and 348. In addition, monotreme sequences have an insertion of five amino acids between position 349 and 353, which is lost in Theria, but retained in lungfish, coelacanth, amphibian, and reptilian sequences (Hunt et al. 2003). These residues are known to interact with rhodopsin kinase (Nathans and Hogness 1983).

Marsupial rhodopsins have a Glutamic acid at residue 26, whereas other tetrapod taxa have a Tyrosine, except for unique substitutions in bovine and polar bear.

Placental sequences differ from all others, except for alligator and lungfish, only at site 63.

At site 333, Afrotheria have a unique substitution: a Glycine.

3.3.3. Similar substitutions in different clades

At site 338, lungfish and coelacanth are the only taxa that bear an amino acid at all; it is lost in all tetrapods. Lungfish and coelacanth sequences share an Aspartic acid with squamates at site 33, while all others have a Glutamic acid. At site 286, lungfish and coelacanth share a Valine with reptilian sequences, except for the chicken, which has an Isoleucine like mammals and amphibians. At residue 39, lungfish and coelacanth and reptiles share an Alanine, monotremes have a Valine, marsupials a Cysteine, and placentals a Methionine, except for the guinea pig.

At residue 290, amphibians share a Valine, reptiles and artiodactyls an Isoleucine, and marsupials, afrotherians, and carnivors a Leucine. All others are not consistent.

Amphibian and archosaur sequences share an Asparagine at site 277, all others have a Histidine.

Monotremes share a Valine with amphibians at site 81. At residue 88, they share a Leucine with amphibians and reptiles, except for salamander and chicken.

At residue 63, monotreme and marsupial rhodopsins share a residue with reptilian ones rather than placentals. And an Isoleucine at site 137 distinguishes monotremes and marsupials from placentals.

At site 37, therian rhodopsin sequences share a Phenylalanine with that of most reptiles.

Afrotheria have a few substitutions that they share with other groups, for example, at site 328 they have a Phenylalanine in common with lungfish and coelacanth and amphibians. At residue 331, they share a Glutamic acid with lungfish and coelacanth and some reptiles.

3.4. Selective constraint acting on the rhodopsin visual pigment

3.4.1. Introduction

In order to test the hypothesis that early mammals had indeed been nocturnal, selective pressure acting on the visual pigment resposible for vision at night, the rhodopsin, was assessed by using a maximum likelihood approach that estimates ω, which is the ratio of non-synonymous substitutions to synonymous substitutions. To determine the type and degree of selective constraint, branches of interest were selected as foreground branches with their own estimated ω, one that is different from the background branches, which have a combined ω estimated for all branches. When these two groups are compared, if one has a higher ω, then either the one with the higher ratio has experienced relaxed purifying selection, or the one with the lower value has undergone stronger purifying selection than the other. Positive selection is indicated if ω is significantly greater than 1.

Here, the amniote, reptilian, mammalian, monotreme, therian, marsupial, and placental branches were of interest and marked separately. Then, comparison of alternative and null models as well as significant LRTs tell us if there was positive or relaxed purifying selection acting on the rhodopsin.

3.4.2. Branch models

A comparison of MB2a and MB1n using siginficant LRTs determines whether the foreground branch is significantly different from the background d_N/d_S ratio. If the ω ratio of the foreground branch in MB2a is estimated to be greater than 1, this indicates either relaxed purifying or positive selection. Comparing MB2a and MB2n tests whether the branch of interest has a d_N/d_S ratio that is significantly different from 1, if supported by significant LRTs. If ω_1 is estimated to be greater than 1, positive selection is indicated.

The first branch of interest is the amniote one. With Amniota marked as a foreground branch, we find a value of 999 in model MB2a (Tab. 14). In PAML 4, the number 999 is the upper bound set for ω, meaning the actual value is not known, it might even represent infinity (Yang 2007). The LRT of the comparison of MB2a and MB1n does not show significance. Hence, the foreground value 999 is not significantly different from the background value 0.0532 and, thus, there is no indication for any positive selection along this branch (Tab. 14). Testing whether this value is significantly different from 1, does not show statistical significance using the LRT comparing models MB2a and MB2n (Tab. 14). However, because the foreground ratio is much larger than the background branch, this indicates slightly relaxed selective constraint.

Table 14. Branch model estimates for the branch Amniota. np is number of parameters, LnL is log likelihood of the model.

Model	ω_0	ω_1	np	LnL	p-value
Alternative model MB2a	0.0532	999	54	-10646.2	
First null model MB1n	0.05432	0.05432	53	-10649.5	MB2a vs MB1n 0.0703

Model	ω_0	ω_1	np	LnL	p-value
Second null model MB2n	0.0533	1	53	-10646.3	MB2a vs MB2n 0.8069

In the reptilian branch, the foreground ratio in null model MB2n is 999 compared to a background ratio of 0.0537 (Tab. 15). However, neither LRTs of comparing models MB2a and MB1n nor models MB2a and MB2n provide statistical support (Tab. 15). As for Amniota, this also suggests slightly relaxed purifying selection.

Table 15. Branch model estimates for the branch Reptilia. np is number of parameters, LnL is log likelihood of the model.

Model	ω_0	ω_1	np	LnL	p-value
Alternative model MB2a	0.0537	999	54	-10647.5	
First null model MB1n	0.05432	0.05432	53	-10649.5	MB2a vs MB1n 0.1549
Second null model MB2n	0.0537	1	53	-10647.6	MB2a vs MB2n 0.7218

For Mammalia, the alternative model MB2a, with foreground and background ratios estimated separately, estimates a foreground ratio of 0.0794 and a background ratio of 0.0538 (Tab. 16). The LRT comparing MB2a and MB1n is not significant and indicates that this value is not significantly different from the background ratio (Tab. 16). However, the LRT comparing MB2a and MB2n is statistically significant (Tab. 16). The foreground ratio is significantly different from 1, and since it is close to the background ratio, this is an indication of purifying selection similar to the background branches.

Table 16. Branch model estimates for the branch Mammalia. * indicates statistical significance. np is number of parameters, LnL is log likelihood of the model.

Model	ω_0	ω_1	np	LnL	p-value
Alternative model MB2a	0.0538	0.0794	54	-10649.0	
First null model MB1n	0.05432	0.05432	53	-10649.5	MB2a vs MB1n 0.4965
Second null model MB2n	0.0522	1	53	-10656.9	MB2a vs MB2n 0.0049*

In monotremes, the estimated foreground ratio is less than 1, more precisely 0.0209 compared to a background ratio of 0.056 (Tab. 17). Both model comparisons that are different from the background and also different from 1, are found to be statistically significant by the LRTs (Tab. 17). Hence, stronger purifying selection than the background branches was detected in the monotreme branch.

Table 17. Branch model estimates for the branch Monotremata. * indicates statistical significance. np is number of parameters, LnL is log likelihood of the model.

Model	ω_0	ω_1	np	LnL	p-value
Alternative model MB2a	0.056	0.0209	54	-10645.6	
First null model MB1n	0.05432	0.05432	53	-10649.5	MB2a vs MB1n 0.0490*
Second null model MB2n	0.0514	1	53	-10681.5	MB2a vs MB2n 0.000000002*

In the therian branch, a foreground ratio of 8.7588 was estimated in the null model MB2a (Tab. 18). The LRT comparing MB2a and MB1n indicates that this foreground ratio is significantly different from the background ratio 0.0528 (Tab. 18). But testing whether the elevated ω is significantly different from 1 by comparing MB2a and MB2n, we do not find statistical support by the LRT (Tab. 18). However, since ω is still greater than the background ratio, this indicates relaxed purifying or weak positive selection compared to the background.

Table 18. Branch model estimates for the branch Theria. * indicates statistical significance. np is number of parameters, LnL is log likelihood of the model.

Model	ω_0	ω_1	np	LnL	p-value
Alternative model MB2a	0.0528	8.7588	54	-10644.3	
First null model MB1n	0.05432	0.05432	53	-10649.5	MB2a vs MB1n 0.0224*
Second null model MB2n	0.0529	1	53	-10644.3	MB2a vs MB2n 0.8332

For Marsupialia, a foreground ratio of 0.0186 and a background ratio of 0.00553 was estimated (Tab. 19). The comparison of models MB2a and MB1n using the LRT does not find statistical support, but there is support when comparing MB2a and MB2n (Tab. 19). Since ω_1 is close to the background ω and significantly smaller than 1, this indicates that purifying selection, similar to that of the background, was acting along this branch.

Table 19. Branch model estimates for the branch Marsupialia. * indicates statistical significance. np is number of parameters, LnL is log likelihood of the model.

Model	ω_0	ω_1	np	LnL	p-value
Alternative model MB2a	0.0553	0.0186	54	-10647.5	
First null model MB1n	0.05432	0.05432	53	-10649.5	MB2a vs MB1n 0.1548
Second null model MB2n	0.0532	1	53	-10659.5	MB2a vs MB2n 0.0005*

The last branch of interest is Placentalia. The foreground ratio is 0.0044, compared to a background ratio of 0.0526 (Tab. 20). Both LRTs provide statistical significance, indicating that ω_1 is not only significantly different from ω_0 but also from 1. Because ω_1 is approaching 0 this is evidence for purifiying selection (Tab. 20). Since the estimated foreground ratio is also much smaller than the background ratio, this indicates even stronger purifying selection along this branch compared to the background branches (Tab. 20).

Table 20. Branch model estimates for the branch Placentalia. * indicates statistical significance. np is number of parameters, LnL is log likelihood of the model.

Model	ω_0	ω_1	np	LnL	p-value
Alternative model MB2a	0.0526	0.0044	54	-10633.0	
First null model MB1n	0.05432	0.05432	53	-10649.5	MB2a vs MB1n 0.00005*
Second null model MB2n	0.0520	1	53	-10692.33	MB2a vs MB2n < 0.0000000001*

3.4.3. Branch-site models

However, positive selection acts on sites. If there are a lot of sites positively selected along a branch of interest, this signal will be detected by branch models. But if there are only a few sites experiencing positive selection, their signal might be overruled by the other negatively selected sites along that branch. In order to test whether positive selection is acting only on a few sites, branch-site models that detect single positively selected sites, were applied as well. In branch-site models, the comparison of alternative model MA and first null model M1a, tests whether there are sites with a ω greater than 1. It is a test for either positive selection or relaxed purifying selection (Yang 2007). Comparing the alternative model MA and the second null model MA1 tests whether sites with an elevated ω ratio are indeed significantly greater than 1. This tests for positive selection only and is called the branch-site test of positive selection (Yang 2007).

For the amniote branch, model MA detects positively selected sites which is indicated by the estimated ω_{2a+b} value 10.643 (Tab. 21). However, the LRT comparing models MA and M1a does not provide statistical support, neither does the LRT comparing models MA and MA1 (Tab. 21). Thus, there is no indication for positive selection, nor for relaxed purifying selection. However, the BEB analysis did identify six positively selected sites, but all show low posterior probabilities < 95% (Tab. 22).

Table 21. Branch-site model estimates for the branch Amniota. np is number of parameters, df is degrees of freedom in Likelihood Ratio Test, LnL is log likelihood of the model.

Model	ω	np	df	LnL	p-value
Alternative model MA	$\omega_0 = 0.04521$ $\omega_1 = 1$ $\omega_{2a} = 10.643$ $\omega_{2b} = 10.643$	56		-10567.6	
First null model M1a	$\omega_0 = 0.04565$ $\omega_1 = 1$	54	2	-10567.7	MA vs M1a 0.40568
Second null model MA1	$\omega_0 = 0.0453$ $\omega_1 = 1$ $\omega_{2a} = 1$ $\omega_{2b} = 1$	55	1	-10569.4	MA vs MA1 0.67395

Table 22. Positively selected sites estimated by BEB analysis in branch-site model MA (Yang et al. 2005), with posterior probabilities, for branches Amniota, Reptilia, Monotremata, Theria, Marsupialia, and Placentalia. Numbers in brackets refer to numbering in bovine rhodopsin. The programm PAML prints out an * if the posterior probability is > 95%, and ** if the probability is > 99% (Yang 2007).

Branch of interest marked as foreground branch	Positively selected site	Posterior probability	Mutation
Amniota	46	0.535	F
	93	0.568	V
	328	0.903	F
	335	0.773	S
	344 (342)	0.899	A
	349 (347)	0.896	S
Reptilia	290	0.611	A
	336	0.900	A
Monotremata	344 (342)	0.992**	Q
Theria	13	0.997**	M
	37	0.967*	Y
	49	0.575	L
	162	0.534	I
	218	0.653	V
	225	0.993**	R
	290	0.921	A
	345 (343)	1.000**	S
	346 (344)	1.000**	S
	348 (346)	0.972**	S
Marsupialia	26	0.987*	Y
	39	0.979*	A
Placentalia	39	0.546	A

In Reptilia, again, the alternative model MA identifies positively selected sites, which is displayed by the elevated ω of 12.236 in site class ω_{2a+b} (Tab. 23). But neither comparing models MA and M1a nor models MA and MA1 show statistical support by the LRTs (Tab. 23). So again, there is no evidence for relaxed purifying or positive selection along this branch. Nevertheless, the BEB analysis estimated two positively selected sites, though with low posterior probabilities < 95% (Tab. 22).

Table 23. Branch-site model estimates for the branch Reptilia. np is number of parameters, df is degrees of freedom in Likelihood Ratio Test, LnL is log likelihood of the model.

Model	ω	np	df	LnL	p-value
Alternative model MA	$\omega_0 = 0.04525$ $\omega_1 = 1$ $\omega_{2a} = 12.236$ $\omega_{2b} = 12.236$	56		-10568.6	
First null model M1a	$\omega_0 = 0.04565$ $\omega_1 = 1$	54	2	-10567.7	MA vs M1a 0.68249
Second null model MA1	$\omega_0 = 0.04527$ $\omega_1 = 1$ $\omega_{2a} = 1$ $\omega_{2b} = 1$	55	1	-10568.6	MA vs MA1 0.8792

In Mammalia, the estimated ω_{2a+b} value is 1 (Tab. 24). This indicates that there are no sites under positive selection in the foreground branch. Also, statistical support for testing for positive selection or relaxed purifying selection is not given by the LRTs (Tab. 24). The results suggest that the mammalian branch has a similar selective constraint to the background branch.

Table 24. Branch-site model estimates for the branch Mammalia. np is number of parameters, df is degrees of freedom in Likelihood Ratio Test, LnL is log likelihood of the model.

Model	ω	np	df	LnL	p-value
Alternative model MA	$\omega_0 = 0.04507$ $\omega_1 = 1$ $\omega_{2a} = 1$ $\omega_{2b} = 1$	56		-10568.9	
First null model M1a	$\omega_0 = 0.04565$ $\omega_1 = 1$	54	2	-10567.7	MA vs M1a 0.77565
Second null model MA1	$\omega_0 = 0.04527$ $\omega_1 = 1$ $\omega_{2a} = 1$ $\omega_{2b} = 1$	55	1	-10568.9	MA vs MA1 1

Also in the monotreme branch, the MA model identified positively selected sites as indicated by the value 50.166 in site class ω_{2a+b} (Tab. 25). Neither model comparison provides statistical significance using the LRTs. The monotreme branch has a selective constraint similar to the background branch (Tab. 25). However, the BEB analysis estimated one positively selected site, but since the LRT comparing models MA and MA1 was not significant, this predicted site is not statistically significant either (Tab. 22).

Table 25. Branch-site model estimates for the branch Monotremata. np is number of parameters, df is degrees of freedom in Likelihood Ratio Test, LnL is log likelihood of the model.

Model	ω	np	df	LnL	p-value
Alternative model MA	$\omega_0 = 0.04537$ $\omega_1 = 1$ $\omega_{2a} = 50.166$ $\omega_{2b} = 50.166$	56		-10566.1	
First null model M1a	$\omega_0 = 0.04565$ $\omega_1 = 1$	54	2	-10567.7	MA vs M1a 0.19004
Second null model MA1	$\omega_0 = 0.04541$ $\omega_1 = 1$ $\omega_{2a} = 1$ $\omega_{2b} = 1$	55	1	-10568.5	MA vs MA1 0.11969

For Theria, the MA model estimates a high ω_{2a+b} ratio of 999 (Tab. 26). This is a signal for positively selected sites. This time, both the comparison of models MA and M1a as well as the one of models MA and MA1 are statistically significant, which is indicated by the LRTs (Tab. 26). This is a clear signal of positive selection acting on sites along this branch. In a second step, the BEB analysis estimated ten BEB sites in total, but only six have posterior probabilites >95% and are, thus, reliable (Tab. 22).

Table 26. Branch-site model estimates for the branch Theria. * indicates statistical significance. np is number of parameters, df is degrees of freedom in Likelihood Ratio Test, LnL is log likelihood of the model.

Model	ω	np	df	LnL	p-value
Alternative model MA	$\omega_0 = 0.04443$ $\omega_1 = 1$ $\omega_{2a} = 999$ $\omega_{2b} =999$	56		-10549.8	
First null model M1a	$\omega_0 = 0.04565$ $\omega_1 = 1$	54	2	-10569.4	MA vs M1a 0.000055*
Second null model MA1	$\omega_0 = 0.04443$ $\omega_1 = 1$ $\omega_{2a} = 1$ $\omega_{2b} = 1$	55	1	-10559.0	MA vs MA1 0.00241*

A signal of positively selected sites was also detected along the marsupial branch, as indicated by the ω_{2a+b} value 509.91 in the alternative model MA (Tab. 27). Statistical support is given by the LRT of comparing MA and MA1, which means that the sites which are greater than 1 are significantly greater than 1, an indication for positive selection (Tab. 27). Two predicted BEB sites with confident posterior probabilities < 95% are shown in Table 22.

Table 27. Branch-site model estimates for the branch Marsupialia. np is number of parameters, df is degrees of freedom in Likelihood Ratio Test, LnL is log likelihood of the model.

Model	ω	np	df	LnL	p-value
Alternative model MA	$\omega_0 = 0.04553$ $\omega_1 = 1$ $\omega_{2a} = 509.91$ $\omega_{2b} = 509.91$	56		-10563.3	
First null model M1a	$\omega_0 = 0.04565$ $\omega_1 = 1$	54	2	-10567.7	MA vs M1a 0.04848*
Second null model MA1	$\omega_0 = 0.04546$ $\omega_1 = 1$ $\omega_{2a} = 1$ $\omega_{2b} = 1$	55	1	-10568.0	MA vs MA1 0.03139*

In the placental branch, the ω_{2a+b} ratio was estimated to equal 1, indicating the presence of no positively selected sites along this branch (Tab. 28). However, neither model comparison is statistically supported by the LRTs (Tab. 28). Thus, no evidence for relaxed purifying or positive selection is found. For placentals, the BEB analysis estimated one positively selected site with a low posterior probability < 95% (Tab. 22).

Table 28. Branch-site model estimates for the branch Placentalia. np is number of parameters, df is degrees of freedom in Likelihood Ratio Test, LnL is log likelihood of the model.

Model	ω	np	df	LnL	p-value
Alternative model MA	$\omega_0 = 0.04565$ $\omega_1 = 1$ $\omega_{2a} = 1$ $\omega_{2b} = 1$	56		-10569.4	
First null model M1a	$\omega_0 = 0.04565$ $\omega_1 = 1$	54	2	-10567.7	MA vs M1a 1

Model	ω	np	df	LnL	p-value
Second null model MA1	$\omega_0 = 0.04565$ $\omega_1 = 1$ $\omega_{2a} = 1$ $\omega_{2b} = 1$	55	1	-10569.4	MA vs MA1 1

3.4.4. Summary

In conclusion, the branch-site analyses found evidence for positive selection acting only on the rhodopsin along the branches Theria and Marsupialia (Fig. 22). All other branches experienced slightly relaxed purifying selection (Amniota and Reptilia), purifying selection similar to background branches (Mammalia), or even stronger purifying selection compared to the background branch (Monotremata and Placentalia) (Fig. 22).

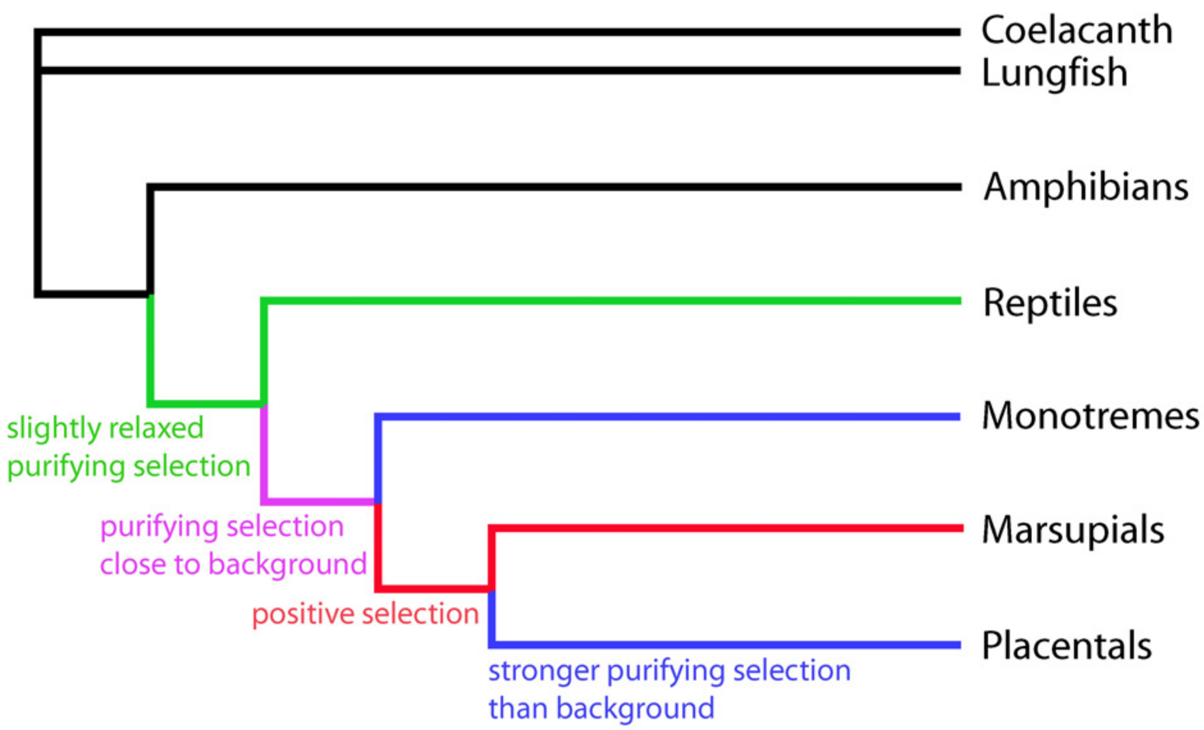

Figure 22. Summary figure showing selective constraints acting on rhodopsin along branches and on sites.

4. Discussion

4.1. Nocturnal vs. diurnal

4.1.1. Characterisation of the echidna rhodopsin

The rhodopsin of the short-beaked echidna was successfully expressed *in vitro* and was found to be functional, as indicated by the dark and light absorption spectra (Fig. 17B, chapter 3.1.4.). With a λ_{max} at 496.5 nm, it absorbs light in a more blue-shifted range than that of bovine. The rhodopsin of its sister taxon, the platypus, has its absorption peak at 498 nm (Davies et al. 2007).

Though the bleaching with HCl acid did not take place as quickly in the echidna as in the bovine, the formation of the protonated Schiff base was complete within the first 5 minutes, which also indicates that this pigment is functional (Fig. 18B, chapter 3.1.5.). The molar extinction coefficient was determined to be 34 921 M^{-1} cm^{-1}, which is much lower than that predicted for bovine (Tab. 11, chapter 3.1.5.) (Wald and Brown 1953, Shichi et al. 1969, Daemen et al. 1970, Hong and Hubbell 1972, Oprian et al. 1987). The molar extinction coefficient is a measure of how strongly a protein absorbs light at a given wavelength. Since one photoexcited rhodopsin molecule activates hundreds of copies of transducin (Sagoo and Lagnado 1997, Menon et al. 2001), one would assume that for vision at low light levels, the rhodopsin would be adapted to absorb a single photon very strongly and trigger the activation of as many transducin molecules as possible. Thus, one would expect the rhodopsin of a nocturnal animal to be better adapted to scotopic vision, displaying a high molar extinction coefficient.

In the hydroxylamine assay, the echidna rhodopsin, as well as its two mutants, reacted to hydroxylamine more than bovine and the ancestral rhodopsins (Fig. 19B, chapter 3.1.6.). Since this assay has commonly been used to characterise rod and cone opsins, this result suggests that the expressed echidna rhodopsin is cone-like. However, cone opsins react to hydroxylamine much stronger (Imai et al. 1995, Das et al. 2004).

The determination of the meta II decay rate, which is the active state of rhodopsin in which the GDP- for GTP-exchange on the G-protein transducin is catalyzed, thereby activating it and eventually generating an electrical response in the photoreceptor cell, provides an interesting result (Tab. 13, chapter 3.1.7.). With a mean value of 7.92 min^{-1}, the echidna rhodopsin has a much lower $t_{1/2}$ than bovine (13.38 min^{-1}).

It has been suggested that having a longer signaling state increases the sensitivity of the photoreceptor cells (Imai et al. 1997, Kuwayama et al. 2002, Shichida and Matsuyama 2009). Thus, a higher meta II time constant would be advantageous for scotopic vision (Sugawara et al. 2010). Cones, which are less photosensitive than rods, show considerably faster meta II decay rates than rods and less activation of the visual transduction cascade (Wald et al. 1955, Wilden et al. 1986, Langlois et al. 1996). Hence, with a $t_{1/2}$ half that of bovine, the echidna rhodopsin displays another cone-like characteristic.

It has also been shown that rhodopsins sometimes display cone-like characteristics and cones sometimes behave rod-like (Crescitelli 1980, Crescitelli 1988, Kawamura and Yokoyama 1998, Yokoyama and Blow 2001). In the gecko, which has a pure rod retina, the green Rh2 cone pigment shows rod-like biochemical characteristics (Crescitelli 1980, Crescitelli 1988). In the anole, the SWS2 cone pigment displays a rod-like insensitivity to hydroxylamine; a result which is still open to interpretation (Kawamura and Yokoyama 1998). On the other hand, the anole rhodopsin is sensitive to hydroxylamine, and thus cone-like, probably as an adaptation to a pure cone retina (Kawamura and Yokoyama 1998). Yokoyama and Blow (2001) suggested that substituting a Glycine (G) for a Methionine (M) at site 89 is likely to serve as determinant of rod and cone properties. However, the echidna has a Glycine (G) at this site, like all other taxa included in this study (Tab. 4, chapter 2.2.2.). Imai et al. (1997) suggested that substitutions at site 122 are associated with rod and cone pigments, as E122Q and E122I bovine rhodopsin mutants showed sensitivity to hydroxylamine. However, both the gecko and the echidna rhodopsin have a Glutamate (E) at this site (Tab. 4, chapter 2.2.2.).
Furthermore, rhodopsins can be expressed in cones, and cone opsins in rods (Kawamura and Yokoyama 1998). In the tiger salamander, the Rh2 rods and SWS2 cones both contain the same SWS2 opsin, but use different transducin types (Ma et al. 2001).
The echidna has long been thought to possess a pure rod retina (Walls 1942, O'Day 1952); a finding which was refuted by the identification of twin cones present in the retina (Young and Pettigrew 1991). Thus, the cone-like meta II decay rate and the hydroxylamine sensitivity of the echidna rhodopsin might reflect an adaptation to rhodopsin being expressed in twin cones as well and thus, show cone-like characteristics as an adapatation to expression in cones, as is the case in the anole (Kawamura and Yokoyama 1998). Investigating the biochemical properties of the cone pigments of the echidna would be an interesting study possibly providing more clearity.

However, the results derived from this study as well as others (Crescitelli 1980, Crescitelli 1988, Kawamura and Yokoyama 1998, Yokoyama and Blow 2001) point out how variable visual pigments, even from the same opsin class, are in their biochemical and functional properties and that changes are not necessarily a result of ecological constraint, as previously assumed.

The echidna rhodopsin displays many reptilian characteristics in its eye, such as morphologically similar bipolar cells, a cartilaginous sclera, and a flattened lense (Bolk et al. 1934, Young and Pettigrew 1991). Interestingy, in the rhodopsin amino acid sequence, there is an observable trend that monotremes more frequently share the same residue with reptiles and other non-mammalian vertebrates than with Theria (see chapter 3.3.2. and 3.3.3.). At rather conservative residues, only nine amino acids are shared with other mammalian taxa, whereas twelve amino acids are shared with non-mammals (Tab. 4, chapter 2.2.2.). Most interesting is an insertion of five amino acids at the end of the amino acid sequence in monotremes and all non-mammalian taxa, which is known to interact with rhodopsin kinase, which is a downstream effector of rhodopsin and, thus, a crucial component in the visual signaling cascade (Nathans and Hogness 1983).

A mosaic of derived and plesiomorphic characters in monotremes, as present in the rhodopsin amino acid sequence, has also been reported from anatomic, genomic, physiological, and developmental studies (Bolk et al. 1934, Gresser and Noback 1935, Griffiths 1989, Young and Pettigrew 1991, Warren et al. 2008, Werneburg and Sánchez-Villagra 2010). On the one hand, these findings strengthen the yet controversial Theria hypothesis that monotremes are the most basal mammals (Janke et al. 2002, Rowe et al. 2008). On the other hand, the odd mosaic pattern in the echidna amino acid sequence might be responsible for the cone-like and yet contradictory results derived from the functional and biochemical assays.

4.1.2. Characterisation of the two echidna mutants

As seen in Figure 17C-D (chapter 3.1.4.), the expression of the two echidna mutants T158A and F169A was also successful and both pigments are functional. With 494.5 nm and 495.5 nm for T158A and F169A, respectively, the determined λ_{max} are close to the one determined for the echidna rhodopsin, which is a bit blue-shifted from where bovine has its absorption peak.

For the acid bleach, the protonated Schiff base had formed in mutant F169A as fast as in bovine, whereas in mutant T158A it took a bit longer. This result nevertheless indicates that both expressed pigments are functional (Fig. 18C-D, chapter 3.1.5.).

The molar extinction coefficients vary: with a value of 31 411 M^{-1} cm^{-1}, mutant T158A has a ε similar to the one determined for echidna, whereas F169A (40 254 M^{-1} cm^{-1}) has a ε similar to bovine rhodopsin (Tab. 11, chapter 3.1.5). The molar extinction coefficient is a measure of how strongly the rhodopsin absorbs light at λ_{max}. Thus, this result suggests that site 169 affects the strength of photon absorption in the echidna. Borhan et al. (2000) figured that site 169, which is not a conserved residue in the GPCR family of proteins, is cross-linked to the all-*trans* chromophore in intermediates lumirhodopsin, meta I, and meta II (Fig. 13, chapter 2.1.8.). Furthermore, this site is likely to be involved in transducin activation (Borhan et al. 2000). Only two of seven rhodopsins expressed in this study, i.e. echidna and T158A mutant, display a low ε, and, interestingly, these two have a Phenylalanine (F) instead of an Alanine (A) at site 169, suggesting that a F, as opposed to an A, decreases the strength of photon absorption as measured by the molar extinction coefficient. However, the benefit of decreasing the strength of photon absorption in the nocturnal echidna remains to be elucidated. For future research, it would be interesting to determine the ε of the platypus rhodopsin, as it has a unique Leucine (L) at this site (Tab. 4, chapter 2.2.2.).

Together with the echidna rhodopsin, the two mutants show sensitivity to hydroxylamine (Fig. 19C-D, chapter 3.1.6.). The strong increase in relative difference absorbance at 363 nm, which is where the retinal oxime absorbs, indicates that the hydroxylamine entered the chromophore binding pocket as it does in cones (Kawamura and Yokoyama 1998). However, the assay was only performed twice for the two mutants, due to technical reasons, and should be reproduced for reliability. Still, the present finding suggests that the echidna is sensitive to hydroxylamine and that substitutions at site 158 and 169 are not involved in regulating this.

4.1.3. Inferring life habits from absorption maxima of living taxa

It has long been hypothesised that the range of absorption maxima in rhodopsin corresponds with life habits in vertebrates (Chang et al. 2002a, Chang 2003, Yokoyama et al. 2008, Zhao et al. 2009b). In particular, a red-shifted absorption range (> 500 nm) is said to be advantageous for vision at low-light levels, whereas a blue-shifted absorption range (< 500 nm) is said to be an adaptation to a deep-water habitat (Muntz 1976, Yokoyama et al. 2008). Yokoyama et al. (2008) classified rhodopsins into four classes based on their absorption maxima and light environments: deep-sea (≈ 480-485 nm), intermediate (≈ 490-495 nm), surface (≈ 500-507 nm), and terrestrial red-shifted (≈ 525 nm). Chang et al. (2003) pointed out that birds tend to have longer wavelength-absorbing rhodopsins. In addition, a number of studies focus on spectral tuning sites, accepting the assumption that the absorption range allows for inferences of life habits (Kochendörfer et al. 1999, Altun et al. 2008, Zhao et al. 2009b). Sugawara et al. (2010) hypothesized that substitutions at sites 83 and 292 are responsible for a blue-shift in λ_{max} values indicating adaptation to a deep-water habitat.

However, this assumption has never been verified nor statistically tested. Thus, the aim was to statistically test if there is a correlation between wavelength absorption and lifestyle, and if a potential correlation is linked to phylogeny. Therefore, absorption maxima of 42 tetrapod taxa were collected from the literature and the life habits of the taxa were classified into three groups, i.e. 1 for diurnal, 2 for nocturnal, and 3 for aquatic or semi-aquatic (Tab. 29).

Table 29. 42 tetrapod taxa used in a Kruskal-Wallis test. Lifestyle: 1 corresponds to diurnal, 2 to nocturnal, and 3 to aquatic life habits.

Taxon	λ_{max}	Lifestyle	Reference
Alligator mississippiensis	499	3	Lythgoe 1972, Smith et al. 1995
Ambystoma tigrinum	502	2	Makino et al. 1999
Anas platyrhynchos	505	1	Bowmaker et al. 1997
Anolis carolinensis	491	1	Kawamura and Yokoyama 1998
Bos taurus	500	1	Nathans and Hogness 1983
Bufo bufo	502	2	Ala-Laurila et al. 2002, Fyhrquist et al. 1998
Bufo marinus	503	1	Ala-Laurila et al. 2002, Fyhrquist et al. 1998
Caluromys philander	504	2	Hunt et al. 2003
Carassius auratus	492	3	Chang et al. 2002a
Columba livia	504	1	Bowmaker et al. 1997, Yokoyama et al. 2008
Coturnix japonica	505	1	Bowmaker et al. 1997
Felis felis	500	2	Bridges 1970
Gallus gallus	504	1	Bowmaker et al. 1997, Yokoyama et al. 2008
Globicephala melas	488	3	Fasick and Robinson 2000
Harbour seal	501	3	Fasick and Robinson 2000
Homo sapiens	495	1	Chang et al. 2002a
Leiothrix lutea	500	1	Bowmaker et al. 1997
Macaca fascicularis	491	1	Baylor et al. 1984, Schnapf et al. 1988, Nickels et al. 1995
Melopsittacus undulatus	509	1	Bowmaker et al. 1997
Mesoplodon bidens	484	3	Fasick and Robinson 2000
Mirounga angustirostris	483	3	Southall et al. 2002
Mus musculus	498	2	Lythgoe 1972, Baehr et al. 1988
Ornithorhynchus anatinus	498	3	Davies et al. 2007

Taxon	λ_{max}	Lifestyle	Reference
Oryctolagus cuniculus	502	2	Chang et al. 2002a
Petromyzon marinus	500	3	Zhang and Yokoyama 1997
Phoca groenlandicus	498	3	Fasick and Robinson 2000
Physeter macrocephalus	483	3	Southall et al. 2002
Polychrus marmoratus	497	1	Loew et al. 2002
Puffinus puffinus	505	1	Bowmaker et al. 1997
Python regius	494	2	Sillman et al. 1999
Raja erinacea	500	3	Chang et al. 2002a
Rana pipiens	502	2	Chang et al. 2002a
Rana temporaria	502	2	Koskelainen et al. 2000
Rattus norvegicus	500	2	Chang et al. 2002a
Sminthopsis crassicaudata	512	2	Hunt et al. 2003.
Spheniscus humboldti	504	3	Bowmaker et al. 1997
Strix aluco	503	2	Bowmaker et al. 1997
Tachyglossus aculeatus	497	2	
Taeniopygia guttata	504	1	Bowmaker et al. 1997, Yokoyama et al. 2008
Trichechus manatus	502	3	Fasick and Robinson 2000
Xenopeltis unicolor	499	2	Davies et al. 2009
Xenopus laevis	502	3	Koskelainen et al. 2000

Analysis of variance (ANOVA) is the most commonly used technique for comparing the means of groups of measurement data. This kind of test is used when one deals with a nominal variable, which classifies observations into categories, and a measurement variable. The Kruskal-Wallis test is the non-parametric version of a one-way ANOVA and compares the medians of three or more samples (Fowler et al. 1995).

With a p-value = 0.5053, there are no significant differences in the medians between the samples. Interestingly, this indicates that inferring a lifestyle based on an animal's rhodopsin absorption maximum is not statistically founded. Though it has been shown that amino acid substitutions at particular sites cause shifts in wavelength absorption, this study shows that ecological inferences based on λ_{max} are not justified (Janz and Farrens 2001).

Since the Kruskal-Wallis test revealed that there is no correlation between wavelength absorption and lifestyle based on our data, a second test for correlation which also considers phylogeny (e.g. Independent Contrast Analysis) was redundant.

However, it should also be pointed out that one weak point of this analysis might be that published absorption maxima were determined inconsistently by differing methods, i.e. either after expression in COS-1 or HEK293 cells, or rhodopsins were purified from ROS, or they were determined using microspectrophotometry (MSP). Others determined the λ_{max} based on a difference spectrum (dark spectrum - light spectrum) after *in vitro* expression. However, the effect on the consistency of the measurement based on the method of data acquisition has never been elucidated either. It would be useful to test if the various methods of λ_{max} determination produce significantly different results.

4.1.4. Conclusions

The expressed echidna and its two mutant rhodopsins are functional pigments as indicated by the dark and light absorption spectra. Acid treatment also showed that the pigments are functional. Hydroxylamine assays and meta II decay rates by fluorescence spectroscopy indicate some cone-like properties of the three rhodopsins, which might have resulted from expression of rhodopsin in twin cones present in the echidna retina. Furthermore, though the role of the molar extinction coefficient in dim-light vision is not yet elucidated in detail, a substitution at site 169 has been found to be involved in decreasing the strength of photon absorption in the echidna. Paradoxically, a low ε appears disadvantegeous for scotopic vision.

The echidna rhodopsin seems to have achieved cone-like characteristics during its evolution, picturing its rhodopsin to be as enigmatic as the animal itself. Furthermore, it was shown that the protein-coding sequence of the rhodopsin of monotremes shares more amino acids with reptiles and amphibians than with other mammals. This mosaic pattern might be responsible for the yet contradictory results from the biochemical and functional assays.

A statistical test rejected any relationship between absorption maxima and life habits at different light levels. Thus, any habitat categorisation based on λ_{max}, as is commonly done, is deficient.

The results interestingly show that, in contrast to prior assumptions, variation in the biochemical and functional properties of visual pigments seem unlikely to be due to ecological constraints, but rather result from interactions of the various proteins involved in the visual signaling cascade.

4.2. The ancestral rhodopsins

4.2.1. Characterisation of the three ancestral rhodopsins

The three inferred and successfully *in vitro* expressed ancestral pigments bound to 11-*cis* retinal to form functional pigments, as indicated by dark and light spectra (Fig. 17E-G, chapter 3.1.4.). The treatment with HCl acid showed that all pigments denatured within the first five minutes, which also indicates that all are functional pigments (Fig. 18E-G, chapter

3.1.5.). The functionality of these pigments is important, as the amino acid sequences were inferred using Maximum likelihood estimates; if they had not shown any functionality, the inference would have borne errors and the models chosen would have to be changed to better fit the data.

The expressed ancestral pigments have absorption peaks at 500 nm, 501 nm, and 500.5 nm for Amniota, Mammalia, and Theria, respectively, which is within the close range of bovine rhodopsin (Oprian et al. 1987, Stavenga et a. 1993).

The determined molar extinction coefficients are all higher than the one predicted for bovine (Tab. 11, chapter 3.1.5.), which indicates that more transducin molecules can be activated by the active state of rhodopsin. It has been shown that substituting a F for an A at site 169 decreases the strength of photon absorption in the echidna, as measured by the ε (see chapter 4.1.2.). Like bovine and all other placentals, the three ancestral pigments share an A at site 169. The determination of a high ε in all ancestral pigments suggests that, in addition to site 169, another site is likely to be involved in regulating the strength of photon absorption. Furthermore, accepting the common belief that a high ε is advantageous for vision at low light levels, the fact that the amniote rhodopsin has a ε similar to Mammalia and Theria indicates that the amniote ancestor had a rhodopsin maintaining a high degree of photon absorption as well, functioning well at low light levels.

The hydroxylamine assays showed that like bovine, neither of the three ancestral pigments reacted to hydroxylamine, also indicating rod-like pigments (Fig. 19E-G, chapter 3.1.6.).

In Figure 21D-F (chapter 3.2.3.), the 3D structure of the three inferred ancestral sequences were predicted based on their secondary structure. Though all three bear a few substitutions which differ from bovine, there is no change in conformation seen in the predicted 3D structure.

4.2.2. The meta II decay rate

The meta II decay assay by fluorescence spectroscopy, which measures the time constant for the active state of rhodopsin that is crucial for the visual signaling cascade, produced a very interesting result. Here, the $t_{1/2}$ of the amniote rhodopsin is as high as that of bovine (Tab. 12, chapter 3.1.7.). They have $t_{1/2}$ mean values of 16.05 min^{-1} (Amniota) and 17.01 min^{-1} (bovine) (Fig. 23), which are within the published range of bovine (Oprian et al. 1987, Stavenga et al. 1993). The Mammalia and Theria pigments, however, show a slower meta II decay rate (Fig. 23). The mammalian rhodopsin displays a mean $t_{1/2}$ of 24.17 min^{-1} and the therian rhodopsin one of 28.17 min^{-1} (Fig. 23). However, the last assay run did not provide a very confident R^2 value in Theria; disregarding this one, the $t_{1/2}$ is even higher, with a mean value of 32.67 min^{-1} (Fig. 23).

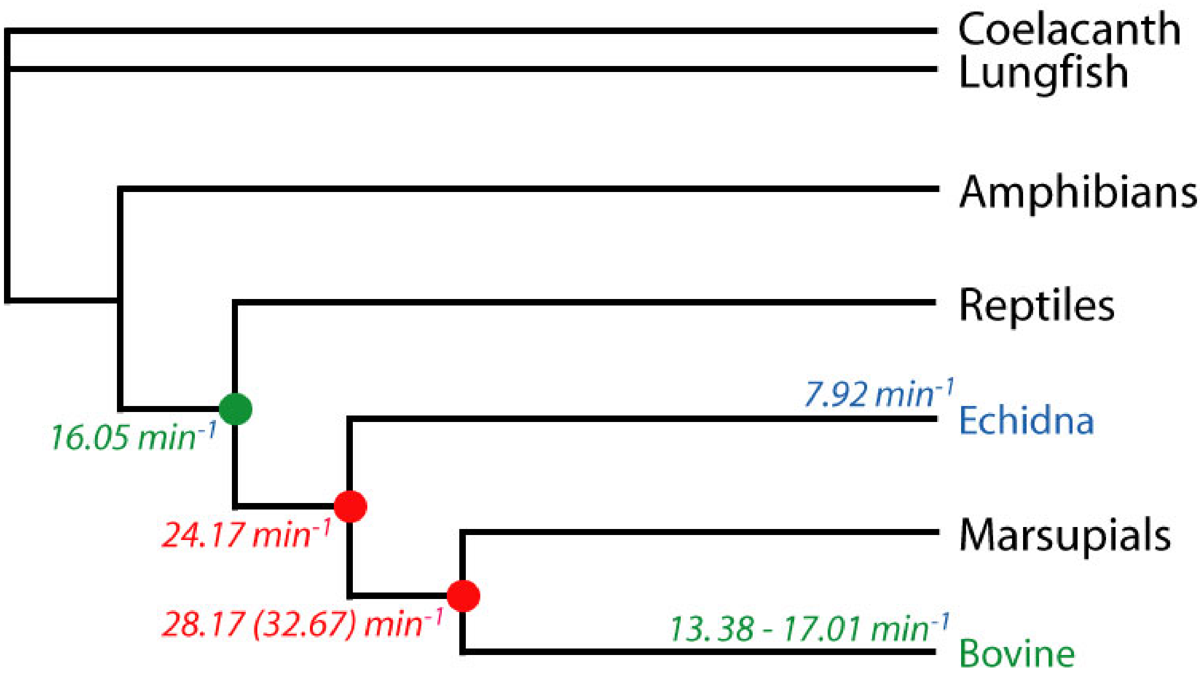

Figure 23. Phylogeny showing meta II decay rates derived from this study.

It has been hypothesised that there is a correlation between the lifetime of meta II and the amplitude of rod response, indicating that larger amounts increase the signal arriving at the brain, as more transducin molecules can be activated (Shichida and Matsuyama 2009, Sugawara et al. 2010). Hence, a low meta II decay rate would be advantageous for scotopic vision (Sugawara et al. 2010). If this assumption was true, the results derived from this study would indicate that the mammalian rhodopsin experienced a change in function leading to better vision at low-light levels compared to the amniote ancestor, and that this functional change was preserved in the therian rhodopsin as well. In contrast, Sakurai et al. (2007) suggested that differences in the amplitude of the photoresponse are more likely due to intrinsic properties such as temperature dependence, rather than interactions between rhodopsin and other proteins from the visual signaling cascade.

Various meta II decay rates with varying assay conditions, such as temperature, have been examined, but most of these lack bovine as positive control. Hence, to ensure reliability, only two studies presenting $t_{1/2}$ of chicken, human, and salamander, including bovine as positive control, were considered here (Okada et al. 1994, Imai et al. 2005). Human rhodopsin has a

$t_{1/2}$ similar to bovine, whereas chicken and salamander rhodopsin also display a $t_{1/2}$ half that of bovine (Imai et al. 2005). However, values listed by Imai et al. (2005) cannot be tracked back in the literature. Thus, only the chicken meta II decay rate by Okada et al. (1994) can be used for comparative interpretations: with a value of 4.42 min^{-1} (bovine: 9.93 min^{-1}), chicken rhodopsin displays a $t_{1/2}$ half that of bovine, as is the case in the echidna. With chicken being a crepuscular animal displaying a rapid meta II decay rate like that of the nocturnal echidna, the $t_{1/2}$ of meta II seems unlikely to allow for inferences on activity patterns as suggested previously (Shichida and Matsuyama 2009, Sugawara et al. 2010). The low $t_{1/2}$ in bovine (9.93 min^{-1}) might be due to experiments being performed at T=15ºC (Okada et al. 1994), whereas in this study, temperature was set to 25ºC. In addition, Imai et al. (2005) pointed out that meta II data obtained from spectroscopic assays using *in vitro* synthesised pigments differs from data acquired by membrane preparations. Okada et al. (1994) prepared chicken rhodopsin from ROS, in contrast to *in vitro* expression used in this study. For future research, assays with chicken should be replicated under the same conditions used in this study.

Alternatively, the rapid meta II decay rates in chicken and echidna, which has a „reptilian-like“ amino acid sequence, could display a phylogenetic pattern. However, the amniote ancestor has a $t_{1/2}$ similar to bovine. But, this finding could be a result of the ancestral sequences being inferred using Maximum likelihood estimates, and, thus, being hypothetical. If indeed chicken and echidna display rapid meta II decay rates due to phylogeny, then the high $t_{1/2}$ values for Mammalia and Theria would indeed indicate an adaptation to dim-light vision, as suggested previously (Shichida and Matsuyama 2009, Sugawara et al. 2010). However, the results rather emphasise that inferring ecological traits based on the investigation of single steps within the visual signaling cascade is problematic.

Sugawara et al. (2010) also found evidence to suggest that substitutions at site 83, among others, were resposible for a blue shift in the absorption spectrum of cichlid fishes, the result of adaptating to the blue-green photic environment in deep water. In nocturnal bats, this substitution was found to cause accelerated meta II formation rates, possibly as an adapatation to dim-light vision (Sugawara et al. 2010). Interestingly, the nocturnal echidna, whose rhodopsin has its λ_{max} at 496.5 nm, which is slightly blue-shifted from bovine rhodopsin, also beares an Asparagine (N), which is said to cause a blue-shift and an accelerated meta II formation rate in fish and bats, in contrast to an Aspartic acid (D) in all others. Though being crepuscular, the chicken rhodopsin, which has a D at site 83, displays a rapid meta II decay rates. However, it has been suggested that, in contrast to meta II formation rates, meta II decay rates are not affected by substitutions at site 83 (Sugawara et al. 2010). Thus, analysing meta II formation rates might be helpful in future research.

Furthermore, Sugawara et al. (2010) discussed that residues 140 to 150 and 226 to 247 are involved in association with transducin, which is the crucial component affected by the meta II state (Weitz and Nathans 1993, Imai et al. 2005). There is one site within these regions where amino acids of the ancestral sequences differ from bovine, i.e. site 228 (Fig. 20, chapter 3.2.1.). Here, Amniota differs from bovine, Mammalia, and Theria in substituting a Cysteine (C) for a Phenylalanine (F) (Fig. 20, chapter 3.2.1.). Since bovine shares the same amino acid with Mammalia and Theria, this residue is unlikely to have influenced the detected high $t_{1/2}$ value. Since all other residues are conserved, the suggested regions are unlikely to be involved in accelerating the meta II decay rate in Mammalia and Theria.

Another amino acid known to cause differences in meta II decay rates between chicken green opsin and rhodopsin is site 189 (Kuwayama et al. 2002). However, Amniota has a different amino acid at this site, i.e. Valine (V), than bovine, Mammalia, and Theria, which share an Isoleucine (I). Thus, this site is unlikely to affect the meta II decay rate in Mammalia and Theria (Fig. 20, chapter 3.2.1.). In addition, the replacement of Isoleucine by a Valine at this site caused no changes in the meta II decay rate, as indicated by site-directed mutagenesis (Kuwayama et al. 2002).

In conclusion, the inconsistency of the results derived from this as well as other studies emphasizes the high variability in the functional properties of visual pigments and demonstrates that single assays do not provide an adequate picture of the highly complex and interconnected visual system; not to mention their problematic use to infer the activity patterns of entire organisms.

4.2.3. Weak points of Maximum likelihood Inferences

Though ancestral sequence reconstruction provides knowledge of ancient organismal biology where the fossil record reaches its limits, Maximum likelihood estimates also have their limits (Chang 2002a).

For example, it is possible that the ancestral reconstructions, which were inferred using likelihood methods, might not reflect the actual ancient gene sequence (Smith et al. 2010). However, they can be used as a good starting point for experimental tests (Chang 2003, Ugalde et al. 2004). Here, ancestral sequences with the highest likelihood were chosen for *in vitro* expression (Tab. 8, chapter 3.1.2.). Future directions already involve *in vitro* expression of additional sequences, which were randomly sampled from the Bayesian distribution, as was done by Gaucher et al. (2010).

Furthermore, codon usage bias describes the phenomenon that the frequencey of occurence of codons in a protein-coding DNA sequence varies among species. It has been found to be present in rhodopsin (Chang and Campbell 2000). For example, reptile and amphibian rhodopsins tend to have more A’s and fewer G/C’s than all other sequences (Chang and Campbell 2000). Thus far, the Maximum likelihood approach used in this study does not account for this bias, which is a weak point of the approach. Unfortunately, at this time there is no better approach.

Also, ancestral reconstruction is sensitive to model choice (Chang 2003). However, since the inferred and expressed ancestral pigments were functional as indicated by dark-light spectra and acid bleach, it seems likely that the models used fit the data well.

4.2.4. Conclusions

It has been suggested that two unique properties were acquired by the rhodopsin from its cone ancestors for mediating scotopic vision: stability and a high amplification ability for phototransduction (Sakurai et al. 2007). A high amplitude of the single-photon response is likely to be achieved by a long lifetime of meta II, as more transducin molecules can be activated (Imai et al. 2005, Imai et al. 2007, Sugawara et al. 2010).

Meta II decay rates have been found to accelerate from node Amniota to Mammalia, suggesting that the mammalian rhodopsin experienced changes in order to adapt to dim-light vision. In Theria, this high meta II $t_{1/2}$ is preserved. In contrast, a rapid meta II decay rate has been measured for the nocturnal echidna in this study and has been reported for the crepuscular chicken (Okada et al. 1994). Thus, the meta II decay data is inconsistent with activity patterns in echidna and chicken, and rather suggests that the visual system is too complex and interconnected, involving many proteins, to allow for ecological interpretations based on single biochemical and functional reactions.

Though the dark and light spectra indicated that all three ancestral pigments are functional, it must be emphasized that ancestral sequence reconstruction has its limitations, such as its hypothetical character as well as the non-consideration of a codon usage bias.

4.3. Positive selection on non-synonymous substitutions along the Therian branch

4.3.1. Therian diversity during the Late Jurassic

The discovery of about 200 additional and exceptionally well preserved Mesozoic mammal fossils in the last 25 years have shaken the view of early mammals being only generalized forms (Luo 2007). Recently, it has been discovered that it is uncommon for any Mesozoic mammalian group to experience little or much delayed diversification (Luo 2007). Instead, early mammalian evolution is characterised by many short lineages in successive clusters (Luo 2007); although, this former view is still valid for the earliest forms such as *Eozostrodon* and *Megazostrodon* as well as for members of the Mesozoic Jehol Biota ecosystem (Luo 2007). However, there is now strong evidence for ecological specializations in many other early mammalian clades (Fig. 24) (Luo 2007). Though not very abundant in the Mesozoic, early mammals were highly diverse: modern lifestyles such as semi-aquatic, swimming, ambulatory, scansorial, climbing, fossorial, volant, and others had already evolved convergently in different taxa and clades during the Triassic and Jurassic (Fig. 24) (Luo 2007). Also a predatory carnivorous diet had evolved multiple times in unrelated mammalian groups during the Jurassic and Cretaceous, indicating an early evolution of food divergence (Luo 2007).

There is now evidence that there were six major diversification events in mammalian evolution, three of which occurred along the mammalian branch. As indicated by a grey dot in Figure 24, a first ecological diversification in early mammalian taxa took place during the Late Triassic and Early Jurassic (Luo 2007). It was followed by another remarkable diversification in ecological specializations in docodonts during the Middle Jurassic (see grey dot in Fig. 24) (Luo 2007). In the Late Jurassic, a third diversification followed within theriiform groups and taxa (see grey dot in Fig. 24) (Luo 2007).

Importantly, these three major diversifications happened along the branch leading from the node Mammalia to the node Theria, which is where the selective constraint analyses detected significant evidence for positive selection acting on the rhodopsin (Fig. 22, chapter 3.4.4.). Assuming that the earliest mammalian forms had indeed been nocturnal, it seems likely that the rhodopsin had undergone major changes in response to these new habitats at different light levels, in particular a semi-aquatic/swimming or fossorial/digging lifestyle; adaptations which are likely to be detected by selective constraint analyses.

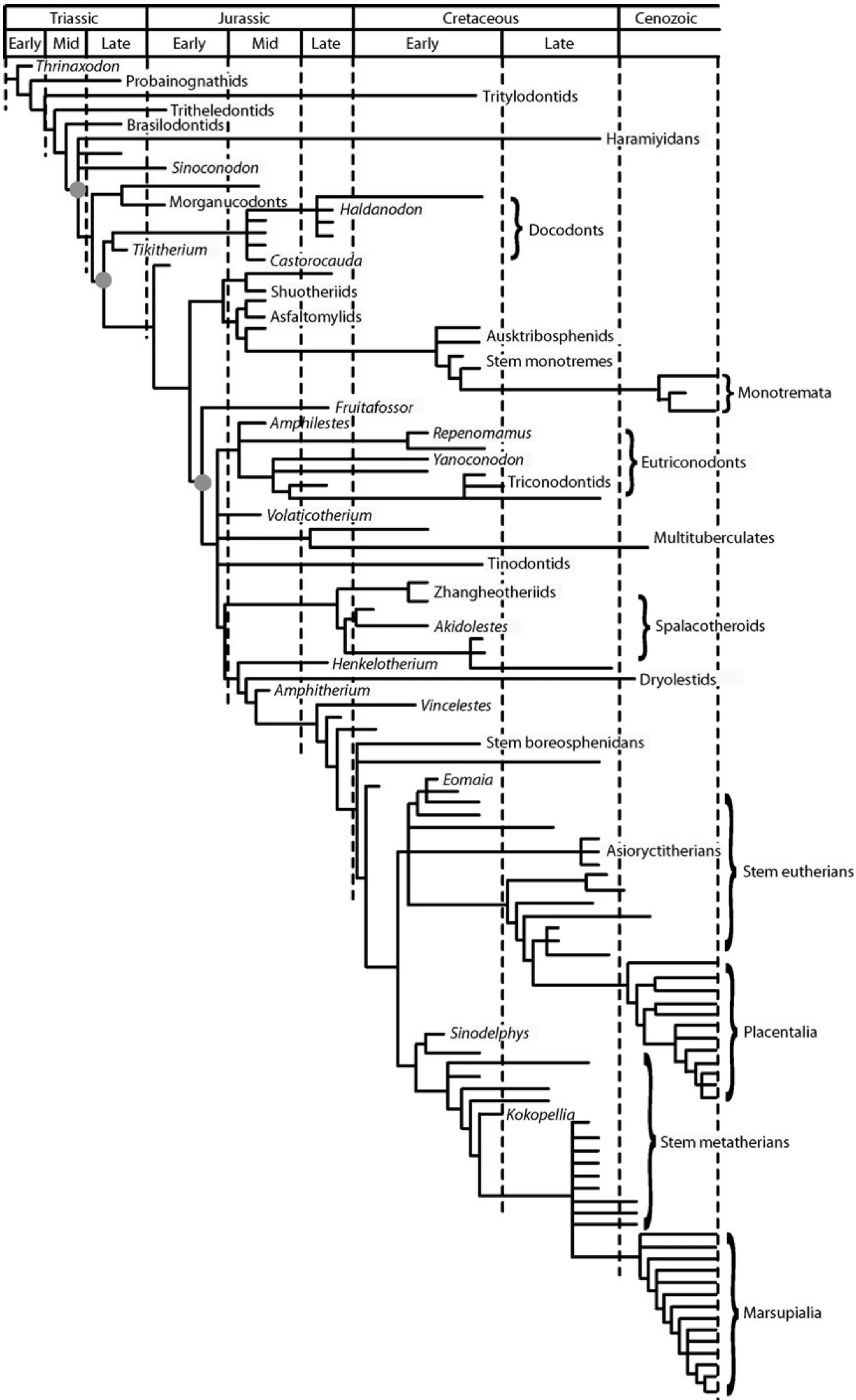

Figure 24. Phylogeny of Mesozoic and extant mammalian groups (after Luo 2007). Grey dots indicate starting points of ecological diversification events.

Ecological specialisations in early mammals include a semi-aquatic, swimming, ambulatory, scansorial, climbing, fossorial, and volant lifestyle. In detail, a swimming lifestyle first evolved in docodonts such as *Haldanodon* and *Castorocauda* (Fig. 24). Haramiyidans as well as early theriiform taxa, such as *Fruitafossor* and *Repenomamus*, were burrowing (Fig. 24). *Volaticotherium* was a gliding form (Fig. 24). *Henkelotherium* was arboreal and *Vincelestes* scansorial (Fig. 24). Early mammalian forms such as *Sinocodon*, *Morganucodon*, and others, as well as the theriiform taxon *Yanoconodon* were ground-dwelling (Fig. 24).

4.3.2. The tetrapod opsin complement

The ancestral complement of visual pigments in tetrapods comprises four cone opsins for colour vision and one rhodopsin for vision at night and/or dim-light. As seen in Figure 25, this ancestral opsin set is reduced in all tetrapod clades. No green-sensitive opsin Rh2 has been found in any amphibian, but since it is found in reptiles and fish, it must have been present in the ancestor of amphibians and amniotes (Fig. 25) (Bowmaker 2008). All mammals have lost Rh2 (Fig. 25) (Hunt et al. 2009).

Davies et al. (2007) found exon 5 of the SWS1 gene in platypus, but Wakefield et al. (2008) found it neither in the platypus nor in the echidna and, thus, SWS1 is not functional in any living monotreme (Fig. 25). Zhao et al. (2009b) hypothesised that an ecological switch to a low-light habitat coincided with the loss or absence of functionality of the SWS1 opsin in marine mammals. All terrestrial mammals that have lost SWS1 are nocturnal (Peichl 2005, Carvalho et al. 2006, Jacobs 2009). One might infer that the early monotreme activity pattern had been nocturnal, as has been suggested by Crompton et al. (1978).

Theria, on the other hand, have lost SWS2, which absorbs blue light at around 410-490 nm (Cowing et al. 2008, Hunt et al. 2009). One might hypothesise that the strong positive selection both at branch level and acting on sites along the Therian branch, might be related to the fact that Theria had lost Rh2 and SWS2, and that their ancestor was only able to absorb UV (SWS1), red (LWS), and dark light (Rh1), as opposed to an amniote ancestor with an opsin set of Rh1, SWS1, SWS2, LWS, and Rh2 (Fig. 25). The loss of a visual pigment possibly puts another opsin, here rhodopsin, under selective constraint, in order to take over functional aspects; a selective constraint which is likely to be detected by the selective constraint analyses used in this study.

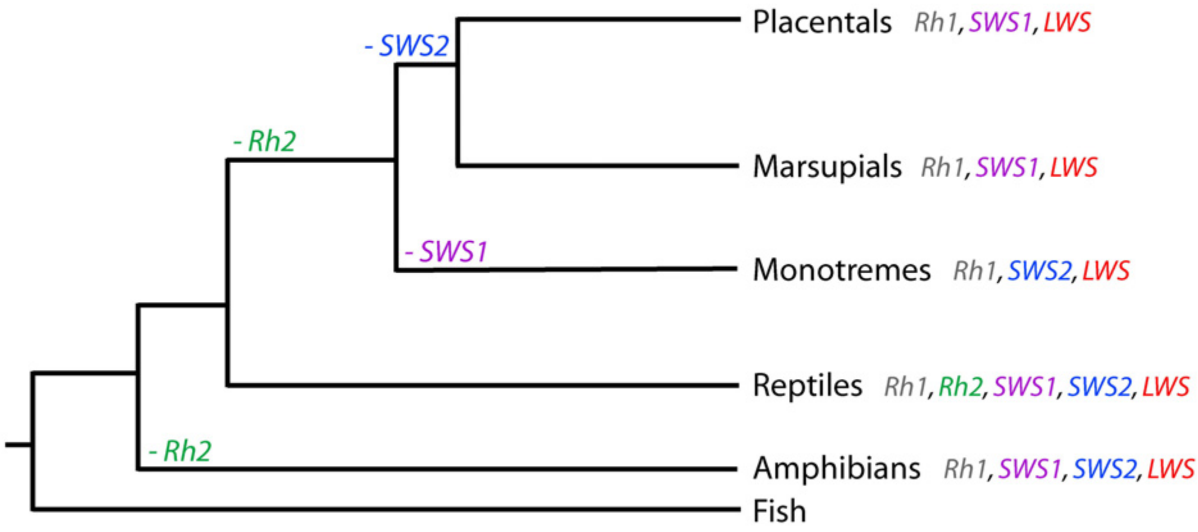

Figure 25. Visual pigment loss in tetrapods.

4.3.3. Selective constraint on synonymous substitutions in the mammalian rhodopsin

Selection for particular codons, i.e. codon usage bias, has long been thought to be free of selection, suggesting an unbiased codon usage, as these substitutions do not lead to adaptive changes in the protein (Kimura 1968). However, this assumption has been challenged, and selection for synonymous sites has been found to be present in plants, bacteria, and invertebrates in order to increase translation efficiency/accuracy (Ikemura 1985, Wright et al. 2004, Cutter and Charlesworth 2006). In mammals, codon usage bias due to selective constraint was found to enhance mRNA stability and tRNA translation efficiency/accuracy, to maintain efficient splice control, and to ensure proper protein folding (Ikemura 1985, Parmley et al. 2006, Shabalina et al. 2006, Drummond and Wilke 2008). Furthermore, it has been suggested that genes with a high level of expression are likely to experience selective constraint on synonymous substitutions (Sharp et al. 1995). Rhodopsin is a highly expressed gene and mammalian rhodopsin has been found to have undergone a strong codon usage bias (Pugh and Lamb 1993, Chang and Campbell 2000).

A collaborative study using the same data set has shown that rhodopsin experienced selective constraint acting on synonymous substitutions in rhodopsin along the branch leading to Mammalia (Du 2010, unpublished MSc thesis). A strong codon usage bias towards G/C nucleotides at the 3rd position of four-fold codons was observed (Fig. 26) (Du 2010, unpublished MSc thesis). The LRTs of estimated data show significance ($p < 0.001$) (Du 2010, unpublished MSc thesis).

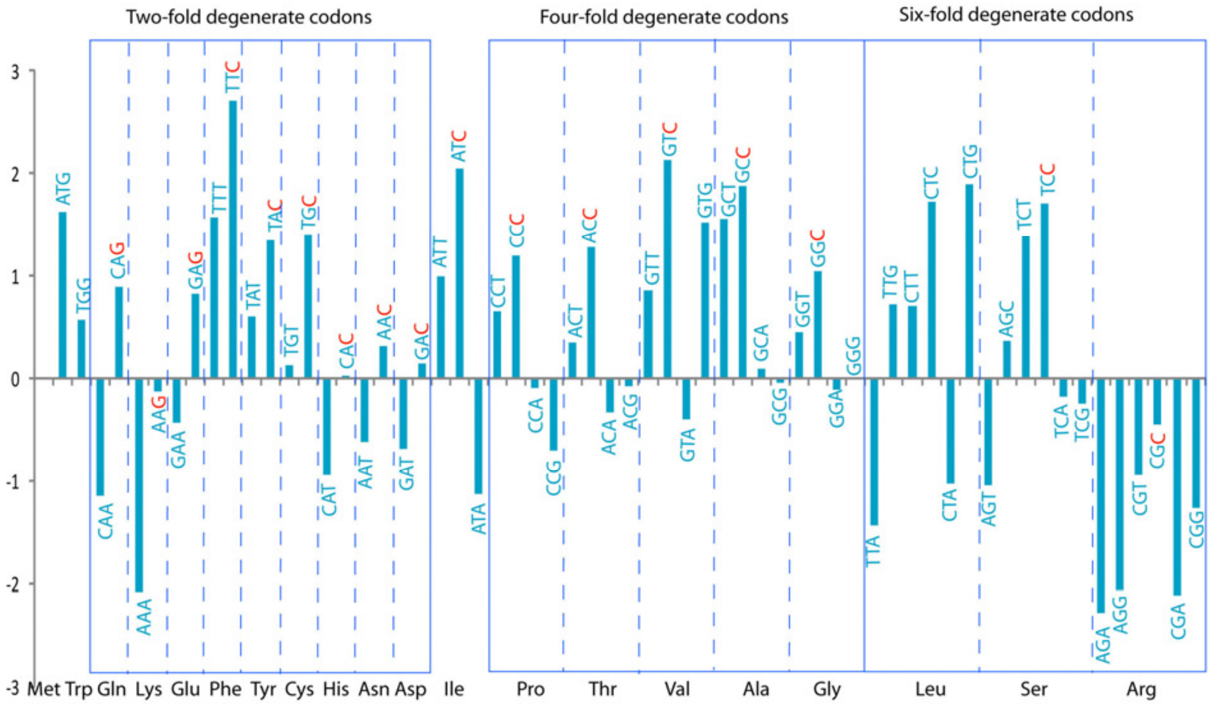

Figure 26. Distribution of G/C-ending codons in mammalian rhodospin gene. Synonymous codons with highest fitness are highlighted by red codon ending.

A preference for G/C-ending codons over A/T-ending codons has been found to increase mRNA stability and tRNA translation efficiency in mammals, suggesting an increase in rhodopsin molecules (Ikemura 1985, Shabalina et al. 2006, Drummond and Wilke 2008). Though in the majority of mammals, the retina is dominated by rods, nocturnal animals have been found to possess even more rod photoreceptors in their retina (Szél et al. 1996, Peichl 2005). An increase in rhodopsin molecules in the retina of the vertebrate eye is said to have resulted when adaptating to vision at night and/or low light leves (Kaskan et al. 2005, Peichl 2005).

This suggests that the mammalian rhodopsin had experienced changes in synonymous sites that led to an increased expression of molecules in the retina, which would have been supportive for adaptating to a nocturnal habitat. In addition, the study showed that there are mechanisms regulating adaptation to dim-light vision other than selection on non-synonymous sites causing adaptive changes.

4.3.4. Conclusions

Selective constraint can act either on synonymous or on non-synonymous substitutions. However, the effect on the protein is different. Positive selection acting on non-synonymous substitutions changes the amino acid sequence, which might affect the functionality or biochemical properties of a protein in order to adapt to external changes, whereas selective constraint on synonymous substitutions does not change the subsequent amino acid but instead increases mRNA stability and tRNA translation efficiency/accuracy (Ikemura 1985, Yang 2002, Shabalina et al. 2006, Drummond and Wilke 2008). Interestingly, selective constraint analyses investigateing both types of selection have shown that the mammalian rhodopsin had experienced important changes in both synonymous and non-synonymous substitutions: selective constraint acting on synonymous substitution sites along the branch leading to Mammalia was detected, and positive selection on non-synonymous substitutions was found within mammals, along the branch leading to Theria. These results suggest that early mammals have increased their number of rhodopsin molecules in order to adapt to a nocturnal habitat. Subsequently, their rhodopsin underwent functional and biochemical changes when taxa began exploring new habitats at different light levels, as indicated by the fossil record.

Furthermore, with only SWS1, LWS, and Rh1 opsins left in the retina, Theria have a very reduced opsin set as opposed to an amniote ancestor with an opsin set of Rh1, SWS1, SWS2, LWS, and Rh2. In order to compensate, the loss of an opsin is likely to put adaptive constraint onto another opsin, which possibly causes adaptive changes which are likely to be detected by selective constraint analyses.

4.4. Summary and future prospects

This thesis represents an integrative approach that combines paleontology and molecular biology in order to address an interesting question in evolutionary history: were the first mammals nocturnal?

1) The *in vitro* expression of the rhodopsin of the nocturnal echidna, together with two mutants T158A and F169A, was successful. All pigments are functional with λ_{max} slightly blue-shifted from that of bovine. Results of the meta II decay assay, which measures the $t_{1/2}$ of the active state of rhodopsin that is a crucial step in the visual signaling cascade, revealed a cone-like characteristic in the echidna rhodopsin, namely, a low $t_{1/2}$. This finding stands in sharp contrast to prior assumptions that a high $t_{1/2}$ is advantageous for scotopic vision.

Hydroxylamine assays also describe these three pigments as cone-like, possibly a result of being expressed in cones as well. Further assays of the two mutants revealed that site 169 is involved in decreasing the strength of photon absorption in the echidna rhodopsin; another contradictory finding as a high strength of photon absorption is believed to be advantageous for vision at low light levels. The echidna rhodopsin is as enigmatic as the echidna itself.

2) Ancestral sequences for the nodes Amniota, Mammalia, and Theria were inferred using Maximum likelihood estimates and their *in vitro* expression was successful. All pigments were found to be functional and rod-like, with λ_{max} within the range of bovine. Mammalia and Theria rhodopsin display high meta II half life times; a finding thought to be linked with adaptation to vision at low-light levels.
However, with regards to inconsistency in the available data, it must be emphasized that the visual signaling cascade is a complex and interconnected system involving numerous proteins. Therefore, inferences based on single biochemical and functional assays are problematic and do not allow for ecological interpretation.

3) Selective constraint analyses on non-synonymous substitutions were carried out. Interestingly, positive selection on non-synonymous sites, which is known to be adaptive, was found along the therian branch. This finding corresponds with recent paleontological data of three major events of ecological diversification along this branch. Changes involved in adapting to a new habitat at different light levels are likely to be detected by selective constraint analyses. Furthermore, selective constraint analyses on synonymous substitutions have revealed that the rhodopsin experienced non-adaptive changes, which nevertheless increase mRNA stability and/or tRNA translation efficiency/accuracy along the mammalian branch. This suggests a scenario in which rhodopsin molecules increased in number somewhere along the branch leading to crown mammals, in order to adapt to a low-light environment, followed by adaptive changes in the rhodopsin due to constraints resulting from ecological diversification or the loss of several cone opsins.

To date, the fossil record does not provide much information concerning nocturnality in early mammals, as preservation of soft-tissue is lacking (Ruben 1995). However, recently, it has been found that eyeball morpholgy is associated with the activity pattern of an animal (Walls 1942, Hall 2008a, Hall 2008b, Schmitz 2009). With scleral plates and other eyeball parameters being well preserved, it is now possible to infer activity patterns of extinct organisms, such as birds (Schmitz 2009). Scleral plates are not found in mammals, not even in the earliest forms or non-mammalian therapsids, but they are present in basal therapsids such as biarmosuchians, dinocephalians, anomodonts, and theriodontids (Fig. 2, chapter 1.1.3.) (Romer 1956, Sidor and Welman 2003, Sidor et al. 2004). Though ocular parameters needed for inferring activity patterns vary in birds and primates (Hall 2008), inferring visual capacities in therapsids based on eyeball dimensions could provide further insight as to whether early mammals had indeed been nocturnal.

Furthermore, from the molecular perspective, a switch from nocturnality to diurnality, or vice versa, has been observed in double-knockout mice lacking the inner-retinal photopigment melanopsin (OPN4) and RPE65, a key protein involved in retinal chromophore recycling (Doyle et al. 2008). Investigating these proteins by means of molecular evolution would be an intriguing direction for future research.

In addition, in order to visualize how the visual system works in a broader sense and to elucidate differences in the rhodopsin of a nocturnal and a diurnal animal, characterising the rhodopsin of a nocturnal placental sister taxon of bovine as second positive control is the next natural step for future research, and further assays, such as retinal regeneration, meta II formation rate, or transducin activation are needed (Chang et al. 2002a, Chang 2003, Janz and Farrens 2004, Sakurai et al. 2007, Sugawara et al. 2010).

In conclusion, this thesis contributes to knowledge about the origin and evolution of mammals in that three ancestral pigments inferred for the nodes Amniota, Mammalia, and Theria by Maximum likelihood estimates were successfully expressed *in vitro*, and were found to be functional and rod-like. The determination of meta II half life times tentatively indicate functional adaptation to vision at low light levels in the mammalian and therian rhodopsin. Furthermore, selective constraint analyses describe a scenario in which early mammals had increased the number of rhodopsin molecules in the retina, which was followed by adaptive changes in the amino acid sequence along the therian branch that were likely the result of exploring various novel habitats. Therefore, Crompton et al.'s hypothesis that early mammals had been nocturnal is supported by the results derived from this study.

In the coming years, the continued collaboration of paleontology and molecular biology could prove fruitful for addressing macroevolutionary questions and for peering deep into the past.

Acknowledgements

Writing this dissertation would not have been possible without the smaller and bigger ways in which many people influenced my personal and intellectual development.

First of all, I want to thank my supervisor Johannes Müller (Berlin). Not only did he give me the opportunity to work on this project, he was also a great mentor and in collaboration with him I deepened my knowledge in various fields (ranging from molecular techniques over bioinformatics to amniote evolution), perfected my drawing techniques and skills pertaining to the writing of scientific manuscripts. I owe him thanks for extensive discussions, reviewing manuscripts and earlier versions of this thesis, as well as emotional support and encouragement. He was of great help whenever needed.

I also want to thank Belinda S.W. Chang (Toronto) for giving me the opportunity to work in her molecular lab in Toronto, where I was able to participate in discussions on vision research, bioinformatics, and molecular techniques. This is a stronger dissertation for these experiences.

I am thankful for the contributions of my collaborator Jingjing Du (Toronto). Her patience in sharing her vast knowledge of bioinformatics with me and, of course, her friendship have been invaluable.

I deeply thank Linda A. Tsuji (Seattle) not only for correcting English grammar, which immensely improved this thesis, but also for help with graphics and abstracts, and, most importantly, for her friendship, advice, patience, emotional support, after-work beers, delicious food, and lots of laughter – I could not have asked for a better person to share an office with. I thank you, my dear friend!

For help in the lab in Toronto, I first want to thank Ilke van Hazel who guided me through expression and cloning techniques and who brought joy and endurance to some long-night experiments. Furthermore, I thank James Morrow for helping with expressing visual pigments and concurrent fluorescence assays. Cameron Weadick helped with the rhodopsin 3D structure. I also want to express my thanks to all the other members of the Chang Lab (actual as well as former), namely Natalie Chan, Yayi Huang, Gloria Lin, Martin R. Smith, Kuan Rai Tan, Johnny Wu, MengShu Xu, Clement Yang, and David Yu.

I deeply appreciate the assistance received while working in the Berlin lab: Robert Schreiber helped during genome walking procedures and PCR, and Antje Sonntag as well as Martin Meixner performed sequence analysis and helped with cloning techniques.

Also, I owe thanks to Zhe-Xi Luo (Pittsburgh) for enriching discussions on early mammalian ecology and diversity, to Jason Head (Toronto) and Johannes Penner (Berlin) for help with statistics, to Dr. G. Crawshaw (Toronto) for kindly providing echidna blood samples, to Julia

Hoffmann (Berlin) for help with formatting, to Jasmina Hugi (Zurich) for providing the photo of the echidna, to Florian Witzmann (Berlin) and Sven Weidemeyer (Berlin) for reviewing earlier versions of this thesis, and to Jörg Fröbisch (Chicago) for help with synapsid phylogeny.

I thank the members of my examining committee, i.e. Belinda S.W. Chang (Toronto), Hannelore Hoch (Berlin), Wolfgang Kiessling (Berlin), Frieder Mayer (Berlin), and Johannes Müller (Berlin).

And I thank my friends and colleagues Nicolas E. Campione (Toronto), Olaf Dülfer (Bonn), David Evans (Toronto), Nadia and Jörg Fröbisch (Chicago), Julia Hoffmann (Berlin), Christian Kolb (Zürich), Dieter Korn (Berlin), Meike Mohneke (Berlin), Ragna Redelstorff (Dublin), Kristian Remes (Bonn), Nicolas Straube (München), Sven Weidemeyer (Berlin), and Florian Witzmann (Berlin) for help, discussion, advice, and support.

Last but not least, I thank my parents, my sister and her family, as well as my friends, in particular Juliane Edler (Toronto), who did a perfect job in encouraging me to sail through the last four years.

This work was funded by the German Research Foundation (DFG Mu 1760/2-3).

Literature cited

Abdala, F. 2007. Redescription of *Platycraniellus elegans* (Therapsida, Cynodontia) from the lower Triassic of South Africa, and the cladistic relationships of Eutheriodonts. Palaeontology 50(3): 591-618.

Abdala, F., Rubidge, B.S., and Van Den Heever, J. 2008. The oldest Therocephalians (Therapsida, Eutheriodontia) and the early diversification of Therapsida. Palaeontology 51(4): 1011-1024.

Abdala, F. and Ribeiro, A.M. 2010. Distribution and diversity patterns of Triassic cynodonts (Therapsida, Cynodontia) in Gondwana. Palaeogeography, Palaeoclimatology, Palaeoecology 286: 202-217.

Ahnelt, P.K. and Kolb, H. 2000. The mammalian photoreceptor mosaic-adaptive design. Progress in Retinal and Eye Research 19(6): 711-777.

Ala-Laurila, P., Saarinen, P., Albert, R., Koskelainen, A., and Donner, K.. 2002. Temperature effects on spectral properties of red and green rods in toad retina. Visual Neuroscience 19: 781-792.

Altun, A., Yokoyama, S., and Morokuma, K. 2008. Spectral tuning in visual pigments: An ONIOM(QM:MM) study on bovine rhodopsin and its mutants. The Journal of Physical Chemistry B 112: 6814-6827.

Asher, R.J. and Helgen, K.M. 2010. Nomenclature and placental mammal phylogeny. BMC Evolutionary Biology 10:102.

Baba, M.L., Goodman, M., Berger-Cohn, J., Demaille, J.G., and Matsuda, G. 1984. The early adaptive evolution of calmodulin. Molecular Biology and Evolution 1(6): 442-455.

Baehr, J.F., Falk, J.D., Bugra, K., Triantafyllos, J.T., and McGinnis, J.F. 1988. Isolation and analysis of the mouse opsin gene. FEBS Letters 238: 253-256.

Bakewell, M.A., Shi, P., and Zhang, J. 2007. More genes underwent positive selection in chimpanzee evolution than in human evolution. Proceedings of the National Academy of Sciences 104: 7489-7494.

Bakker, R.T. 1971. Dinosaur physiology and the origin of mammals. Evolution 25: 636-658.

Baylor, A., Lamb, T.D., and Yau, K.-W. 1979. Responses of retinal rods to single photons. Journal of Physiology 288: 613-634.

Baylor, D.A., Nunn, B.J., and Schnapf, J.L. 1984. The photocurrent, noise, and spectral sensitivity of rods of the monkey *Macaca fascicularis*. Journal of Physiology 357: 575-607.

Bennett, A.F. and Ruben, J. 1979. Endothermy and the activity in vertebrates. Science 206: 649-654.

Bininda-Emonds, O., Cardillo, M., Jones, K.E., MacPhee, R.D.E., Beck, R.M.D., Grenyer, R., Price, S.A., Vos, R.A., Gittleman, J.L., and Purvis, A. 2007. The delayed rise of present-day mammals. Nature 466: 507-512.

Blumer, K.J. 2004. The need for speed. Nature 427: 20-21.

Boisvert, M. and Grisham, J. 1988. Reproduction of the short-nosed echidna *Tachyglossus aculeatus* at the Oklahoma City Zoo. International Zoo Yearbook 27: 103-108.

Bolk, L., Göppert, E., Kallius, E., Lubosch, W. 1934. Handbuch der vergleichenden Anatomie der Wirbeltiere. Urban & Schwarzenberg, Berlin.

Bonaparte, C.L. 1837. New systematic arrangement of vertebrated animals. Transactions of the Linnean Society of London 18: 247-304.

Borhan, B., Souto, M.L., Imai, H., Schichida, Y., and Nakanishi, K. 2000. Movement of retinal along the visual transduction path. Science 288: 2209-2212.

Bowmaker, J.K. 2008. Evolution of vertebrate visual pigments. Vision Research 48: 2022-2041.

Bowmaker, J. K., Heath, L. A., Wilkie, S. E., and Hunt, D. M. 1997. Visual pigments and oil droplets from six classes of photoreceptors in the retinas of birds. Vision Research 37: 2183-2194.

Bowmaker, J.K. and Hunt, D.M. 2006. Evolution of vertebrate visual pigments. Current Biology 16(13): R484-489.

Bridges, C.D.B. 1970. Biochemistry of vision. pp. 564-635 *In* Biochemistry of the eye. *Edited by* C.N. Graymore. Academic Press, New York.

Brink, A.S. 1956. Speculations on some advanced mammalian characteristics in the higher mammal-like reptiles. Paleontologia Africana 4: 77-95.

Broom, R. 1905. On the use of the term Anomodontia. Record of the Albany Museum 1: 266-269.

Campbell, N.A. and Reece, J.B. 2009. Biologie. 8th edition. Pearson Studium, München.

Carleton, K.L., Spady, T.C., and Cote, R.H. 2005. Rod and cone opsin families differ in spectral tuning domains but not signal transducing domains as judged by Saturated Evolutionary Trace Analysis. Journal of Molecular Evolution 61: 75-89.

Carroll, R.L. 1988. Vertebrate paleontology and evolution. Freeman, New York.

Carvalho, L. d.S., Cowing, J.A., Wilkie, S.E., Bowmaker, J.K., and Hunt, D.M. 2006. Shortwave visual sensitivity in tree and flying squirrels reflects changes in lifestyle. Current Biology 16: R81-83.

Chang, B.S.W. 2003. Ancestral gene reconstruction and synthesis of ancient rhodopsins in the laboratory. Integrative and Comparative Biology 43(4): 500-507.

Chang, B.S.W. and Campbell, D.L. 2000. Bias in phylogenetic reconstruction of vertebrate rhodopsin sequences. Molecular Biology and Evolution 17(8): 1220-1231.

Chang, B.S.W. and Donoghue, M.J. 2000. Recreating ancestral proteins. Tree 15(3): 109-114.

Chang, B.S.W., Jönsson, K., Kazmi, M.A., Donoghue, M.J., and Sakmar, T.P. 2002a. Recreating a functional ancestral archosaur visual pigment. Molecular Biology and Evolution 19(9): 1483-1489.

Chang, B.S.W., Kazmi, M.A., and Sakmar, T.P. 2002b. Synthetic gene technology: applications to ancestral gene reconstruction and structure-function studies of receptors. Methods in Enzymology 343: 274-294.

Chang, B.S.W., Matz, M.V., Field, S.F., Müller, J., and van Hazel, I. 2007. Dealing with model uncertainty in reconstructiong ancestral proteins in the laboratory: examples from archosaur visual pigments and coral fluorescent proteins. pp. 164-180. *In* Ancestral sequence reconstruction. *Edited by* D.A. Liberles. Oxford University Press, New York.

Cowing, J.A., Arrese, C.A., Davies, W.L., Beazley, L.D., and Hunt, D.M. 2008. Cone visual pigments in two marsupial species: The fat-tailed dunnart (*Sminthopsis crassicaudata*) and the honey possum (*Tarsipes rostratus*). Proceedings of the Royal Society B 275: 1491-1499.

Crescitelli, F. 1980. The two visual pigments of the gecko: the labile behaviour. Journal of Comparative Physiology 138: 121-129.

Crescitelli, F. 1988. The gecko visual pigment: the chromophore dark exchange reaction. Experimental Eye Research 46: 239-248.

Crompton, A.W., Taylor, C.R., and Jagger, J.A. 1978. Evolution of homeothermy in mammals. Nature 272: 333-336.

Crompton, A.W. and Sun, A.-L. 1985. Cranial structure and relationships of the Liassic mammal *Sinocodon*. Zoological Journal of the Linnean Society 85: 99-119.

Crompton, A.W. and Luo, Z.-X. 1993. Relationships of the Liassic mammals Sinocodon, Morganucodon oehleri, and Dinnetherium. pp.30-43. *In* Mammalian phylogeny: Mesozoic differentiation, multituberculates, monotremes, early therians, and marsupials. *Edited by* F.S. Szalay, M.C. McKenna, and M.J. Novacek. Springer Verlag, New York.

Cutter, A.D. and Charlesworth, B. 2006. Selection intensity on preferred codons correlates with overall codon usage bias in *Caenorhabditis remanei*. Current Biology 16: 2053-2057.

Daemen, F.J.M., Borggreven, J.M.P.M., and Bonting, S.L. 1970. Molar absorbance coefficient of rhodopsin. Nature 227:1258-1260.

Davies, W.L., Carvalho, L.S., Cowing, J.A., Beazley, L.D., Hunt, D.M., and Arrese, C.A. 2007. Visual pigments of the platypus: A novel route to mammalian colour vision. Current biology 17(5): R161-163.

Dawson, T.J., Grant, T.R., and Fanning, D. 1979. Standard metabolism of monotremes and the evolution of homeothermy. Australian Journal of Zoology 27: 511-515.

Doi, T., Molday, R.S., and Khorana, G. 1990. Role of the intradiscal domain in rhodopsin assembly and function. Proceedings of the National Academy of Sciences 87: 4991-4995.

Doyle, S.E., Yoshikawa, T., Hillson, H., and Menaker, M. 2008. Retinal pathways influence temporal niche. Proceedings of the National Academy of Sciences 105(35): 13133-13138.

Drummond, D.A. and Wilke, C.O. 2008. Mistranslation-induced protein misfolding as a dominant constraint on coding-sequence evolution. Cell 134: 341-352.

Du, J. 2010. Investigating molecular evolution of rhodopsin using Likelihood/Bayesian phylogenetic methods. Unpublished Master thesis, University of Toronto.

Ernst, O.P., Gramse, V., Kolbe, M., Hofmann, K.P., and Heck, M. 2007. Monomeric G protin-coupled receptor rhodopsin in solution activates its G protein transducin at the diffusion limit. Proceedings of the National Academy of Sciences 104(26): 10859-10864.

Fager, L.Y. and Fager, R.S. 1981. Chicken blue and chicken violet, short wavelength sensitive visual pigments. Vision Research 21: 581-586.

Farmer, C.G. 2000. Parental care: The key to understanding endothermy and other convergent features in birds and mammals. The American Naturalist 155: 326-334.

Farrens, D.L., and Khorana, H.G. 1995. Structure and function in rhodopsin. Measurement of the rate of metarhodopsin II decay by fluorescence spectroscopy. Journal of Biological Chemistry 270(10): 5073-5076.

Fasick, J.I. and and Robinson, P.R. 2000. Spectral-tuning mechanisms of marine mammal rhodopsins and correlations with foraging depth. Visual Neuroscience 17: 781-788.

Flannery, T.F. and Groves, C.P. 1998. A revision of the genus *Zaglossus* (Monotremata, Tachyglossidae), with description of new species and subspecies. Mammalia 62(3): 367-396.

Fowler, J., Cohen, L., and Jarvis, P. 1995. Practical statistics for field biology. John Wiley & Sons, Chichester.

Frank, R.N. and Rodbard, D. 1975. Precision of sodium dodecyl-polyacrylamide-gel electrophoresis for the molecular weight estimation of a membrane glycoprotein: studies on bovine rhodopsin. Archives of Biochemistry and Biophysics 171: 1-13.

Fröbisch, J. Schoch, R.R., Müller, J., Schindler, T., and Schweiss, D. in press. A new basal sphenacodontid synapsid from the Late Carboniferous of the Saar-Nahe basin, Germany. Acta Palaeontologica Polonica. doi: 10.4202/app.2010.0039

Fyhrquist, N., Donner, K., Hargrave, P. A., McDowell, J. H., Popp, M. P., and Smith, W. C. 1998. Rhodopsins from three frog and toad species: Sequences and functional comparisons. Experimental Eye Research 66: 295-305.

Gaucher, E.A., Thomson, J.M., Burgan, M.F., and Benner, S.A. 2003. Inferring the paleoenvironment of ancient bacteria on the basis of resurrected proteins. Nature 425: 285-288.

Gill, T. 1872. Arrangement of the families of mammals and synoptical table of the characters of the subdivisions of mammals. Smithsonian Miscellaneous Collection 11:1-89.

Goldman, N. and Yang, Z. 1994. A codon-based model of nucleotide substitution for protein-coding DNA sequences. Molecular Biology and Evolution 11(5): 725-736.

Govardovskii, V.I., Fyhrquist, N., Reuter, T., Kuzmin, D.G., and Donner, K. 2000. In search of the visual pigment template. Visual Neuroscience 17: 509-528.

Gow, C.E. 1985. Apomorphies of the Mammalia. South African Journal of Science 81: 558-560.

Gresser, E.B. and Noback, C.V. 1935. The eye of the monotreme, *Echidna hystrix*. Journal of Morphology 58(1): 279-284.

Griffiths, M. 1989. Tachyglossidae. pp. 407-435 *In* Fauna of Australia. Mammalia. *Edited by* Walton, D.W. and Richardson, B.J. Canberra, Australian Capital Territory 1B.

Griffiths, M. and Simpson, K.G. 1966. A seasonal feeding habit of spiy ant-eaters. CSIRO Wildlife Research 11: 137-143.

Grützner, F. and Graves, J.A.M. 2004. A platypus' eye view of the mammalian genome. Current Opinion in Genetics and Development 14: 642-649.

Hall, M.I. 2008a. Comparative analysis of the size and shape of the lizard eye. Zoology 111: 62-75.

Hall, M.I. 2008b. The anatomical relationships between the avian eye, orbit and sclerotic ring: Implications for inferring activity patterns in extinct birds. Journal of Anatomy 712: 781-794.

Hanson-Smith, V., Koladzkowski, B., and Thornton, J.W. 2010. Robustness of ancestral sequence reconstruction to phylogenetic uncertainty. Molecular Biology and Evolution 27(9): 1988-1999.

Heck, M., Schädel, S.A., Maretzki, D., Bartl, F.J., Ritter, E., Palczewski, K., and Hofmann, K.P. 2003. Signaling states of rhodopsin – Formation of the storage form, metarhodopsin III, from active metarhodopsin II. The Journal of Biological Chemistry 278(5): 3162-3169.

Hildebrand, P.W., Scheerer, P., Park, J.H., Choe, H.-W., Piechnick, R., Ernst, O.P., Hofmann, K.P., and Heck, M. 2009. A ligand channel through the G protein coupled receptor opsin. PloS ONE 4(2): e4382.

Hillenius, W.J. 1992. The evolution of nasal turbinates and mammalian endothermy. Paleobiology 18(1): 17-29.

Hillenius, W.J. 1994. Turbinates in therapsids: Evidence for Late Permian origins of mammalian endothermy. The Society for the Study of Evolution 48(2): 207-229.

Hofreiter, M., Serre, D., Poinar, H.N., Kuch, M., and Pääbo, S. 2001. Ancient DNA. Nature Reviews Genetics 2: 353-359.

Hong, K. and Hubbell, W.L. 1972. Preparation and properties of phospholipid bilayers containing rhodopsin. Proceedings of the National Academy of Sciences 69: 2617-2621.

Hong, K., Knudsen, P.J., and Hubbell, W.L. 1982. Purification of rhodopsin on hydroxyapatite columns, detergent exchange, and recombination with phospholipids. Methods in Enzymology 81: 144-50.

Hopson, J.A. 1973. Endothermy, small size, and the origin of mammalian reproduction. The American Naturalist 107(955): 446-452.

Hulbert, A.J., Beard, L.A., and Grigg, G.C. 2008. The exceptional longevity of an egg-laying mammal, the short-beaked echidna (*Tachyglossus aculeatus*) is associated with peroxidation-resistant membrane composition. Experimental Gerontology 43: 729-733.

Hunt, D. M., Arrese, C. A., von Dornum, M., Rodger, J., Oddy, A., Cowing, J. A., Ager, E. I., Bowmaker, J. K., Beazley, L. D., and Shand, J. 2003. The rod opsin pigments from two marsupial species, the South American bare-tailed woolly opossum and the Australian fat-tailed dunnart. Gene 323: 157-162.

Hunt, D.M., Carvalho, L.S., Cowing, J.A., and Davies, W.L. 2009. Evolution and spectral tuning of visual pigments in birds and mammals. Philosophical Transactions of the Royal Society B 364: 2941-2955.

Ikemura, T. 1985. Codon usage and tRNA content in unicellular and multicellular organisms. Molecular biology and evolution 2(1): 13-34.

Imai, H., Kojima, D., Oura, T., Tachibanaki, S., Terakita, A., and Shichida, Y. 1997. Single amino acid residue as a functional determinant of rod and cone visual pigments. Proceedings of the National Academy of Sciences 94: 2322-2326.

Imai, H., Kuwayama, S., Onishi, A., Morizumi, T., Chisaka, O., and Shichida, Y. 2005. Molecular properties of rod and cone visual pigments from purified chicken cone pigments to mouse rhodopsin in situ. Photochemical and Photobiological Sciences 4: 667-674.

Imai, H., Kefalov, V., Sakurai, K., Chisaka, O., Ueda, Y., Onishi, A., Morizumi, T., Fu, Y., Ichikawa, K., Nakatani, K., Honda, Y., Chen, J., Yau, K.-W., and Shichida, Y. 2007. Molecular properties of rhodopsin and rod function. The Journal of Biological Chemistry 282(9): 6677-6684.

Jacobs, G.H. 2009. Evolution of colour vision in mammals. Philosophical Transactions of the Royal Society B 364: 2957-2967.

Janke, A., Magnell, O., Wieczorek, G., Westerman, M., and Arnason, U. 2002. Phylogenetic analysis of 18S rRNA and the mitochondrial genomes of the wombat, *Vombatus ursinus*, and the spiny anteater, *Tachyglossus aculeatus*: Increased support for the Marsupionta hypothesis. Journal of Molecular Evolution 54(1): 71-80.

Janz, J.M. and Farrens, D.L. 2001. Engineering a functional blue-wavelength-shifted rhodopsin mutant. Biochemistry 40: 7219-7227.

Janz, J.M. and Farrens, D.L. 2004. Role of the retinal hydrogen bond network in rhodopsin Schiff base stability and hydrolysis. Journal of Biological Chemistry 279(53): 55886-55894.

Jerison, H.J. 1971. More on why birds and mammals have big brains. The American Naturalist 105(942): 185-189.

Ji, Q., Luo, Z.-X., Wible, J.R., Zhang, J.-P., and Georgi, J.A. 2002. The earliest known eutherian mammal. Nature 416: 816-822.

Ji, Q., Luo, Z.-X., Yuan, C.-X., and Tabrum, A.R. 2006. A swimming mammaliaform from the Middle Jurassic and ecomorphological diversification of early mammals. Science 311: 1123-1126.

Kaskan, P.M., Franco, E.C.S., Yamada, E.S., de Lima Silveira, L.C., Darlington, R.B., Finlay, B.L. 2005. Peripheral variability and central constancy in mammalian visual system evolution. Proceedings of the Royal Society B 272: 91-100.

Kawamura, S. and Yokoyma, S. 1998. Functional characterization of visual and nonvisual pigments of American chameleon (*Anolis carolinensis*). Vision Research 38: 37-44.

Kemp, T.S. 2005. The origin and evolution of mammals. Oxford University Press, New York.

Kemp, T.S. 2006. The origin of mammalian endothermy: a paradigm for the evolution of complex biological structure. Zoological Journal of the Linnean Society 147: 473-488.

Kielan-Jaworowska, Z., Cifelli, R.L., and Luo, Z.-X. 2004. Mammals from the age of dinosaurs: Origins, evolution, and structure. Columbia University Press, New York.

Kimura, M. 1968. Genetic variability maintained in a finite population due to mutational production of neutral and nearly neutral isoalleles. Genetic Research 11: 247-269.

Kimura, M. 1983. The neutral theory of molecular evolution. Cambridge University Press, Cambridge.

Kito, Y., Suzuki, T., Azuma, M., and Sekoguti, Y. 1968. Absorption spectrum of rhodopsin denatured with acid. Nature 218: 955-957.

Kochendörfer, G.G., Lin, S.W., Sakmar, T.P., and Mathies, R.A. 1999. How color visual pigments are tuned. Trends in Biochemical Sciences 24: 300-305.

Koshi, J.M. and Goldstein, R.A. 1996. Probabilistic reconstruction of ancestral protein sequences. Journal of Molecular Evolution 42: 313-320.

Koskelainen, A., Ala-Laurila, P., Fyhrquist, N., and Donner, K. 2000. Measurement of thermal contribution to photoreceptor sensitivity. Nature 403: 220-223.

Koteja, P. 2000. Energy assimiltaion, parental care, and the evolution of endothermy. Proceedings of the Royal Society of London B 267: 479-484.

Koteja, P. 2004. The evolution of concepts on the evolution of endothermy in birds and mammals. Physiological and Biochemical Zoology 77(6): 1043-1050.

Kuwayama, S., Imai, H., Hirano, T., Terakita, A., and Shichida, Y. 2002. Conserved proline residues at position 189 in cone visual pigments as a determinant of molecular properties different from rhodopsins. Biochemistry 41: 15245-15252.

Kuwayama, S., Imai, H., Morizumi, T., and Shichida, Y. 2005. Amino acid residues responsible for the meta-III decay rates in rod and cone visual pigments. Biochemistry 44: 2208-2215.

Laaß, M., Hampe, O., Schudack, M., Hoff, C., Kardjilov, N., and Hilger, A. 2010. New insights into the respiration and metabolic physiology of *Lystrosaurus*. Acta Zoologica. doi: 10.1111/j.1463-6395.2010.00467 .x

Lamb, T.D., Pugh Jr., E.N., Collin, S.P. 2007. The origin of the vertebrate eye. Evolution: Education and Outreach 1:415-426.

Langlois, G., Chen, C.-K., Palczewski, K., Hurley, J.B., and Vuong, M. 1996. Responses of the phototransduction cascade to dim light. Proceedings of the National Academy of Sciences 93: 4677-4682.

Li, G. and Luo, Z.-X. 2006. A Cretaceous symmetrodont therian with some monotreme-like postcranial features. Nature 439: 195-199.

Li, G., Steel, M., and Zhang, L. 2008. More taxa are not necessarily better for the reconstruction of ancestral character states. Systematic Biology 57 (4): 647-653.

Linnaeus, C. 1758. Systema naturae per regna triae naturae, secundum classis, ordines, genera, species cum characteribus, differentiis, synonyms locis; edito decima, reformata. Laurentii salvii, Stockholm, Vol. 1.

Loew, E.R., Fleishman, L.J., Foster, R.G., and Provencio, I. 2002. Visual pigments and oil droplets in diurnal lizards: A comparative study of Caribbean anoles. The Journal of Experimental Biology 205: 927-938.

Long, C.A. 1972. Two hypotheses on the origin of lactation. The American Naturalist 106(947): 141-144.

Luo, Z.-X. 1994. Sister-group relationships of mammals and transformations of diagnostic mammalian characters. pp. 98-128. *In* In the shadow of the dinosaurs: Early Mesozoic tetrapods. *Edited by* Fraser, N.C. and Sues, H.-D. Cambridge University Press, Cambridge.

Luo, Z.-X. 2007. Transformation and diversification in early mammal evolution. Nature 450: 1011-1019.

Luo, Z.-X., Crompton, A.W., and Sun, A.-L. 2001. A new mammal from the early Jurassic and evolution of mammalian characteristics. Science 292: 1535-1540.

Luo, Z.-X., Kielan-Jaworowska, Z., and Ciflli, R.L. 2002. In quest for a phylogeny of Mesozoic mammals. Acta Palaeontologica Polonica 47(1): 1-78.

Luo, Z.-X. and Wible, J.R. 2005. A late Jurassic digging mammal and early mammalian diversification. Science 308: 103-107.

Luo, Z.X., P. Chen, G. Li, and M. Chen. 2007. A new eutriconodont mammal and evolutionary development in early mammals. Nature 446: 288-293.

Lythgoe, J.N. 1972. List of vertebrate visual pigments. pp. 604-623. *In* Photochemistry of vision. *Edited by* H.J.A. Dartnall. Springer Verlag, New York.

Ma. J.-X., Znoiko, S., Othersen, K.L., Ryan, J.C., Das, J., Isayama, T., Kono, M., Oprian, D.D., Corson, D.W., Cornwall, M.C., Cameron, D.A., Harosi, F.I., Makino, C.L., and Crouch, R.K. 2001. A visual pigment expressed in both rod and cone photoreceptors. Neuron 32: 451-461.

MacKenzie, D., Arendt, A., Hargrave, P., McDowell, J.H., and Molday, R.S. 1984. Localization of binding sites for carboxyl terminal specific anti-rhodopsin monoclonal antibodies using synthetic peptides. Biochemistry 23: 6544-6549.

Makino, C.L. Groesbeek, M., Lugtenburg, J., and Baylor, D.A. 1999. Spectral tuning in salamander visual pigments studied with dihydroretinal chromophores. Biophysical Journal 77: 1024-1035.

Martin, T. 2005. Postcranial anatomy of *Haldanodon expectatus* (Mammalia, Docodonta) from the Late Jurassic (Kimmeridgian) of Portugal and its bearing for mammalian evolution. Zoological Journal of the Linnean Society 145: 219-248.

McKibbin, C., Toye, A.M., Reeves, P.J., Khorana, H.G., Edwards, P.C., Villa, C., and Booth, P.J. 2007. Opsin stability and folding: The role of Cys185 and abnormal disulfide bond formation in the intradiscal domain. Journal of Molecular Biology 374: 1309-1318.

McNab, B.K. 1978. The evolution of hoemeothermy in the phylogeny of mammals. The American Naturalist 112: 1-21.

Meng, J., Hu, Y., Wang, Y., Wang, X., and Li, C. 2006. A mesozoic gliding mammal from northeastern China. Nature 444: 889-893.

Menon, S.T., Han, M., and Sakmar, T.P. 2001. Rhodopsin: Structural basis of molecular physiology. Physiological Reviews 81: 1659-1688.

Meredith, R.W., Westerman, M., Case, J.A., and Springer, M.S. 2007. A phylogeny and timescale for marsupial evolution based on sequences for five nuclear genes. Journal of Mammalian Evolution 15: 1-36.

Metzger, K.J. and Thomas, M.A. 2010. Evidence of positive selection at codon sites localized in extracellular domains of mammalian CC motif chemokine receptor proteins. BMC Evolutionary Biology 10: 139.

Modesto, S.P. and Anderson, J.S. 2004 The phylogenetic definition of Reptilia. Systematic Biology 53(5): 815-821.

Molday, R.S. and MacKenzie, D. 1983. Monoclonal antibodies to rhodopsin: Characterization, cross-reactivity, and application as structural probes. Biochemistry 22: 653-660.

Morrow, J.M. and Chang, B.S.W. 2010. The p1D4-hrGFP II expression vector: A tool for expressing and purifying visual pigments and other G protein-coupled receptors. Plasmid. doi:10.1016/j.plasmid.2010.07.002

Muntz, W.R.A. 1976. Visual pigments of cichlid fishes from Malawi. Vision Research 16: 897-903.

Murphy, W.J., Pringle, T.H., Crider, T.A., Springer, M.S., and Miller, W. 2007. Using genomic data to unravel the root of the placental mammal phylogeny. Genome Research 17: 413-421.

Nathans, J. and Hogness, D.S. 1983. Isolation, sequence analysis, and intron-exon arrangement of the gene encoding bovine rhodopsin. Cell 34: 807-814.

Nathans, J. and Hogness, D.S. 1984. Isolation and nucleotide sequence of the gene encoding human rhodopsin. Proceedings of the National Academy of Sciences 81: 4851-4855.

Navidi, W.C., Churchill, G.A., and von Haeseler, A. 1991. Methods for inferring phylogenies from nucleic acid sequence data by using maximum likelihood and linear invariants. Molecular Biology and Evolution 8(1): 128-143.

Nickels, R.W., Bourgoyne, C.F., Quigley, H.A., and Zack, D.J. 1995. Cloning and characterization of rod opsin cDNA from the old world monkey, *Macaca fascicularis*. Investigative Ophtalmology and Visual Science 36: 72-82.

Nicol, S. and Andersen, N.A. 2006. Body temperature as an indicator of egg-laying in the echidna, Tachyglossus aculeatus. Journal of Thermal Biology 31: 483-490.

Nicol, S. and Andersen, N.A. 2007. The life-history of an egg-laying mammal, the echidna (*Tachyglossus aculeatus*). Ecoscience 14(3): 275-285.

Novacek, M.J. 1992. Mammalian phylogeny: Shaking the tree. Nature 356(6365): 121-125.

O'Day, K.J. 1952. Observations on the eye of the monotreme. Transactions of the Ophthalmological Society of Australia 12: 95-104.

Okada, T, Matsuda, T., Kandori, H., Fukada, Y., Yoshizawa, T., and Shichida, Y. 1994. Circular dichroism of metaiodopsin II and its binding to transducin: A comparative study between meta II intermediates of iodopsin and rhodopsin. Biochemistry 33: 4940-4946.

Okano, T., Fukada, Y., Artamonov, I.D., and Yoshizawa, T. 1989. Purification of cone visual pigments from chicken retina. Biochemistry 28: 8848-8856.

Okano, T., Kojima, D., Fukada, Y., Shichida, Y., and Yoshizawa, T. 1992. Primary structures of chicken cone visual pigments: Vertebrate rhodopsins have evolved out of cone visual pigments. Proceedings of the National Academy of Sciences 89: 5932-5936.

Olson, L.E. and Hassanin, A. 2003. Contamination and chimerism are perpetuating the legend of the snake-eating cow with twisted horns (*Pseudonovibus spiralis*). A case study of the pitfalls of ancient DNA. Molecular Phylogenetics and Evolution 27: 545-548.

Oprian, D.D., Molday, R.S., Kaufman, R.J., and Khorana, H.G. 1987. Expression of a synthetic bovine rhodopsin gene in monkey kidney cells. Proceedings of the National Academy of Sciences 84: 8874-8878.

Oprian, D.D., Asenjo, A.B., Lee, N., and Pelletier, S.L. 1991. Design, chemical synthesis, and expression of genes for the three human color vision pigments. Biochemistry 30: 11367-11372.

Page, R.D.M. and Holmes, E.C. 2006. Molecular evolution. A phylogenetic approach. Blackwell Publishing, Oxford.

Palczewski, K. 2006. G protein-coupled receptor rhodopsin. Annual Review of Biochemistry 75: 743-767.

Palczewski, K., Kumasaka, T., Hori,T., Behnke, C.A., Motoshima, H., Fox, B.A., Le Trong, I., Teller, D.C., Okada, T., Stenkamp, R.E., Yamamoto, M., and Miyano, M. 2000. Crystal structure of rhodopsin: A G protein-coupled receptor. Science 289: 739-745.

Park, J.H., Scheerer, P., Hofmann, K.P., Choe, H.-W., and Ernst, O.P. 2008. Crystal structure of the ligand-free G-protein-coupled receptor opsin. Nature 454: 183-187.

Parmley, J.L., Chamary, J.V., and Hurst, L.D. 2006. Evidence for purifying selection against synonymous mutatins in mammalian exonic splicing enhancers. Molecular Biology and Evolution 23: 301-309.

Parry, J.W.L., Carleton, K.L., Spady, T., Carboo, A., Hunt, D.M., and Bowmaker, J.K. 2005. Mix and match color vision: Tuning spectral sensitivity by differential opsin gene Expression in Lake Malawi cichlids. Current Biology 15: 1734-1739.

Pauling, L. and Zuckerkandl, E. 1963. Chemical paleogenetics: molecular „restoration studies“ of extinct forms of life. Acta Chemica Scandinavica 17: S9-16.

Peichl, L. 2005. Diversity of mammalian photoreceptor properties: Adaptations to habitat and lifestyle? The Anatomical Record A 287: 1001-1012.

Peters, W. and Doria, G. 1876. Diagnosi di alcune nuove specie di Marsupiali appartenenti Fauna papuana. Ann. Mus. Civ. Stor. Nat. Gen. 7: 541.

Phillips, M. J., Bennett, T.H., and Lee, M.S.Y. 2009. Molecules, morphology, and ecology indicate a recent, amphibious ancestry for echidnas. Proceedings of the National Academy of Sciences 106(40): 17089-17094.

Pie, M.R. 2006. The influence of phylogenetic uncertainty on the detection of positive Darwinian selection. Molecular Biology and Evolution 23(12): 2274-2278.

Pugh, E.N.Jr. and Lamb, T.D. 1993. Amplification and kinetics of the activation steps in phototransduction. Biochimica et Biophysica Acta 1141: 111-149.

Pupko, T., Pe'er, I., Shamir, R., and Graur, D.. 2000. A fast algorithm for joint reconstruction of ancestral amino acid sequences. Molecular Biology and Evolution 17: 890-896.

Radding, C.M. and Wald, G. 1956. Acid-base properties of rhodopsin and opsin. Journal of General Physiology 39(6): 909-922.

Reeves, P.J., Thurmond, R.L., and Khorana, H.G. 1996. Structure and function in rhodopsin: high level expression of a synthetic bovine opsin gene and its mutants in stable mammalian cell lines. Proceedings of the National Academy of Sciences 93: 11487-11492.

Reisz, R.R. 1986. Pelycosauria. *In* Handbuch der Paläoherpetologie Part 17A. *Edited by* Kuhn, O. and Wellnhofer, P. Gustav Fischer Verlag.

Rismiller, P. 1999. The Echidna - Australia's enigma. Hugh Lauter Levin Associates, Inc. Hong Kong.

Romer, A.S. 1956. Osteology of the reptiles. University of Chicago Press, Chicago.

Rowe, M.P. 2000. Inferring the retinal anatomy and visual capacities of extinct vertebrates. Palaeontologia Electronica 3(1): 43 pp.

Rowe, T. 1988. Definition, diagnosis, and origin of Mammalia. Journal of Vertebrate Paleontology 8(3): 241-264.

Rowe, T., Rich, T.H., Vickers-Rich, P., Springer, M., and Woodburne, M.O. 2008. The oldest platypus and its bearing on divergence timing of the platypus and echidna clades. Proceedings of the National Academy of Sciences 105(4): 1238-1242.

Ruben, J. 1995. The evolution and endothermy in mammals and birds: from physiology to fossils. Annual Review of Physiology 57: 69-95.

Sagoo, M.S. and Lagnado, L. 1997. G-protein deactivation is rate-limiting for shut-off of the phototransduction cascade. Nature 389: 392-395.

Sakamoto, T. and Khorana, H.G. 1995. Structure and function in rhodopsin: The fate of opsin formed upon the decay of light-activated metarhodopsin II *in vitro*. Proceedings of the National Academy of Sciences 92: 249-253.

Sakmar, T.P., Franke, R.R., and Khorana, H.G. 1989. Glutamic acid-113 serves as the retinylidene Schiff base counterion in bovine rhodopsin. Proceedings of the National Academy of Sciences 86: 8309-8313.

Sakmar, T.P., Menon, S.T., Marin, E.P., and Awad, E.S. 2002. Rhodopsin: Insights from recent structural studies. Annual Review of Biophysics and Biomolecular Structure 31: 443-484.

Sakurai, K., Onishi, A., Imai, H., Chisaka, O., Ueda, Y., Usukura, J., Nakatani, K., and Shichida, Y. 2007. Physiological properties of rod photoreceptors cells in green-sensitive cone pigment knock-in mice. Journal of General Physiology 130(1): 21-40.

Salom, D., Lodowski, D.T., Stenkamp, R.E., Le Trong, I., Golczak, M., Jastrzebska, B., Harris, T., Ballesteros, J.A., and Palczewski, K. 2006. Crystal structure of a photoactivated deprotonated intermediate of rhodopsin. Proceedings of the National Academy of Sciences 103(44): 16123-16128.

Sánchez-Villagra, M.R. 2010. Developmental palaeontology in synapsids: the fossil record of ontogeny in mammals and their closest relatives. Proceedings of the Royal Society B: 277: 1139-1147.

Schädel, S.A., Heck, M., Maretzki, D., Filipek, S., Teller, D.C., Palczewski, K., and Hofmann, K.P. 2003. Ligand channeling within a G-protein-coupled receptor. Journal of Biological Chemistry 278(27): 24896-24903.

Schmidt-Nielsen, K., Dawson, T.J., and Crawford, E.C.Jr. 1966. Temperature regulation in the echidna (*Tachyglossus aculeatus*). Journal of Cellular Physiology 67: 63-72.

Schmitz, L. 2009. Quantitative estimates of visual performance features in fossil birds. Journal of Morphology 270: 759-773.

Schnapf, J.L., Kraft, T.W., Nunn, B.J., and Baylor, D.A. 1988. Spectral sensitivity of primate photoreceptors. Visual Neuroscience 1: 255-261.

Schweitzer, M.H., Zheng, W., Organ, C.L., Avci, R., Suo, Z., Freimark, L.M., Lebleu, V.S., Duncan, M.B., Heiden, M.G.V., Neveu, J.M., Lane, W.S., Cottrell, J.S., Horner, J.R., Cantley, L.C., Kalluri, R., and Asara, J.M. 2009. Biomolecular characterization and protein sequences of the Campanian hadrosaur *B. canadensis*. Science 324: 626-631.

Shabalina, S.A., Ogutsov, A.Y., and Spiridonov, N.A. 2006. A periodic pattern of mRNA secondary structure created by the genetic code. Nucleic Acids Research 34(8): 2428-2437.

Sharp, P.M., Cowe, E., Higgins, D.G., Shields, D.C., Wolfe, K.H., and Wright, F. 1988. Codon usage patterns in *Escherichia coli*, *Bacillus subtilis*, *Saccharomyces cerevisiae*, *Schizosaccharomyces pombe*, *Drosophila melanogaster*, and *Homo sapiens*: A review of the considerable within-species diversity. Nucleic Acids Research 16(17): 8207-8211.

Shaw, G., 1792. Museum Leverianum, containing select specimens from the Museum of the Late Sir Ashton Lever with descriptions in Latin and English. 2 vols. London.

Shaw, G. 1799. The duck-billed platypus. *In* The naturalists' miscellany. Vol. 10. London.

Shaw, C.N., Wilson, P.J., and White, B.N. 2003. A reliable molecular method of gender determination for mammals. Journal of Mammalogy 84(1): 123-128.

Shen, Y.-Y., Liu, J., Irwin, D.M., and Zhang, Y.-P. 2010. Parallel and convergent evolution of the dim-light vision gene RH1 in bats (Order: Chiroptera). PloS ONE 5(1): e8838.

Shi, Y. and Yokoyama, S. 2003. Molecular analysis of the evolutionary significance of ultraviolet vision in vertebrates. Proceedings of the National Academy of Sciences 100(14): 8308-8313.

Shichi, H., Lewis, M.S., Irreverre, F., and Stone, A.L. 1969. Biochemistry of visual pigments. The Journal of Biological Chemistry 244(3): 529-536.

Shichida, Y., Imai, H., Imamoto, Y., Fukada, Y., and Yoshizawa, T. 1994. Is chicken green-sensitive cone visual pigment a rhodopsin-like pigment? A comparative study of the molecular properties between chicken green and rhodopsin. Biochemistry 33: 9040-9044.

Shichida, Y. and Matsuyama, T. 2009. Evolution of opsins and phototransduction. Philosophical Transactions of the Royal Society B 364: 2881-2895.

Sidor, C.A. and Welman, J. 2003. A second specimen of *Lemurosaurus pricei* (Therapsida: Burnetiamorpha). Journal of Vertebrate Paleontology 23: 631-642.

Sidor, C.A., Hopson, J.A., and Keyser, A.W. 2004. A new burnetiamorph therapsid from the Teekloof Formation, Permian, of South Africa. Journal of Vertebrate Paleontology 24: 938-950.

Sillman, A.J., CARVER, J.K., and LOEW, R. 1999. The photoreceptors and visual pigments in the retina of a boid snake, the ball python (*Python regius*). The Journal of Experimental biology 202: 1931-1938.

Smith, W.C., Adamus, G., Van Der Wel, H., Timmers, A., Palczewski, K., Ulshafer, R.J., Hargrave, P.A., and McDowell, J.H. 1995. Alligator rhodopsin: Sequence and biochemical properties. Experimental Eye Research 61(5): 569-578.

Southall, K.D., Oliver, G.W., Lewis, J.W., Le Boeuf, B.J., Levenson, D.H., and Southall, B.L., 2002. Visual pigment sensitivity in three deep diving marine mammals. Marine Mammal Science 18: 275-281.

Spady, T.C., Seehausen, O., Loew, E.R., Jordan, R.C., Kocher, T.D., and Carleton, K.L. 2005. Adaptive molecular evolution in the opsin genes of rapidly speciating cichlid species. Molecular Biology and Evolution 22: 1412-1422.

Stackhouse, J., Presnell, S.R., McGeehan, G.M., Nambiar, K.P., and Benner, S.A. 1990. The ribonuclease from an extinct bovid ruminant. FEBS Letters 262(1): 104-106.

Starace, D.M. and Knox, B.E. 1998. Cloning and expression of a short wavelength cone pigment. Experimental Eye Research 67: 209-220.

Stavenga, D.G., Smits, R.P., and Hoenders, B.J. 1993. Simple exponential functions describing the absorbance bands of visual pigment spectra. Vision Research 33(8): 1011-1017.

Sues, H.D. 1986. Relationships and biostratigraphic significance of thge Tritylodontidae (Synapsida) from the Kayenta Formation of northeastern Arizona. pp. 279-284. *In* The beginning of the age of dinosaurs: Faunal change across the Triassic-Jurassic boundary. *Edited by* Padian, K. Cambridge University Press, Cambridge.

Sugawara, T., Terai, Y., and Okada, N. 2002. Natural selection of the rhodopsin gene during the adaptive radiation of East African great lakes cichlid fishes. Molecular Biology and Evolution 19: 1807-1811.

Sugawara, T., Imai, H., Nikaido, M., Imamoto, Y., and Okada, N. 2010. Vertebrate rhodopsin adaptation to dim light via rapid meta-II intermediate formation. Molecular Biology and Evolution 27(3): 506-519.

Swofford, D.L. 1985. PAUP: Phylogenetic analysis using parsimony. Version 2.4. Illinois Natural History Survey, Champaign.

Szél, À., Röhlich, P., Caffé, A.R., and Van Veen, T. 1996. Distribution of cone photoreceptors in the mammalian retina. Microscopy Research and Technique 35: 445-462.

Tan, Y., Yoder, A.D., Yamashita, N., and Li, W.-H. 2005. Evidence from opsin genes rejects nocturnality in ancestral primates. Proceedings of the National Academy of Sciences 102(41): 14712-14716.

Tamura, K., Dudley, J., Nei, M., and Kumar, S. 2007. MEGA4: Molecular evolutionary genetics analysis (MEGA) software version 4.0. Molecular Biology and Evolution 24: 1596-1599.

Thomas, M.O.1907. A new *Acanthoglossus* from the island of Salawatti. Ann. Mag. Nat. Hist. Lond. 20: 498-499.

Thornton, J.W. 2004. Resurrecting ancient genes: Experimental analysis of extinct molecules. Nature Reviews Genetics 5: 366-375.

Thornton, J.W., Need, E., and Crews, D. 2003. Resurrecting the ancestral steroid receptor: ancient origin of estrogen signaling. Science 301: 1714-1717.

Ugalde, J.A., Chang, B.S., and Matz, M.V. 2004. Evolution of coral pigments recreated. Science 305(5689): 1433.

Wakefield, M.J., Anderson, M., Chang, E., Wei, K.-J., Kaul, R., Graves, J.A.M., Grützner, F., and Deeb, S.S. 2008. Cone visual pigments of monotremes: Filling the phylogenetic gap. Visual Neuroscience 25: 257-264.

Wald, G. 1968. The molecular basis of visual excitation. Nature 219: 800-807.

Wald, G. and Brown, P.K. 1953. The molar extinction of rhodopsin. The Journal of General Physiology: 189-199.

Wald, G., Brown, P.K., and Smith, P.H. 1955. Iodopsin. Journal of General Physiology 38: 623-681.

Wald, G. and Brown, P.K. 1958. Human rhodopsin. Science 127(3292): 222-249.

Walls, G.L. 1942. The vertebrate eye and its adaptive radiation. Cranbrook Institute of Science, Bloomfield Hills, Michigan.

Wang, S.-Z., Adler, R., and Nathans, J. 1992. A visual pigment from chicken that resembles rhodopsin: Amino acid sequence, gene structure, and functional expression. Biochemistry 31: 3309-3315.

Warren, W.C., Hillier, L.W., Graves, J.A.M., Birney, E., Ponting. C.P., Grützner, F., Belov, K., Miller, W., Clarke, L., Chinwalla, A.T., Yang, S.-P., Heger, A., Locke, D.P., Miethke, P., Waters, P.D., Veyrunes, F., Fulton, L., Fulton, B., Graves, T., Wallis, J., Puente, X.S., López-Otín, C., Ordóñez, G.R., Eichler, E.E., Chen, L., Cheng, Z., Deakin, J.E., Alsop, A., Thompson, K., Kirby, P., Papenfuss, A.T., Wakefield, M.J., Olender, T., Lancet, D., Huttley, G.A., Smit, A.F.A., Pask, A., Temple-Smith, P., Batzer, M.A., Walker, J.A., Konkel, M.K., Harris, R.S., Whittington, C.M., Wong, E.S.W., Gemmell, N.J., Buschiazzo, E., Vargas Jentzsch, I.M., Merkel, A., Schmitz, J., Zemann, A., Churakov, G., Kriegs, J.O., Brosius, J., Murchison, E.P., Sachidanandam, R., Smith, C, Hannon, G.J., Tsend-Ayush, E., McMillan, D., Attenborough, R., Rens, W., Ferguson-Smith, M, Lefèvre, C.M., Sharp, J.A., Nicholas, K.R., Ray, D.A., Kube, M., Reinhardt, R., Pringle, T.H., Taylor, J., Jones, R.C., Nixon, B., Dacheux, J.-L., Niwa, H., Sekita, Y., Huang, X., Stark, A., Kheradpour, P., Kellis, M., Flicek, P., Chen, Y., Webber, C., Hardison, R., Nelson, J., Hallsworth-Pepin, K., Delehaunty, K., Markovic, C., Minx, P., Feng, Y., Kremitzki, C., Mitreva, M., Glasscock, J., Wylie, T., Wohldmann, P., Thiru, P., Nhan, M.N., Pohl, C.S., Smith, S.M., Hou, S., Renfree, M.B., Mardis, E.R., and Wilson, R.K. 2008. Genome analysis of the platypus reveals unique signatures of evolution. Nature 455: 175-256.

Watson, J.M., Meyne, J., and Graves, J.A.M. 1996. Ordered tandem arrangement of chromosomes in the sperm heads of monotreme mammals. Proccedings of the National Academy of Sciences 93(19): 10200-10205.

Weitz, C.J. and Nathans, J. 1993. Rhodopsin activation: Effects on the metarhodopsin I-metarhodopsin II equilibrium of neutralization or introduction of charged amino acids within putative transmembrane segments. Biochemistry 32: 14176-14182.

Werneburg, I. and Sánchez-Villagra, M.R. 2010. The early development of the echidna, *Tachyglossus aculeatus* (Mammalia: Monotremata), and patterns of mammalian development. Acta Zoologica. doi: 10.111/j.1463-6395.2009.00447.x

Wible, J.R., Rougier, G.W., Novacek, M.J., and Asher, R.J. 2007. Cretaceous eutherians and Laurasian origin for placental mammals near the K/T boundary. Nature 447: 1003-1006.

Wilden, U., Hall, S.W., and Kohn, H. 1986. Phosphodiesterase activation by photoexcited rhodopsin is quenched when rhodopsin is phosphorylated and binds the intrinsic 48-kDa protein of rod outer segments. Proceedings of the National Academy of Sciences 83: 1174-1178.

Wong, D.W.S. 2006. The ABCs of gene cloning. 2nd edition. Springer science and business media, New York.

Woodburne, M.O., Rich, T.H., and Springer, M.S. 2003. The evolution of tribospheny and the antiquity of mammalian clades. Molecular Phylogenetics and Evolution 28: 360-385.

Wright, S.I., Yau, C.B., Looseley, M, and Meyers, B.C. 2004. Effects of gene expression on molecular evolution in *Arabidopsis thaliana* and *Arabidopsis lyrata*. Molecular Biology and Evolution 21: 1719-1726.

Yang, Z. 1998. Likelihood ratio tests for detecting positive selection and application to primate lysozyme evolution. Molecular Biology and Evolution 15(5): 568-573.

Yang, Z. 2002. Inference of selection from multiple species aligments. Current Opinion in Genetics and Development 12: 688-694.

Yang, Z. 2007. PAML 4: Phylogenetic analysis using maximum likelihood. Molecular Biology and Evolution 24: 1586-1591.

Yang, Z., Kumar, S., and Nei, M. 1995. A new method of inference of ancestral nucleotide and amino acid sequences. Genetics 141: 1641-1650.

Yang, Z. and Nielsen, R. 1998. Synonymous and nonsynonymous rate variation in nuclear genes of mammals. Journal of Molecular Evolution 46: 409-418.

Yang, Z. and Nielsen, R. 2002. Codon-substitution models for detecting molecular adaptation at individual sites along specific lineages. Molecular Biology and Evolution 19: 908-917.

Yang, Z. and Bielawski, J.P. 2000. Statistical methods for detecting molecular adaptation. Tree 15: 496-503.

Yang, Z., Wong, W.S.W., and Nielsen, R. 2005. Bayes empirical bayes inference of amino acid sites under positive selection. Molecular Biology and Evolution 22(4): 1107-1118.

Yau, K.-W. 1994. Phototransduction mechanism in retinal rods and cones. Investigative Ophthalmology and Visual Science 35(1): 9-32.

Yokoyama, S. 2008. Evolution of dim-light and color vision pigments. Annual Review of Genomics and Human Genetics 9: 259-282.

Yokoyama, S. and Blow, N.S. 2001. Molecular evolution of the cone visual pigments in the pure rod-retina of the nocturnal gecko, *Gekko gekko*. Gene 276: 117-125.

Yokoyama, S., Tada, T., Zhang, H., and Britt, L. 2008. Elucidation of phenotypic adaptations: molecular analyses of dim-light vision proteins in vertebrates. Proceedings of the National Academy of Science 105(36): 13480 -1348.

Young, H.M. and Pettigrew, J.D. 1991. Cone photoreceptors lacking oil droplets in the retina of the echidna, *Tachyglossus aculeatus* (Monotremata). Visual Neuroscience 6: 409-420.

Zhang, H. and Yokoyama, S. 1997. Molecular evolution of the rhodopsin gene of the marine lamprey, *Petromyzon marinus*. Gene 191: 1-6.

Zhang, J., Nielsen, R., and Yang, Z., 2005. Evaluation of an improved branch-site likelihood method for detecting positive selection at the molecular level. Molecular Biology and Evolution 22: 2472-2479.

Zhao, H., Rossiter, S.J., Teeling, E.C., Li, C., Cotton, J.A., and Zhang, S. 2009. The evolution of colour vision in nocturnal mammals. Proceedings of the National Academy of Sciences 106(22): 8980-8985.

Zhao, H., Ru, B, Teeling, E.C., Faulkes, C.G., Zhang, S., and Rossiter, S.J. 2009b. Rhodopsin molecular evolution in mammals inhabiting low light environments. PloS ONE 4(12): e8326.

Publications

Sander, M., Klein, N., Albers, P., **Bickelmann, C.**, and Winkelhorst, H. (submitted). Postcranial morphology of a basal Pistosauroidea from the Lower Muschelkalk of Winterswijk, The Netherlands and a revised and extended phylogenetic analysis of Triassic Sauropterygia. Jounal of Vertebrate Paleontology.

Hampe, O., Schwarz-Wings, D., **Bickelmann, C.**, and Klein, N. 2010. Fore limb bones of late Pleistocene dwarf hippopotamuses (Mammalia, Cetartiodactyla) from Madagascar previously determined as belonging to the crocodylid *Voay* Brochu, 2007. Fossil Record 13(2): 303-307.

Bickelmann, C. Müller, J. & Reisz, R.R. 2009. The enigmatic diapsid *Acerosodontosaurus piveteaui* (Reptilia: Neodiapsida) from the Upper Permian of Madagascar and the paraphyly of "younginiform" reptiles. Canadian Journal of Earth Sciences, 46: 651-661.

Bickelmann, C. & Klein, N. 2009. A Late Pleistocene horned crocodile *Voay robustus* (Grandidier & Vaillant, 1872) from Madagascar in the collection of the Museum für Naturkunde, Berlin. Fossil Record, 12(1): 13-21.

Bickelmann, C. & Sander, P.M., 2008. A partial skeleton and isolated humeri of *Nothosaurus* (Reptilia: Eosauropterygia) from Winterswijk, The Netherlands. Journal of Vertebrate Paleontology, 28(2): 326-338.

Conference presentations

- *06/2010*
  - Evolution Meeting, Portland, Oregon, USA
    Bickelmann, C., Du, J., Müller, J. & Chang, B.S.W. „Ancestral visual pigments and their implications for early mammlian paleobiology“
- *10/2009*
  - Annual Meeting of the Society of Vertebrate Paleontology, Bristol, UK
    Bickelmann, C., Müller, J., Du, J. & Chang, B.S.W. “Inferring early mammalian paleobiology from vertebrate visual pigments“
- *05/2009*
  - Meeting of the German Paleoherpetologists, Bonn, Germany
    Bickelmann, C., Müller, J. & Reisz, R.R. „*Acerosodontosaurus piveteaui* und die Paraphylie der ‚Younginiformes‘“
- *10/2008*
  - Annual Meeting of the Society of Vertebrate Paleontology, Cleveland, Ohio, USA
    Bickelmann, C., Müller, J. & Reisz, R.R. “*Acerosodontosaurus* and the monophyly of younginiform reptiles”
- *09/2008*
  - Annual Meeting of the German Paleontological Society, Erlangen, Germany
    Bickelmann, C., Müller, J. & Chang, B.S.W. “The genetic basis for scopic vision in the living echidna and its implications for the paleobiology of early mammals.”

    Buchwitz, M., Klein, N. & **Bickelmann, C.** “Isolated bones as a paleobiological data source: a case study on sauropterygian humeri.”
- *10/2007*
  - Annual Meeting of the Society of Vertebrate Paleontology, Austin, Texas, USA
    Bickelmann, C. & Sander, P.M. „Postcranial material of *Nothosaurus* from the Lower Muschelkalk of Winterswijk, The Netherlands: the systematic value of humerus morphology.“
- *09/2007*
  - Annual Meeting of the German Paleontological Society, Freiberg, Germany
    Bickelmann, C. & Sander, P.M. “*Nothosaurus* aus dem Unteren Muschelkalk von Winterswijk, Niederlande: ein Postkranialskelett im Vergleich mit Humerus-Morphotypen.“
- *03/2007*
  - Meeting of the German Vertebrate Paleontologists, Freyburg a.d. Unstrut, Germany
    Bickelmann, C. & Sander, P.M. „Ein teilweise erhaltenes Postkranialskelett und Humeri-Morphotypen der Sauropterygier-Gattung *Nothosaurus* aus dem Unteren Muschelkalk von Winterswijk, Niederlande.“
- *05/2006*
  - Meeting of the German Paleoherpetologists, Mainz, Germany
    Bickelmann, C. & Sander, P.M. „Die postkraniale Anatomie von *Nothosaurus* aus dem Unteren Muschelkalk von Winterswijk, Niederlande“

Erklärung

Hiermit verischere ich, dass ich diese Dissertation eigenständig und nur unter Verwendung der angegebenen Quellen und Hilfsmittel angefertigt habe.

Berlin, den 20.02.2011

Constanze Bickelmann